A NEW COMPOUND MODULATION TECHNIQUE FOR MULTI-CHANNEL ANALOG VIDEO TRANSMISSION ON FIBER

by

Alfred S. Andrawis

Dissertation submitted to the Faculty of the

Virginia Polytechnic Institute and State University

in partial fulfillment of the requirements for the degree of

Ph.D.

in Electrical Engineering

APPROVED:

Ira Jacobs,
Chairperson

Charles W. Bostian

Richard O. Claus

Timothy Pratt

Werner E. Kohler

December, 1991

Blacksburg, Virginia

A NEW COMPOUND MODULATION TECHNIQUE FOR MULTI-CHANNEL ANALOG VIDEO TRANSMISSION ON FIBER

by

Alfred S. Andrawis

Ira Jacobs, Chairperson

Electrical Engineering

(ABSTRACT)

Present analog optical fiber multi-channel video transmission systems are very sensitive to laser nonlinearities and are consequently limited in the optical modulation depth (OMD) that may be used. This, in turn limits the power budget achievable, signal-to-noise ratio, and the channel capacity.

In this dissertation a new analog transmission technique for multi-channel TV transmission on fiber using frequency modulation/pulse amplitude modulation/time division multiplexing (FM/TDM) is described and compared with present digital and analog systems. Parameters for the proposed system are selected and the relationship between the performance and parameter values is discussed. Analysis and simulations indicate that the proposed system has a very low sensitivity to nonlinearities and is similar to that of digital systems, and much better than current Frequency Modulated/Frequency Division Multiplexed (FM/FDM) systems. This permits the use of higher OMD (as high as in digital systems), which results in achieving a high signal-to-noise ratio and a large power budget. Analysis of the number of channels as a function of adjacent channel

intersymbol interference indicates that the proposed system has a better spectral efficiency than present analog systems. Simulations are also used to predict the performance of the proposed system with laser diodes poorer than the ones presently used for multi-channel analog systems. Considerably poorer lasers may be used while achieving acceptable transmission quality. Finally, carrier-to-noise penalty caused by timing errors and jitter effects are analyzed.

ACKNOWLEDGEMENTS

I would like to express my sincere gratitude to my advisor, Dr. Ira Jacobs, for his sincere help, support, and guidance throughout this work. Without his guidance, encouragement and support this dissertation could have never been completed

Special thanks are also due to the members of my advisory committee: Dr. Bostian, Dr. Claus, Dr. Pratt, and Dr. Kholer for their time and effort in the presentation and defense of my dissertation. Your comments have been very helpful. Dr. Bostian has been always a source of encouragement, not only in this dissertation, but since the first day I came to Virginia Tech. I would also like to thank Dr. Pratt, for his technical comments and for helping me in preparing for my preliminary examination. I would also like to thank Dr. Claus for his encouragement and support in the last three years.

I also wish to thank all faculty and staff of the Electrical Engineering Department who made my stay at the university a memorable and valuable experience. Specially, I would like to thank Dr. Stephenson for his cooperation and encouragement. I also wish to express my appreciation to Dr. Nunnally for his kindness, generosity, and encouragement.

The greatest amount of thanks goes to my lovely wife, children, and family. If it were not for you, this dissertation would be only a dream. I hope this dissertation will be a testament to your persistence and love.

Alfred 12/19/1991

TABLE OF CONTENTS

LIST OF ILLUSTRATIONS

LIST OF TABLES

CHAPTER 1

INTRODUCTION

1.1 STATEMENT OF THE PROBLEM

In the CATV industry the demand for wider bandwidth, larger power budget, and higher signal-to-noise ratio is escalating [1],[2]. This is due to the increasing need for more television channels, expansion of the coverage areas, and better picture quality. The introduction of wide screen, improved resolution NTSC TV receivers (IDTV), makes video impairments more evident. Thus picture quality delivered to the home should be comparable to studio quality. As advanced television systems (ATV) and high definition TV (HDTV) are introduced, still more demands will be made on cable system performance.

Present analog optical fiber systems do not provide an easy solution for all the demands needed by the CATV operators. They are still limited in power budget, signal-to-noise ratio (S/N), and number of channels. To achieve a large value of any of these parameters, a large optical signal should be launched into the fiber. Optical sources are generally intensity modulated around a bias point. A large signal causes large deviation from the bias point, which means large optical modulation depth (OMD) of the light source. On the other hand light sources are inherently nonlinear devices. Large OMD further degrades the linearity of the source, raising the level of nonlinear distortions.

In this dissertation a proposal for a new analog transmission technique,

using frequency modulation / pulse amplitude modulation / time division multiplexing (*FM/TDM*) is presented. The proposed system and present digital and analog FM, systems are compared. Analysis and simulations indicate that the proposed system's sensitivity to nonlinearities is similar to digital systems and much lower than present analog systems. This permits the use of higher optical modulation depth, which results in achieving a higher signal-to-noise ratio, larger power budget, better spectrum efficiency, and/or the use of lower cost optical components, than current analog systems. Relative to digital systems, the proposed system avoids the need for analog-to-digital conversion and provides more flexible control of performance parameters. Furthermore, with aging and other performance degradation factors, the proposed system offers what is termed "graceful degradation", in contrast to digital systems which exhibit a sharp threshold.

1.2 CHARACTERISTICS OF CATV NETWORKS

1.2.1 CATV HISTORY

The original purpose of cable television was to deliver broadcast signals in areas where they were not received in an acceptable manner with an antenna. These systems were called Community Antenna Television (CATV). The first operators of these systems were TV receiver dealers who sought to expand the market for the sale of their products by also providing the signal required. By the late 1960s, nearly all the areas of the U.S. that could benefit from a community antenna had been served. In the mid-1970s, a new technology gave new life to cable television. Satellite broadcasting added more channels than were available from terrestrial broadcasters. While satellites and earth stations

were very expensive investments, these programming pioneers understood that the cost could be spread over many cable operators who, in turn, could serve many subscribers.

CATV is made possible by the technology of coaxial cable. The principal negatives of coaxial cable are its relatively high loss and limited bandwidth. Coaxial cable signal loss is a function of its diameter, dielectric construction, and frequency of operation. Half-inch-diameter aluminum cable has a typical attenuation value of 1 dB/100 ft; the attenuation drops to 0.59 dB/100 ft, for 1 inch diameter (at frequency of 300 MHz). This limits the distance between amplifiers to at most 2000 feet for 1 inch diameter coaxial cable. Furthermore the attenuation of the cable varies with the square root of the frequency. Thus, the attenuation at 214 MHz (TV channel 13) is twice that of 54 MHz (TV channel 2). This phenomenon limits the usable bandwidth of the cable to $\sim$500 MHz (i.e. a maximum of $\sim$60 NTSC TV channels).

1.2.2 NETWORK TOPOLOGY

Coaxial CATV distribution systems are based mainly on the tree-and-branch architecture [3]. Figure 1.1 shows a typical coaxial cable system topology. Television, FM radio, and other services are processed and/or generated at a master signal processing center (headend). Depending on the size of the system, this headend may transmit signals to several regional centers (hubs). Each of the hubs is connected to one or more "tree-and-branch" coaxial networks. Within the coaxial network, large trunk cables (approximately one inch diameter) and repeater amplifiers carry the signal throughout a service area. Separate branching amplifiers (bridgers) feed the signal to smaller (distribution) cables which carry the signals within the neighborhoods. In-line

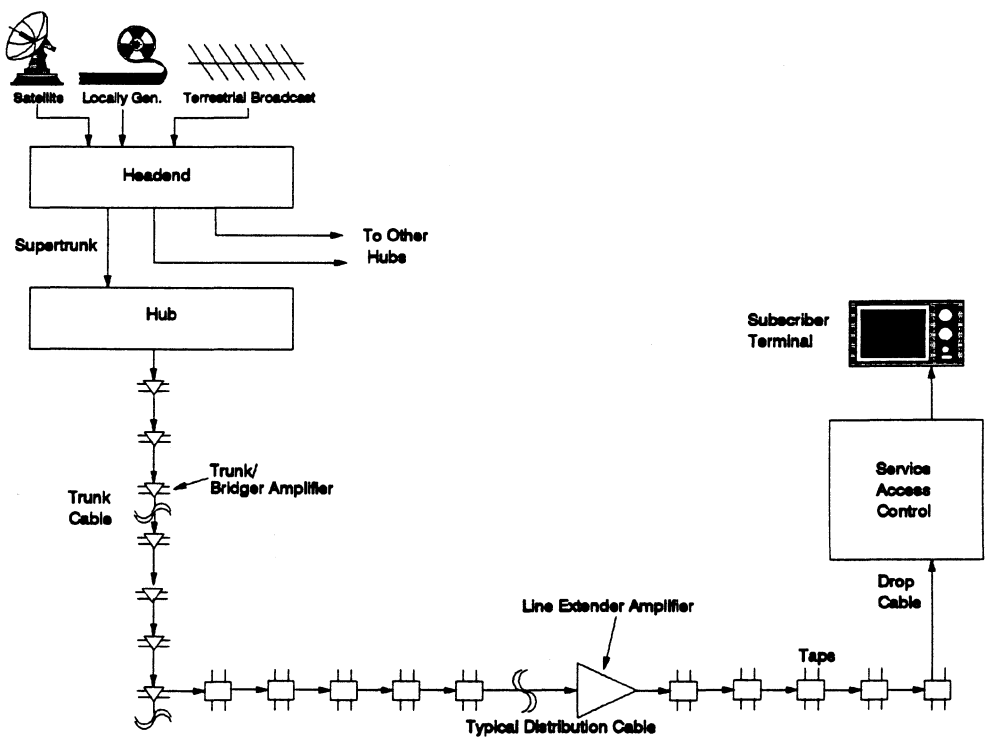

Figure 1.1: Coaxial tree-and-branch system.

directional coupler/splitter assemblies (taps) siphon off a portion of the signal to feed individual homes through small flexible cables (drops). In some cases booster amplifiers (line extenders) are used to increase the number of taps served by an individual bridger output.

1.2.3 PICTURE QUALITY

The ultimate goal of the cable system is to deliver pictures of adequate quality at a reasonable price. Subscriber satisfaction is a complicated function of a variety of factors led by program quality and variety, reliability of service, video and sound quality, and the size of the monthly bill.

The principal picture impairments can be divided into two categories, coherent and non-coherent. Coherent impairments result in a recognizable interfering pattern or picture. They tend to be more objectionable than non-coherent impairments of the same level.

Coherent interference include reflections of the signal from transmission-line impedance discontinuities, and amplifier/cable nonlinearities. Reflections cause picture ghosts, while nonlinearities cause harmonics and cross-modulation, of video carriers. This last phenomenon gives rise to patterns on the screen that are called "beats". Composite triple beat (CTB): is the ratio of the peak carrier to the peak power in the composite third-order intermodulation tone. Composite second order (CSO): is the ratio of the peak carrier to the peak power in the composite second-order intermodulation tone. These patterns often look like moving diagonal bars.

The principal non-coherent picture impairment is random noise. Random noise is the consequence of the statistical nature of the movement of

electric charges in conductors and semiconductors. This creates an added signal of its own. This noise is inescapable yielding a snowy picture, and a seashore-sounding background to audio.

For CATV distribution the target values of S/N is $\simeq$ 45 dB, CSO is $\simeq$ -53 dB, CTB is $\simeq$ -53 dB, and signal level at the television receiver is $\simeq$ 0 dBmV. Visibility of noise and picture impairments depends on the quality of the TV receiver. For an average receiver, picture impairments are not noticeable when the target values are met. For high resolution wide screen-size receivers a better signal quality is needed.

1.2.4 CATV TRADE-OFFS

It is important to balance noise, nonlinear distortions, and cost to a near-optimal balance. Starting at the home, the objective is to deliver at least 0 dBmV but not more than 10 dBmV to the terminal on the television receiver. Lower numbers produce snowy pictures and higher numbers overload the television receiver's tuner. Going back up the plant, a signal level of 10 to 15 dBmV is needed to compensate for losses in the drop cable. This energy diverted to the subscriber is lost from the distribution cable. This loss is called "flat loss" (also called "splitting loss") because it is independent of frequency. Loss in the cable itself is a square root function of frequency in contrast to flat losses. Because of flat loss, relatively high power levels are required in the distribution part of the plant, typically 48 dBmV at the input to the distribution plant. These levels force the amplifiers in the distribution part of the plant to reach into regions of their transfer characteristics that are slightly nonlinear. As a result, only one or two amplifiers, called line extenders, can be cascaded in the distribution part of the plant. These amplifiers are spaced 300

to 900 ft. apart, depending on the number of taps required by the density of homes.

If a design level of noise and nonlinear distortion is assigned at the subscriber's television receiver that is below the threshold of visibility, a budget of noise and distortion can be established to be "spent" in the various parts of the system. The distribution part of the system has relatively high powers and uses up most of the budget for nonlinear distortions. On the other hand, little of the noise budget has been consumed. It can be allocated to the trunk part of the system that brings the signal into the neighborhood.

The design objective of the trunk part of the system is to transmit the signal over substantial distances with minimal degradation. Because distances are substantial, lower-loss cables are used (1 inch or 0.75 inch diameter cable). Since the signal is not repeatedly tapped off in the trunk part of the system, high power levels are not required to feed splitting losses. As a result, signal levels are lower than in the distribution portion of the plant. For the most part, the amplifiers of the trunk are operated within their linear regions. The principal challenge of trunk design is keeping noise under control. It has been determined through analysis and confirmed through experience that the optimum noise performance is obtained when signal is not allowed to be attenuated more than about 20 to 22 dB before being amplified again. Each doubling of the number of amplifiers in the cascade results in a 3 dB decrease in the C/N at the end of the cascade and a 6 dB increase in the amount of CTB. For a trunk with a C/N of 49 dB and CTB of -59 dB the number of cascaded amplifiers is found to be at most ~ 22 amplifiers. Therefore, for a 1 inch diameter cable the maximum length of a trunk section is ~ 8.3 miles.

1.3 OPTICAL-FIBER VIDEO DELIVERY SYSTEMS

Prior to the mid-1980's, most analog lightwave video delivery systems operated in the 0.8-μm region. The large attenuation (~ 5 dB/km) and material dispersion (~ 90 ps/nm-km) in the optical fiber at that wavelength, the severe modal noise problems of multi-mode fiber, and the relatively small bandwidth of early laser diodes, all combined to limit the system capacity. The rapid increase in broadband systems capacity (transporting multi-channel analog/digital video signals, and multi-gigabit/second data) in the late 1980's is largely due to the development of high-speed 1.3-μm InGaAsP laser diodes (10-20 GHz bandwidth), photodetectors (10-20 GHz bandwidth), as well as traveling-wave laser amplifiers. The optical fiber itself has characteristics which are intriguing to most telecommunications system engineers. It has an extremely wide bandwidth, very low loss, small size, light weight, and resistance to electromagnetic interference. Thus there has been recently strong interest in the use of optical fibers in CATV applications.

As indicated in Chapter 2, presently there are three major fiber video modulation schemes, amplitude modulated vestigial sideband/frequency division multiplexed (AM-VSB/FDM), frequency modulated/time division multiplexed (FM/FDM), and pulse code modulation/time division multiplexing (PCM/TDM). The simplest and the most widely used is the AM-VSB/FDM system. The main disadvantage of this scheme is its high sensitivity to nonlinearities which limits the optical modulation index (OMD) of the light source. Thus AM-VSB/FDM systems have very limited S/N, channel capacity, and optical power budget. Since passive optical fiber splitters need very high power budgets [4], present optical-fiber video delivery systems are limited to supertrunk/trunk applications. Digital systems have relatively high power budgets and may be used in optical fiber video delivery,

but their high cost is the main hurdle for CATV applications.

1.4 RESEARCH MOTIVATION

As indicated above, nonlinearity of the laser source is the main limiting factor in achieving large OMD. Efforts at several research and development labs continue to focus on improving linearity of lasers, as well as their relative intensity noise (RIN), (this is a signal-dependent noise phenomenon in lasers which limits their maximum S/N). Sources of nonlinearities and noise have been addressed with processing and structural improvements in the laser chips. In spite of very significant progress, present analog modulation techniques still have limited OMD, consequently limited power budget, and limited S/N.

This dissertation employs a different approach for solving the problem. An alternative modulation/multiplexing scheme which is less sensitive to nonlinearities is presented. The expected behavior of this proposed system is then analyzed. The optimum test for any new system is prototyping, which may involve high cost and a long time. Instead, computer simulations (with the simulation package The Block Oriented Systems Simulator[1] BOSS^{TM}) is used to verify analytical results.

1.5 SCOPE OF RESEARCH

Similar to the frequency modulation/frequency division multiplexing (FM/FDM) system, the proposed system employs frequency modulation to obtain the advantage of the FM improvement factor. But instead of frequency domain multiplexing, time domain multiplexing is used, i.e. frequency modulation/pulse

[1]

amplitude modulation/time division multiplexing (FM/TDM). This eliminates inter-modulation and cross-modulation products, which are associated with FDM systems. Analytical and simulation results (Chapters 4 and 6)indicate that the proposed system has many advantages over existing analog fiber optic systems, not the least its very low sensitivity to nonlinearities. This allow the use of very high optical modulation index resulting in higher power budget, better signal-to-noise ratio, and/or the use of lower cost optical components.

The goals of this research are:

1. to relate the performance of the proposed modulation scheme vis-a-vis existing modulation schemes; i.e., calculate and compare the following:
   a. the nonlinear distortion;
   b. the overall carrier-to-noise ratio;
   c. the detected baseband signal-to-noise ratio;
   d. the optical power budget;
   e. the spectrum efficiency;
2. to simulate the complete proposed system (baseband to baseband) and verify the results whenever applicable with the analytical results;
3. to find from simulations the limits under which the proposed system can operate with acceptable performance;
4. to find the effects of jitter and static phase offset, and determine their limits for acceptable performance.

1.6 APPROACH AND OUTLINE

First the performance of the proposed system is analyzed. Then this performance is compared with the expected performance of two representative

contemporary multi-channel video transmission systems. Typical optical components are used for all systems under consideration. The same optical components are also used for simulations of the proposed system. Simulation results are then used to verify the validity of analysis assumptions.

The following chapter outlines the existing broadband video distribution systems and selects the ones which are used for the comparison. Chapter 3 describes the general idea of the proposed system, and the basis of selecting system parameters. In Chapter 4, laser diode's characteristics are selected, corresponding to those of moderate cost laser, and its parameters are calculated. This laser diode is then utilized in the systems under consideration. Then, spectrum efficiency, power budget, IF carrier-to-noise ratio (C/N), and baseband signal-to-noise ratio (S/N) are estimated for all systems under consideration. Modules used for the simulations, representing optical and electrical components, are described in Chapter 5. Also simulations parameters are calculated and discussed in the same chapter. In Chapter 6 simulation results are presented and compared with analytical results. Jitter and static phase off-set effects on the signal are discussed in Chapter 7. The dissertation ends with conclusions and discussion of further research opportunities.

CHAPTER 2

PRESENT SYSTEMS REVIEW

2.1 SYSTEM CONFIGURATION

The basic configuration of a frequency division multiplexed (FDM) video transmission system is shown in Figure 2.1. A number of subcarrier signals are first multiplexed by using local oscillators (LO's) of different radio frequencies. These signals could be analog baseband, frequency modulated (FM), or pulse code modulated (PCM). The upconverted subcarrier signals are then combined to drive a high speed light source (typically a laser diode). At the receiver site, a user can receive any one of the FDM channels by tuning a local oscillator, and down converting the RF signal to the corresponding signal (baseband, FM, or PCM). Some digital systems use time-division multiplexing (TDM) instead of FDM. FDM systems have an advantage over TDM systems in that services carried by different subcarriers are independent of each other, and require no synchronization. In addition, FDM systems are often more cost-effective than high-capacity TDM lightwave systems. On the other hand, the TDM systems have the advantage of being less sensitive to nonlinear distortions, and pulse regeneration (if PCM is used) could be accomplished without converting the signals to baseband.

In this chapter, noise and degradation factors limiting the overall carrier-to-noise ratio in sub-carrier multiplexed systems are reviewed. Then the most widely used fiber optic broadband video transmission modulation/multiplexing schemes

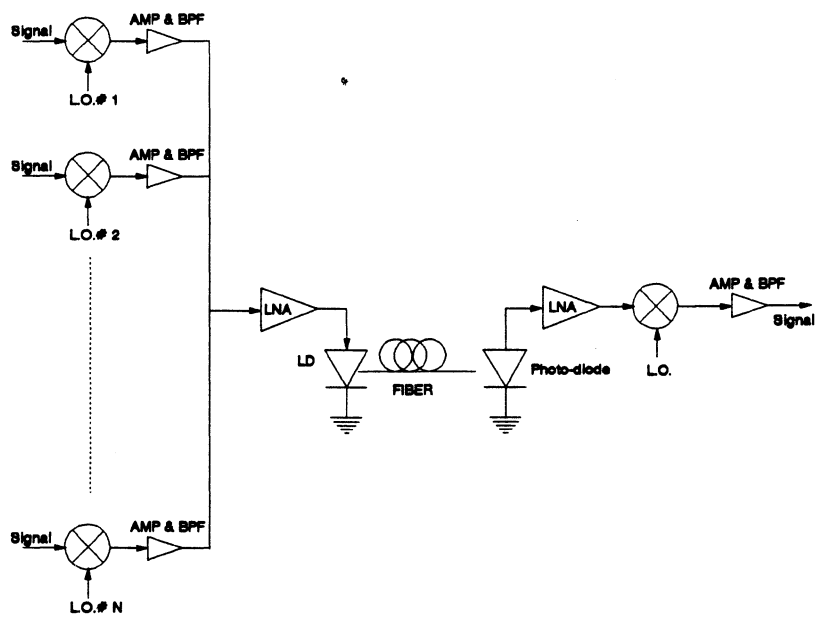

Figure 2.1: Basic FDM video distribution system.

are described.

2.2 IF CARRIER-TO-NOISE RATIO

Several components in an optical fiber system contribute to the overall noise and distortion power. Referring to Figure 2.2, the laser starts by adding nonlinear distortions and intensity noise. The splices and discontinuities in the fiber converts laser phase noise into intensity noise which adds to the intrinsic laser relative intensity noise. The photo-diode does its share by adding shot, dark, and excess noise in the process of converting the optical signal to an electrical signal. Last but not least, the receiver's electronics adds thermal noise. Thus, the overall IF carrier-to-noise at the receiver's output for any subcarrier multiplexed system, $(C/N)^{-1}$ in ratio can be expressed by [5]

$$(C/N)^{-1} = (C/N)^{-1}_{RIN} + (C/N)^{-1}_{shot+dark+excess}$$

$$+ (C/N)^{-1}_{thermal} + (C/N)^{-1}_{NLD} \tag{2.1}$$

where $(C/N)^{-1}_{RIN}$ is the carrier-to-noise ratio limitation caused by the laser relative intensity noise; $(C/N)^{-1}_{shot+dark+excess}$ is the carrier-to-noise ratio limitation caused by shot noise, dark current, and excess noise; $(C/N)^{-1}_{thermal}$ is the carrier-to-noise ratio limitation caused by receiver circuit thermal noise; and $(C/N)^{-1}_{NLD}$ is the carrier-to-noise ratio limitation caused by laser nonlinearities. The level of the received optical power determines which of the noise phenomena are the limiting factors. Systems requiring low C/N are generally limited by thermal noise; systems requiring high C/N are generally limited by either laser

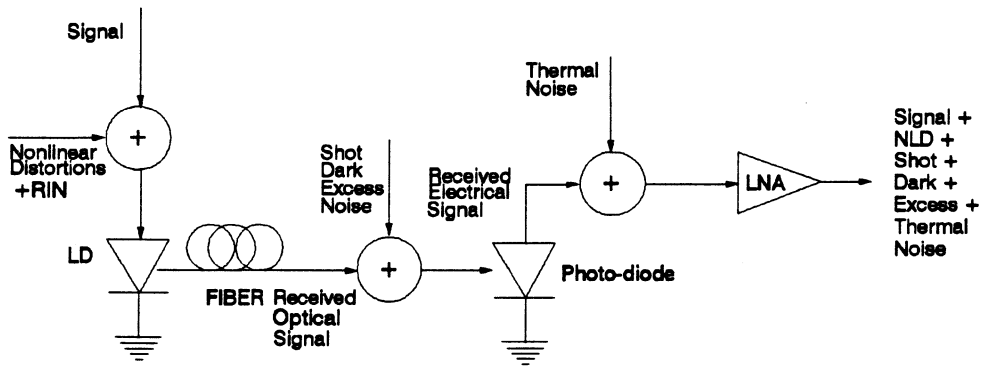

Figure 2.2: Fiber-optic system noise model.

noise or by shot noise. The following sections discuss each limitation in more detail.

2.2.1 INTENSITY NOISE

Intensity noise embedded in a received signal directly degrades the signal quality. Intensity noise is usually specified by a normalized quantity, relative intensity noise (*RIN*) [5], defined as

$$RIN = \frac{\sigma_i^2}{<i>^2}, \tag{2.2}$$

where σ_i is the noise current spectral density in A/Hz, and $<i>$ is the detected dc photo-current in A. The units of *RIN* are Hz^{-1} (or dB/Hz) . The total system intensity noise (RIN_t) is the summation of two terms: intrinsic intensity noise of the laser diode (RIN_i) and extrinsic degradation factors encountered in practical lightwave systems (RIN_e). The following discussion will briefly describe each intensity noise term.

Normally, both Fabry-Perot multi-longitudinal-mode (MLM) lasers and distributed-feedback (DFB) lasers that are free from optical reflection exhibit very low intensity noise. For a laser diode, the intrinsic RIN_i decreases as the bias current increases proportionate to $\frac{1}{(I_b/I_{th} - 1)^3}$, where I_b is the bias current, and I_{th} is the threshold current.

However, in a practical lightwave system, the total system intensity noise may be significantly increased due to reflections from fiber discontinuities (for example, fiber connectors/splices) back into the laser cavity, or by multiple reflections between fiber discontinuities (i.e. extrinsic factors). The extrinsic

degradation factors encountered in a practical lightwave systems may increase the total *RIN* to a level substantially higher than the intrinsic *RIN* of a laser diode (RIN_e). The amount of reflections which can be tolerated depends critically on the degree of coherence of the laser light. In general, the more coherent a laser is, the more sensitive it will be to optical reflections.

The *RIN* is further affected by applying an RF modulating signal. The coherence property of a laser is reduced when the modulating signal power is increased. Therefore, the *RIN* of a laser with external reflections is decreased when the optical modulation depth (*OMD*) is increased. (The *OMD* is defined as $I_{ac}/(I_b - I_{th})$ where I_{ac} is half the peak-to-peak amplitude of the modulating current).

The system total *RIN* is the sum of both intrinsic and extrinsic intensity noise sources, thus

$$RIN_t = RIN_i + RIN_e. \tag{2.3}$$

The total intensity noise in the received signal is proportional to its RF bandwidth. On the other hand the signal power is proportional to the square of the *OMD* (for sinusoidal normalized signals applied to 1Ω load, the received signal power is equal to $OMD^2/2$). Thus the limitation caused by the system relative intensity noise, is given by [5]

$$(C/N)^{-1}_{RIN} = \frac{RIN_t \cdot BW}{\frac{1}{2} OMD^2}, \tag{2.4}$$

where RIN_t is the system's total intensity noise in Hz^{-1}, typical values

are in the range from 1 x 10^{-12} Hz^{-1} to 1 x $10^{-15}Hz^{-1}$ (i.e. from -120 dB/Hz to -150 dB/Hz), and a representative value of -130 dB/Hz is used in the following chapters,

BW is the sub-carrier bandwidth in Hz, and

OMD is the optical modulation depth.

2.2.2 SHOT, DARK, AND EXCESS NOISE

The generation of photo-current is a sequence of discrete events that includes the creation of electron-hole pairs and the motion of these charges under the influence of the local electric field. Each electron-hole pair will result in a pulse of current. The total current is the sum of many pulses. The total current is not a smooth continuous flow, but has variations about an average value. This variation is known as "shot noise". The power density of the shot noise associated with the photo-current is proportional to the received current (I_{ph}), dark current (I_{dark}) (i.e. the reverse saturation current in the diode with no incident light) [6]. The mean square value of the noise is

$$<i_{sh}^2> = 2q.(I_{ph} + I_{dark}).BW, \tag{2.5}$$

where q is the electron charge (1.6 x 10^{-19}C),

I_{ph} is the received photodetector d.c. current (A),

I_{dark} is the photodetector dark current (A), typical value is between 1 and 20 nA

BW is the received signal bandwidth (Hz).

The received signal power is proportional to the photo-diode current, and the OMD. Hence the mean-squared value of the current for a sinusoidal received signal is

$$< i_s^2 > = \frac{1}{2} OMD^2 . I_{ph}^2 \tag{2.6}$$

Therefore, for a *p-i-n* photo-diode (diode with an intrinsic region between the p and n regions), the limitation cased by shot noise and dark current is given by

$$(C/N)^{-1}_{shot+dark} = \frac{2\, q.(I_{ph} + I_{dark}) \, . \, BW}{\frac{1}{2} OMD^2 . I^2_{ph}}, \tag{2.7}$$

Note that for small dark current, *(C/N)* is proportional to the photo-detector current I_{ph} which in turn is proportional to the received optical power. As an example, for *OMD* of 40% and a bandwidth of 40 MHz, the level of the shot noise for a received photo-current of 1 μA is only -38 dBc (dB below carrier), while it is -28 dBc for received photo-current of 100 nA.

An avalanche photo-diode (APD) can produce a "bunch" of electron-hole pairs in response to a primary photon-generated pair [4]. This gain mechanism can help to overcome the limitations of noise added by the preamplifier electronics (thermal noise). However, the number of secondary pairs produced by a given primary pair is only statistically predictable. An APD gain of G means that each primary electron-hole pair produces an average of G secondary pairs via collision ionization. Note that although each primary produces on average G secondary pairs, the actual number of secondary pairs produced by any primary pair is not predictable. As the avalanche gain is increased, the

randomness of the gain mechanism increases the shot noise by a factor which is dependent on the gain. This factor is known as excess noise factor $F(G)$. Thus the limitation caused by shot noise, dark current, and excess noise is given by [5]

$$(C/N)^{-1}_{shot+dark+excess} = \frac{2\,q.(I_{ph} + I_{dark})\,.\,G^2.F(G).\,BW}{\frac{1}{2}\,OMD^2.\,G^2.I^2_{ph}}, \tag{2.8}$$

In the above equation, G appears in both the numerator and the denominator. Thus, increasing G will not improve $(C/N)^{-1}_{shot+dark+excess}$, but on the contrary it may reduce the C/N. That is because increasing G increases the excess noise factor $F(G)$ which decreases the C/N. However, a large received signal may help to overcome the thermal noise generated in the receiver's electronics (see next section). A good APD may have large gain G with a noise excess factor $F(G)$ close to unity ($F(G) > 1$). The opposite is true for a low performance APD.

2.2.3 RECEIVER THERMAL NOISE

The noise added by the receiver's electronics is characterized by a measure called the noise figure (F_e) [4]. The noise figure is the ratio of total noise at the receiver's output to the portion of the output noise due to the intrinsic noise of the signal itself. If the receiver's electronics adds noise which is small compared to the intrinsic noise of the signal, then the noise figure is close to unity. If the noise figure is close to unity, there is little benefit in trying to further reduce the receiver's noise contribution. The equivalent input noise power spectral density $< i^2_{ckt} >$ in W/Hz of a receiver with a 50 Ω front-end preamplifier is given by

$$< i_{ckt}^2 > = \frac{4\ kTF_e}{50}, \tag{2.9}$$

where k is Boltzmann's constant (1.38×10^{-23} J/K), T is temperature in Kelvin. For a typical 50-Ω front-end receiver with a preamplifier noise figure of 1.5 dB, $< i_{ckt}^2 >$ is about 5 x 10^{-22}A^2/Hz. Recent state-of-the-art high impedance GaAs MESFET front-end amplifiers can have about 20 dB lower noise than a 50-Ω front-end receiver with noise figure of 1.5 dB. A regular 50-Ω front-end receiver, with input noise power spectral density equal to 5 x 10^{-22}A^2/Hz, is used in the following chapters. The limitation caused by receiver's circuit thermal noise given by

$$(C/N)^{-1}_{thermal} = \frac{< i^2_{ckt} > \ .\ BW}{\frac{1}{2}\ OMD^2.\ G^2.\ I^2_{ph}}. \tag{2.10}$$

As G increases this term decreases (i.e. $(C/N)_{thermal}$ increases). However, from Equation 2.8, we see that as G is increased from unity the $(C/N)_{shot+dark+excess}$ decreases (because of $F(G)$). As long as the shot and excess noise is smaller than thermal noise, increasing the gain G will increase the overall C/N. Beyond this, further increase in G may decrease the overall carrier-to-noise ratio. At this point, the C/N is limited by shot and excess noise rather than thermal noise. Therefore, there is an optimum value for the gain G to reach the highest overall C/N possible.

For FM subcarrier multiplexed systems the carrier-to-noise limitation imposed by the thermal noise should be less than ~ -20 dBc. For a 50 Ω front-end receiver with thermal noise power density equal to 5 x 10^{-22}A^2/Hz, and a *p-i-n* diode receiver ($G = 1$ & $F(G) = 1$), the minimum received photo-

current should be at least 10 μA to establish a $C/N = 20$ dB (assuming that *OMD* is 40% and the IF bandwidth is 40 MHz). If the responsivity of the photo-diode is 0.5 A/W, then the minimum optical power needed at the receiver is ~ 20 μW. If the optical power launched into the fiber is 1 mW, then the optical power budget is about 17 dB. For a fiber with attenuation of 0.5 dB/km (this includes connectors and splices loss), the maximum link span is ~ 35 km. For AM-VSB systems (see next section for details), baseband signal-to-noise (*S/N*) is the same as IF carrier-to-noise (*C/N*), thus, minimum *C/N* should be as high as the required *S/N*. To meet *S/N* CATV target values, *C/N* should be at least 45 dB or better. Furthermore, *OMD* can not be as high as in an FM system due to the limitations of the intermodulation products (composite triple beats and composite second order). This combination of high *C/N* and low *OMD* limits the power budget of the AM-VSB to values between 5 to 10 dB. Satisfactory operation of digital systems requires *C/N* of about 16 dB. Thus, the thermal noise limitation gives a power budget of the order of ~ 20 dB (similar to the FM subcarrier systems). Furthermore, the *OMD* is not limited by coherent distortions as in the two previous cases. Thus, the *OMD* could be nearly as high as 100%. The combination of low *C/N* with high *OMD* gives a very large optical power budget for digital systems (~ 10 dB more than for FM subcarrier systems).

2.2.4 NONLINEAR DISTORTIONS

Nonlinearities result in two types of distortion [5]:

- *Harmonics and Inter-modulation Distortions (IMD)*: For multi-channel signal transmission through a nonlinear device such as a laser diode, second

order IMD ($A-B$ or $A+B$ type, where A and B stand for two arbitrary RF frequencies) are the dominant second order nonlinear distortions. Composite triple beat products (especially $A+B-C$ type, which fall within the signal band) are the dominant third order nonlinear distortions. The number of two-tone third order IMPs is proportional to N^2, where N is the number of channels, while the number of triple beat products is proportional to $N^3/2$. Therefore, triple beat nonlinear products tend to be the dominant nonlinear distortion for large numbers of channels. For RF and microwave signals occupying a bandwidth of more than one octave, the second order nonlinear distortions must be taken into account. Otherwise, only third order nonlinear distortions have to be considered.

- *Cross Modulation:* Cross modulation is the transfer of modulation energy from one or more carriers to another in a multi-channel system; it occurs as a result of the triple beat [7]. Cross modulation distorts the modulated signal itself. Thus it can't be reduced by filtering.

The nonlinear distortion limitation caused by laser's nonlinearities is given by [5]

$$(C/N)^{-1}_{NLD} = \frac{\sigma^2_{NLD}\, BW}{\frac{1}{2}\, OMD^2.\ G^2.\ I^2_{ph}} \tag{2.11}$$

where σ^2_{NLD} is the nonlinear distortion spectral noise density (A^2/Hz). The nonlinear distortion current density σ_{NLD} is proportional to OMD^2 for second order distortion and OMD^3 for third order distortion. Nonlinear distortion generates a coherent type distortion (see Section 1.2.3). As indicated previously, the human eye is more sensitive to coherent distortion than to random noise. Therefore $(C/N)_{NLD}$ should be limited to 53 dB or less. On the

other hand, σ^2_{NLD} is a function of both the *OMD* and the number of channels. Thus, the limiting factor for both *OMD* and the number of channels in a typical analog system (FM or AM-VSB) tends to be nonlinear distortion. Because the $(C/N)_{NLD}$ requirements are considerably more stringent than the carrier-to-noise requirement, *NLD* may be neglected in calculating overall *C/N*. A more detailed discussion of nonlinear distortions is presented in Chapter 5.

2.3 PRESENT BROADBAND DISTRIBUTION SYSTEMS

Present video distribution systems fill into two main categories: analog and digital. There are many different analog schemes as well as digital schemes. The most widely used modulation/multiplexing schemes are described below.

2.3.1 ANALOG SYSTEMS

Most analog transmission systems use frequency-division multiplexing (FDM), to combine the subcarrier signals into an RF signal as shown in Fig 2.1. The subcarrier may be straight amplitude modulated or frequency modulated.

2.3.1.1 Amplitude modulated vestigial sideband/frequency-division multiplexed (AM-VSB/FDM)

AM-VSB/FDM has many advantages, not the least of which is its compatibility with present CATV multiplexing methods. The input for an AM-VSB/FDM link is simply the broadband signal consisting of AM-VSB channels. They occupy the range from 50 to 550 MHz, each channel occupying 6 MHz. The principal disadvantage of this scheme is its high sensitivity to

nonlinearities and noise. Furthermore, the baseband signal-to-noise ratio (S/N) is equal to the received carrier-to-noise ratio (C/N). Therefore requirements for linearity and relative intensity noise (RIN) of the light source are very stringent [5]. Furthermore, as mentioned in Section 2.2.1, RIN of any optical-fiber system is a function of splice reflections and fiber discontinuities. Therefore, AM systems may also entail higher construction/maintenance care than FM/FDM or PCM/TDM counterparts. There is considerable research and development effort directed towards optical sources and equalization techniques suitable for AM-VSB/FDM [8 – 13]. In spite of technical progress reported from various manufacturers, detected Signal-to-Noise ratio (S/N) is limited to only ~ 45-55 dB, with optical power budget of merely ~ 5-10 dB [4],[12]. These limitation not withstanding, AM-VSB/FDM systems are currently used widely in CATV trunking applications.

2.3.1.2 Frequency modulated/frequency-division multiplexed (FM/FDM)

Frequency modulation is applied first to the baseband TV signal resulting in an intermediate frequency (IF) bandwidth of ~ 36 MHz/channel. In exchange for the wider bandwidth, a considerable S/N improvement factor is gained. As long as the input C/N is larger than a threshold value (typically 10 dB), the FM improvement factor can be calculated from the following equation [14]

$$\left(\frac{S}{N}\right)_W = \frac{C}{N} + 1.76 + 10\log\left(\frac{B_{IF}}{B_{BB}}\right) + 20\log\left(\frac{\Delta f}{B_{BB}}\right) + P + Q \qquad (2.12)$$

where $\left(\frac{S}{N}\right)_W$ is the weighted signal-to-noise ratio of the demodulated signal

in dB,

$(\frac{C}{N})$ is the carrier-to-noise ratio in dB,

B_{IF} is the IF bandwidth in Hz,

B_{BB} is the baseband bandwidth in Hz,

Δf is the peak frequency deviation in Hz,

P is the improvement factor due to preemphasis, and

Q is a weighting factor to account for the non-uniform response of the eye to white noise in the video bandwidth. ($P+Q$=18 $\sim$ 26, a value of 23 dB is selected [15]).

If the TV baseband frequency is assumed to be 4.2 MHz and the IF bandwidth is $\sim$ 36 MHz, then by using Carson's rule the FM peak frequency deviation Δf is $\sim$ 13.7 MHz. From the above equation the FM improvement factor is $\sim$ 39.2 dB. Therefore the minimum carrier-to-noise ratio (C/N) needed to meet the studio quality transmission standard (weighted baseband S/N = 56 dB) is $\sim$ 16.8 dB. Studio quality transmissions with higher power budgets and larger numbers of channels than AM-VSB/FDM systems have been reported [16-19]. However, the need for an FM modulator/demodulator at both transmitter and receiver and the additional FDM equipment makes this a more expensive alternative than AM systems. To date FM/FDM systems are used only in super trunks where high quality transmission is needed over extended distances.

2.3.2 DIGITAL SYSTEMS

Pulse code modulated/time-division multiplexed (PCM/TDM) transmission has the advantage of offering high transmission quality over literally unlimited distances, as its binary codes can be recovered and regenerated as needed. The most commonly used modulation methods in

optical systems are on-off-keying (OOK). In subcarrier multiplexed systems frequency-shift-keyed (FSK) is often used. In theory, both OOK and FSK need ~ 15.5 dB C/N, to reach a bit error rate of 10^{-9}. In practice the required C/N is somewhat greater than the theoretical value because of inter-symbol interference and other degradation factors [18].

In PCM, the information to be transmitted is contained in the coded waveform. However, in order to encode a continuous signal it must be sampled and then quantized to a finite number of discrete amplitude levels. Once quantized, the instantaneous values of the continuous signal can never be reconstructed exactly. The random error is called quantization noise ($\overline{\epsilon^2}$). It can be reduced to any desired degree by increasing the number, and distribution, of quantizing levels. Furthermore, noise added in the transmission may cause errors in recognition of the message sent. These code errors will introduce additional noise to the demodulated signal ($\overline{n^2}$). But if the signal pulses are received above a certain C/N threshold, the average error rate can be kept very low, and the dominant noise in such a case is the quantization noise [20-21].

To calculate the mean-square quantization noise, we assume equal amplitude increments between levels. Specifically, let the input signal be quantized into q levels, each spaced by an amplitude increment, a Volts. If the signal amplitude is assumed to be bipolar with average value zero (no dc off-set), the quantizing levels are $\pm a/2$, $\pm 3a/2$, $\pm 5a/3$,. . . . $\pm qa/2$. (For binary PCM, q should be an integer power of two). The quantizing error ϵ is the difference between the signal level and the nearest allowed quantizing level. If all the values of ϵ are equally likely anywhere in the range $-a/2 \leq \epsilon \leq a/2$, then the mean-square quantization noise is given by

$$\bar{\epsilon^2} = \frac{a^2}{12} \text{ Watts.} \tag{2.13}$$

Other noise sources, such as thermal noise, shot noise, intensity noise etc., contribute to code errors, which add to the baseband demodulated noise. The mean-square noise per code word caused by the errors is found to be proportional to the probability that a given bit is in error, P_e, and to the square of the peak-to-peak amplitude range. It is given by [21]

$$\bar{n^2} = \frac{P_e\ (q^2 - 1)\ a^2}{3}, \text{ Watts} \tag{2.14}$$

where the code probability of error P_e is dependent on the input C/N. If $x = \sqrt{C/2N}$, then $P_e = Q(x) = \int_x^\infty \frac{1}{\sqrt{2\pi}}\ e^{-z^2/2}\ dz \simeq \frac{1}{\sqrt{2\pi}\ x}\ e^{-x^2/2}$, for x $\gg 1$ [29]. Because the peak signal magnitude is $qa/2$, then the unweighted S/N is

$$(S/N)_{PCM} = \frac{\text{Signal power}}{\text{Noise power}} = \frac{(qa/2)^2}{\bar{\epsilon^2} + \bar{n^2}} \tag{2.15}$$

Substituting Equations 13 and 14 in Equation 15 we get an expression for the output S/N in terms of the input C/N. Expressed in decibels, the weighted S/N becomes

$$(S/N)_{PCM_{(dB)}} = 10log\left(\frac{3(q^2 - 1)}{1 + 4(q^2 - 1)\frac{1}{\sqrt{2\pi C/2N}}\ e^{-(C/4N)}}\right) + W \tag{2.16}$$

where W is the weighting factor (let $W = \sim 8$ dB [22]). Weighted baseband S/N as a function of the C/N for both FM and PCM are shown in Figure 2.3. The

PCM system has a better performance for the range of input C/N from 15 to 16 dB. For higher received C/N, the detected S/N for the FM system is better than S/N for the PCM system where the performance is limited mainly by quantization errors.

A typical digital video system with: 256 levels of linear quantization; a bit rate of 85.9 Mbit/s (8 bit/sample with $f_s = 3$ x color subcarrier); IF bandwidth of 42.95 MHz; and with input $C/N \geq$ 16 dB, has a weighted S/N of $\sim$ 55 dB [23].

PCM/TDM is an obvious approach to video distribution systems. But since the cost of terminal equipment is presently high, and code regeneration is not essential for short distances (and also extremely expensive), video digital transmission currently is used more in long haul links.

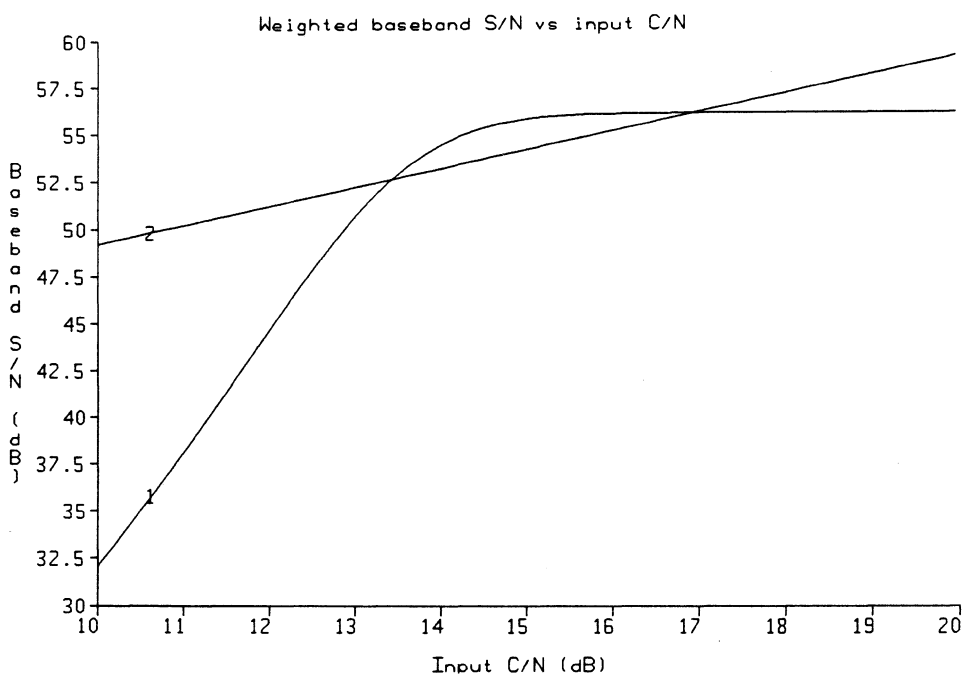

Figure 2.3 : Weighted baseband signal-to-noise vs input carrier-to-noise in dB

1) for PCM 2) for FM.

CHAPTER 3

PROPOSED SYSTEM

3.1 INTRODUCTION

It is generally desirable to achieve a large power budget and high S/N in lightwave video distribution networks. This means that the laser should be modulated with a large *OMD*, but this results in non-linear distortion in analog modulation systems. Although FM/FDM systems are less sensitive to this distortion than AM-VSB/FDM systems, non-linear distortion still limits the performance of these systems. Digital systems are less sensitive to nonlinear distortion than FM/FDM systems, but since the cost of terminal equipment is presently very high, and code regeneration is not essential for short distances, video digital transmission currently is used more in long haul links.

In this chapter an alternative analog modulation / multiplexing scheme less sensitive to non-linearities is described. The spectrum of the proposed system is discussed when only two tones are applied to the baseband. From that, the expected spectrum is estimated when an NTSC TV signal is transmitted on the system. Finally, suitable parameters for the proposed system are selected, to be used for the analysis and simulation in the following chapters.

3.2 SYSTEM DESCRIPTION

3.2.1 TRANSMITTER

Referring to Figure 3.1, frequency modulation (FM) is applied first to each baseband TV signal to spread its spectrum. As shown in Equation 2.1, in exchange for a wide bandwidth, a considerable signal-to-noise improvement factor is gained. The FM signal bandwidth is first limited with a bandpass filter (BPF), it is then sampled at the minimum subNyquist rate (i.e. the sampling rate f_s is twice the IF bandwidth B_{IF}). It is essential to limit the IF signal bandwidth to at most half the sampling frequency, otherwise aliasing may degrade the signal quality. The N sample trains (where N is the number of channels) are then combined by using time division multiplexing (TDM). The combined pulse stream is then shaped and applied to the light source. The selection of the FM carrier frequency, the sampling rate and the IF bandwidth is discussed later in Section 3.3.

3.2.2 RECEIVER

For CATV applications there could be two types of receivers:

3.2.2.1 Hub-Point Receiver

This type of receiver could be used for hub distribution points, where all channels should be available for further distribution with coaxial cables. As shown in Figure 3.2, the front end of the receiver consists of a photo-detector and a Nyquist filter, followed by a full "time domain demultiplexer" and a bank of BPFs and FM demodulators. A block diagram of this type of

receiver is shown in Figure 3.2.

3.2.2.2 Single-Channel Receiver

A single-channel receiver could be integrated with the "Set-Top Convertor Box" in the subscriber's premises when a "Fiber To The Home" network is used. As shown in Figure 3.3, the front end consists of a photo-detector and a Nyquist filter. The timing circuit might be simply a notch filter tuned to a harmonic of the sample repetition rate (the sample repetition rate = Nxf_s. The timing signal is then applied to an N counter. In this counter, the input rate is divided by N, the output is a trigger signal with frequency equal to f_s (i.e. the sampling frequency of a single channel). For a simpler receiver circuit, the sampling frequency f_s may be sent to the receiver on a separate channel. A user can select any particular channel by applying a time delay between 0 and T_s seconds (with respect to the framing signal) to this trigger signal in increments of T_s/N seconds. The time gate circuitry should pass only the samples indicated by the delayed trigger signal. The gated samples are then filtered and frequency demodulated to recover the baseband TV signal.

3.3 SPECTRUM OF THE SAMPLED SIGNAL

The spectrum of the i_{th} channel flat top sampled signal (rectangular samples) can be represented by [5]

$$V_i(f) = \frac{\tau}{T_s}\left[\sum_{k=-\infty}^{\infty} Y_i(f\text{-}kf_s)\right] sinc\left(\frac{\tau\omega}{2}\right), \tag{3.1}$$

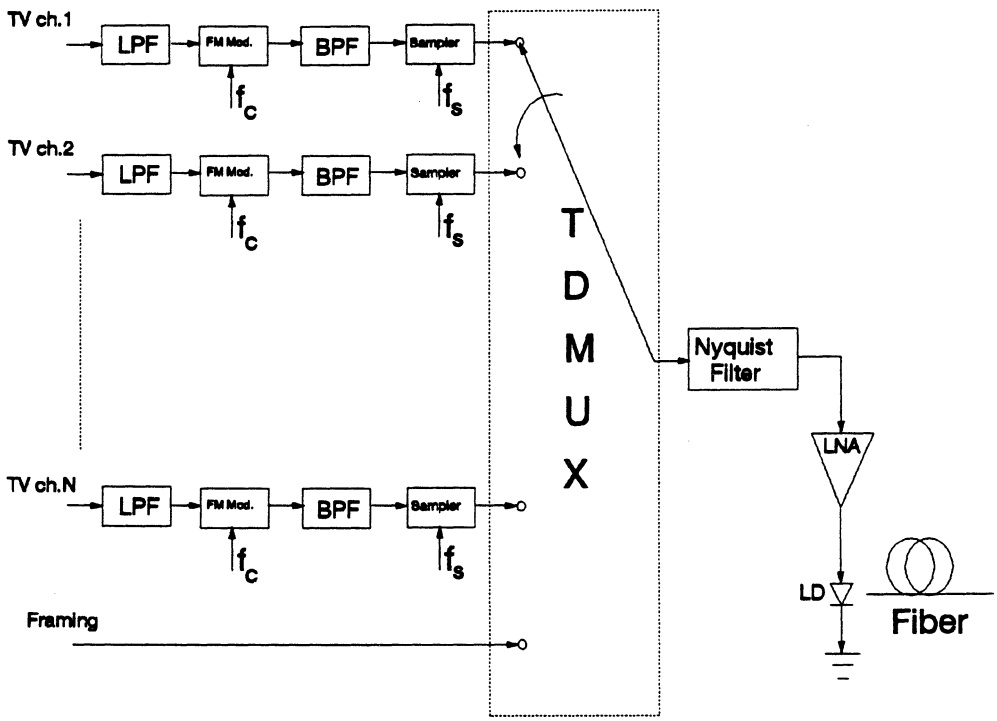

Figure 3.1: Transmitter block diagram.

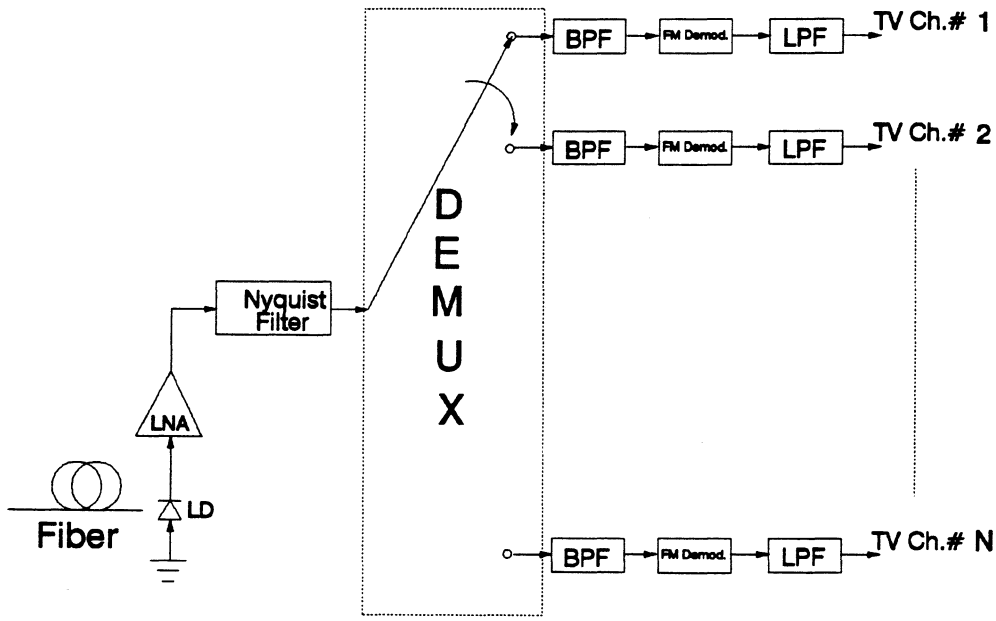

Figure 3.2: Hub-Point receiver block diagram.

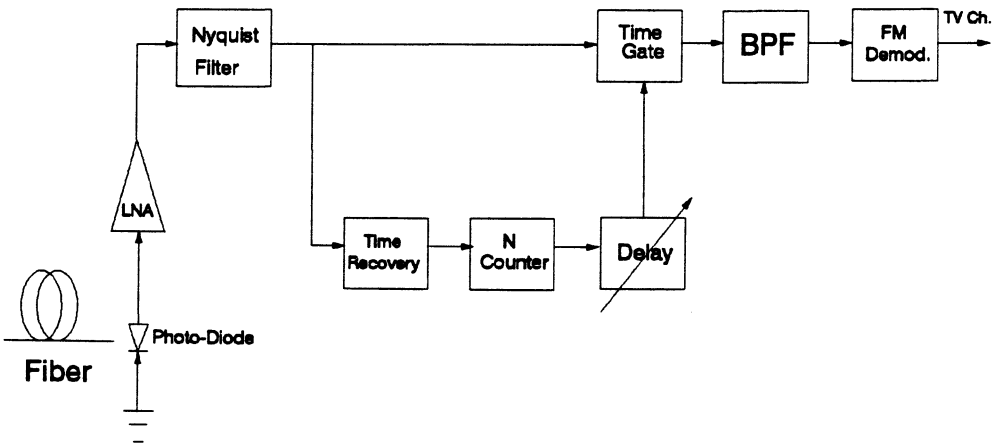

Figure 3.3: Single channel receiver block diagram.

where $Y_i(f)$ is the spectrum of the i_{th} FM channel,

τ is the width of the sample in seconds,

$T_s = \frac{1}{f_s}$ in seconds,

$sinc(x) = sin(x)/x$ is the aperture effect (flat top samples).

For 60 channels with sampling frequency $f_s = 71.6$ MHz, $T_s \simeq 14$ nanoseconds, and $\tau \simeq 233$ picosecond. For the case in which the baseband signal is a single sinusoidal tone, the FM amplitude spectrum $Y_i(f)$ is given by [6]

$$
\begin{aligned}
Y_i(f) = A\,\frac{J_0(\beta)}{2}\,[\delta(f+f_c)+\delta(f-f_c)] \\
+\ \frac{A}{2}\sum_{k=0}^{\infty} J_{2k}(\beta)\{[\delta(f-[f_c-2kf_m])+\delta(f+[f_c-2kf_m])] \\
+[\delta(f-[f_c+2kf_m])+\delta(f+[f_c+2kf_m])]\} \\
+\ \frac{A}{2}\sum_{k=0}^{\infty} J_{2k\text{-}1}(\beta)\{[\delta(f-[f_c-(2k-1)f_m])+\delta(f+[f_c-(2k-1)f_m])] \\
-[\delta(f-[f_c+(2k-1)f_m])+\delta(f+[f_c+(2k-1)f_m])]\}\ \text{Volts} \qquad (3.2)
\end{aligned}
$$

where $J_k(\beta)$ is the k^{th} order Bessel function,

β is the FM modulation index $= \frac{A_m \Delta f}{f_m}$,

Δf is the peak-to-peak frequency deviation in Hz/V,

A_m is the amplitude of the modulating frequency in V, and

f_m is the frequency of the modulating signal in Hz.

The power spectrum of such a signal is shown in Figure 3.4 with $f_m = 1.12$ MHz, Δf=13.8 MHz/V, and A_m=1 V. It can be observed that the spectrum of the sampled FM with sinusoidal modulating frequency consists of a residual carrier and

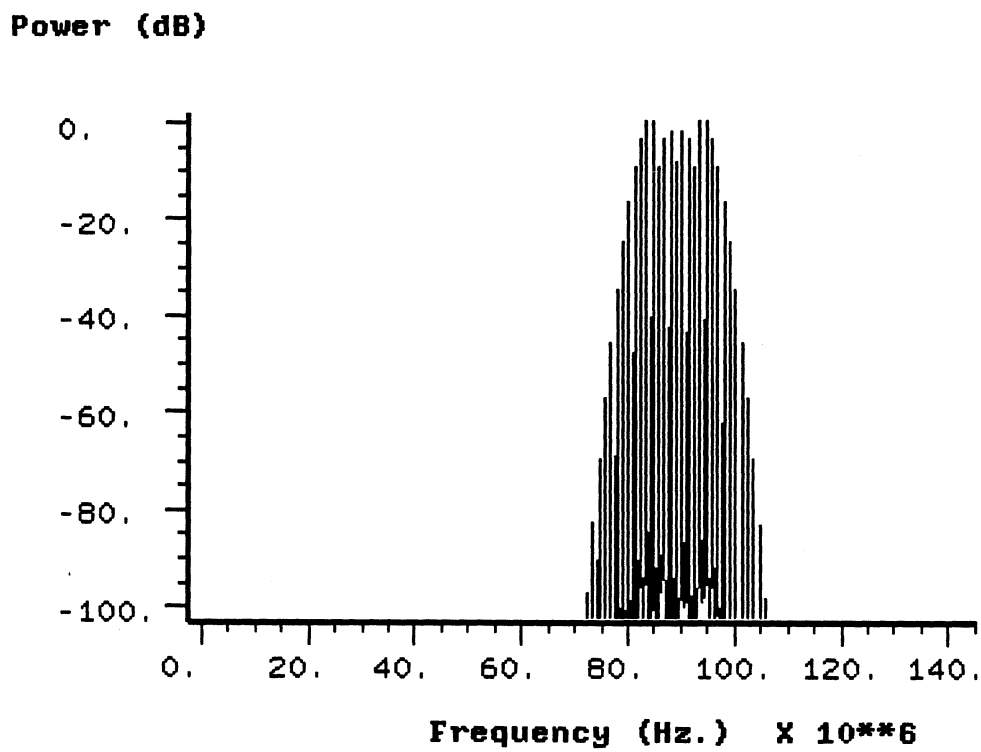

Figure 3.4: Spectrum of a single FM channel with a sinusoidal modulating frequency.

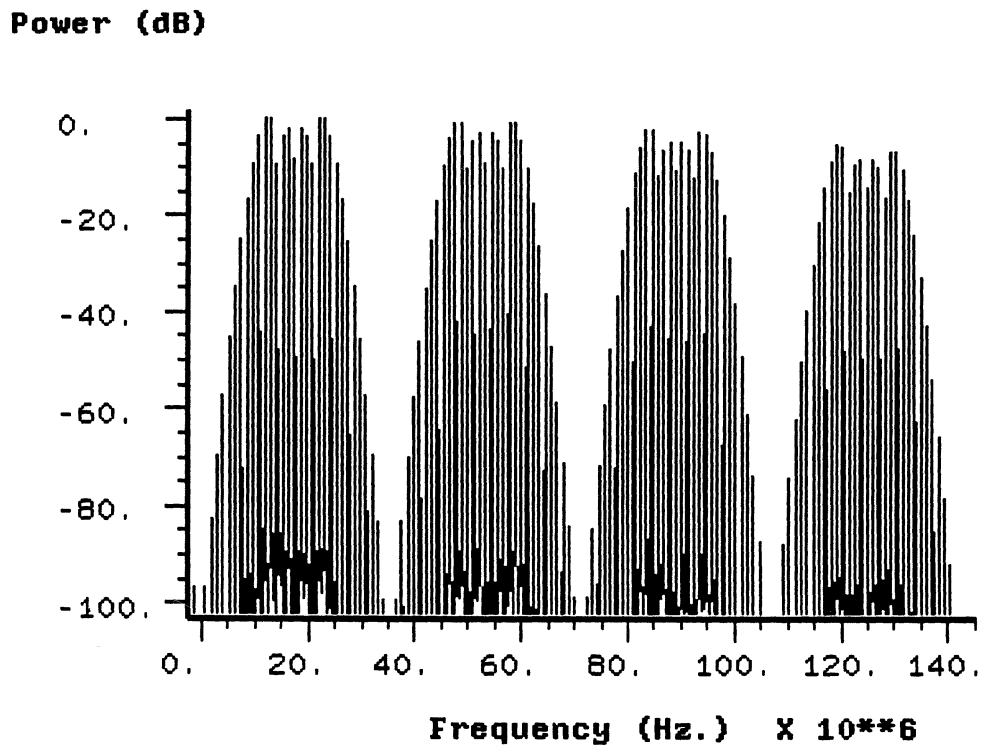

Figure 3.5 : Spectrum of the sampled FM with a sinusoidal modulating frequency.

an infinite number of even-order and odd-order harmonics in the upper and the lower side bands. Figure 3.5 shows the spectrum of the sampled FM signal. This spectrum exhibits the side bands owing to the frequency modulation and the periodicity resulting from sampling (explained more in Figure 3.6).

3.4 PARAMETER SELECTION

In this section, parameter values for the proposed system are chosen. The three parameters, the FM carrier frequency f_c, the FM signal bandwidth B_{IF} (hence the modulation index β), and the sampling frequency f_s, are related to each other. On the other hand each one of them should satisfy certain conditions. These conditions and the selection process is explained in this section. There are many values which could be chosen to fit a particular application. Values selected here are meant to be close to presently used video transmission systems. They will be used later in Chapter 4 for system performance evaluation.

3.4.1 FM CARRIER FREQUENCY

To avoid nonlinear distortion in the FM modulator/demodulator, the FM carrier frequency f_c should satisfy the following relationship:

$$f_c \geq \frac{3 \cdot B_{IF}}{2}, \tag{3.3}$$

where B_{IF} if the FM signal bandwidth. If f_c is less than $\frac{3 \cdot B_{IF}}{2}$, then the second order products will lie within the FM bandwidth, resulting in distortion.

3.4.2 SAMPLING FREQUENCY

From the sampling theorem, it is known that a sampling rate of $f_S \geq 2B$ is always sufficient to avoid spectral overlap (aliasing). For a band limited signal with a bandwidth $B = f_{max} - f_{min}$ Hz, the minimum sampling rate may be less than twice the highest frequency f_{max}. As illustrated in Figure 3.6.*a* and 3.6.*b* a baseband signal with $f_{max} = B$ Hz and $f_{min} = 0$ Hz, a sampling frequency $f_s = 2f_{max} = 2B$ Hz is the minimum rate to avoid aliasing. As f_{max} increases to $1.5B$ (3.6.*c*), the minimum rate is still $f_S = 2f_{max} = 3B$ Hz (3.6.*d*). Finally, as f_{max} approaches $2B$, the required sampling rate will approach $2f_{max}$ or $4B$, as can be deduced from Figure 3.6.*d*. However, when f_m reaches $2B$ (3.6.*e*), a clear frequency slot of width B, from 0 to B, exists where the lower side of the image around $+f_S$ could be placed; likewise, from 0 to $-B$ for the lower sideband of the image around $-f_S$, a rate of only $2B$ is necessary (part *f*). In general, each time f_{max} attains an integer multiple of B, (for example, $f_{max} = \nu B$, where $\nu = 1,2,3...$), the passband B will lie between $(\nu - 1)B$ and νB, and the required sampling rate will drop to $2B$. For the case when

$$f_{max} = f_c + \frac{B_{IF}}{2} = \nu B_{IF}, \tag{3.4}$$

then

$$f_S = 2B. \tag{3.5}$$

As shown in Section 3.2, the frequency spectrum of a sampled FM

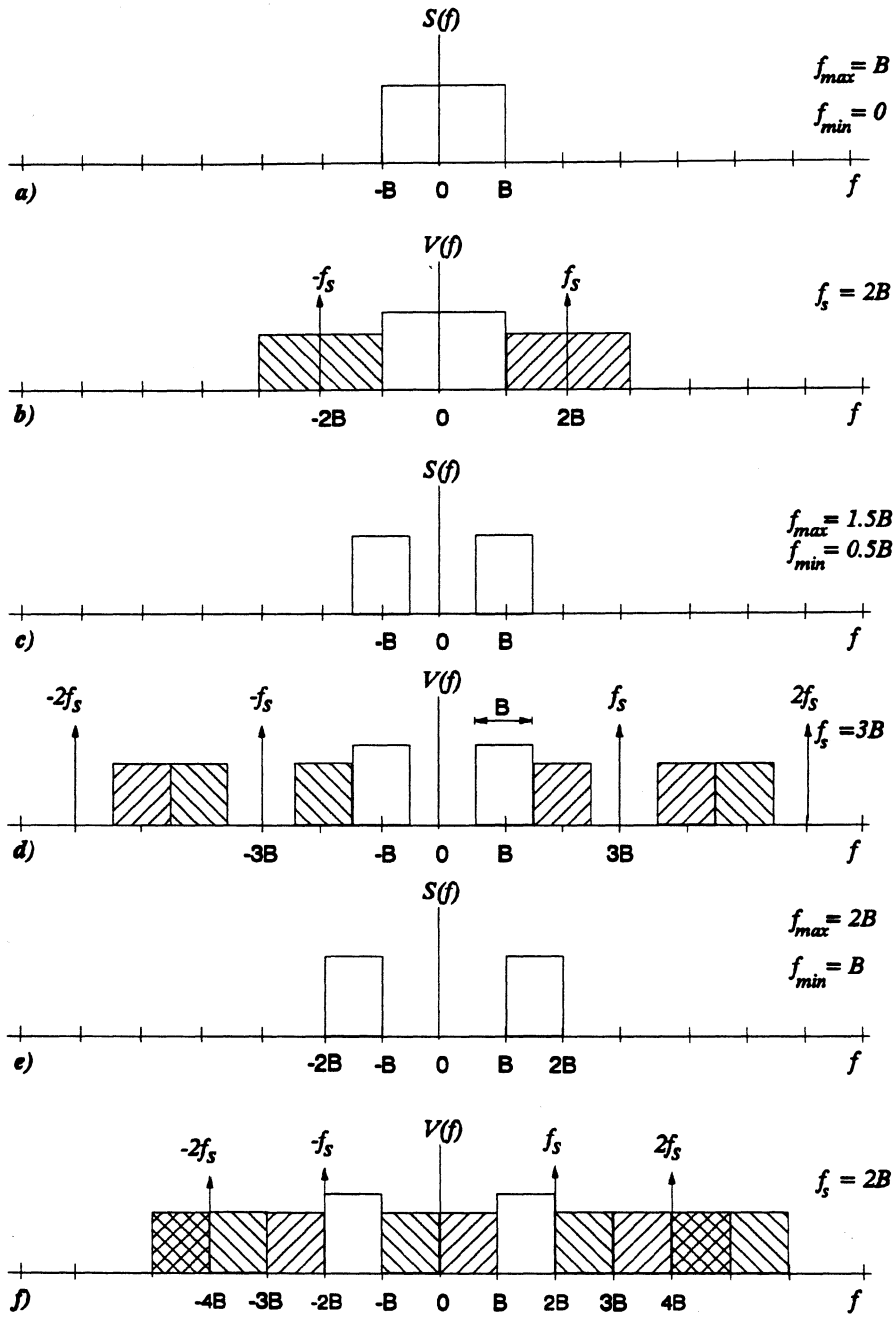

Figure 3.6: Strictly band-limited spectra *S(f)* for various values of highest frequency f_{max}, lowest frequency f_{min} and associated sampled spectra *V(f)*.

signal, with a sinusoidal modulating frequency, is a discrete periodic spectrum. The frequency spectrum of a typical NTSC TV signal consists of harmonics of the line frequency and the color subcarrier frequency [6]. Therefore the spectrum of the FM signal with an NTSC TV modulating signal consists of a residual carrier and harmonics of the line frequency and the color subcarrier and their cross terms, similar to the spectrum shown in Figure 3.6 but with smaller intervals between harmonics. Thus, the NTSC TV FM signal consists of a residual carrier and harmonics separated by a distance $f_l/2$, where f_l is the line frequency. As indicated, the spectrum of the sampled FM signal is periodic, with a period equal to that of the original FM signal bandwidth.

When such a periodic spectrum is passed through a non-linearity, nonlinear distortion is added to the signal. Memoryless nonlinearity of the laser may be modeled by a power series given by

$$P_o(t) = a_o + a_1.i(t) + a_2.i^2(t) + a_3.i^3(t) + ..., \tag{3.6}$$

where P_O is the output optical power, a_o, a_1, a_2, a_3, .. are the coefficient of the power series. The desired signal is $a_1.i(t)$, while second, and third order nonlinear distortion results from the terms $a_2.i^2(t)$ and $a_3.i^3(t)$ respectively. From the Fourier theorem, multiplication in the time domain is equivalent to convolution in the frequency domain (and vice-versa). Therefore, the spectrum of the second order of such a periodic signals may be estimated by the periodic convolution (a form of convolution for periodic signals with equal periods) of the periodic spectrum $V_i(f)$ by itself (multiplied by the nonlinearity coefficient a_2'). The result of such a convolution is a periodic

signal $D2_i(f)$ with the same period as the original signal. Hence

$$D2_i(f) = a_2' \cdot (V_i(f) \otimes V_i(f)), \tag{3.7}$$

where $\otimes$ denotes a periodic convolution operation and a_2' is the second order nonlinearity coefficient (filtering may reduce second order distortion, thus a_2' $\leq a_2$). The third order distortion $D3_i(f)$ is the periodic convolution of the second order distortion sequence by the original periodic signal spectrum $V_i(f)$, hence

$$D3_i(f) = \frac{a_3'}{a_2'} (D2_i(f) \otimes V_i(f)) = a_3' (V_i(f) \otimes V_i(f) \otimes V_i(f)) \tag{3.8}$$

where a_3' is the third order nonlinearity coefficient (similarly $a_3' \leq a_3$). If the sampling frequency f_s and bandwidth of the FM signal are integer multiples of the separation between harmonic components, then second and third order distortion harmonics will have exactly the same frequencies as the original undistorted sampled signal. Figure 3.7 shows an example where the sampling frequency is not an integer multiple of the baseband modulating frequency. It is seen that second and third order distortions introduce tones between the original frequency components. Figure 3.8 shows an example where the sampling frequency is an integer multiple of the baseband modulating frequency. Here the second and third distortion components lie exactly on the original frequency components. The same analogy may be applied to the NTSC TV signal, the spectrum components of the chrominance signal are precisely interleaved among the components of the luminance spectrum. If this signal is sampled with a rate which is not an integer multiple of both

components, the nonlinear distortions will then introduce interfering component to each side of the chrominance components. Because these two interfering components could be very close to the original subcarrier component, they may phase modulate the color subcarrier component which may result in color distortion. The overlap between original and interfering components eliminates phase distortion. This may reduce differential gain and differential phase (i.e. inter-modulation/cross-modulation between luminance and chrominance signals). Hence we conclude that the sampling frequency and the FM bandwidth should be an integer multiple of the line frequency and the color subcarrier.

3.4.3 IF BANDWIDTH

As indicated, for a band limited signal with a bandwidth $B = f_{max} - f_{min}$ the minimum sampling rate can be less than twice the highest frequency f_{max}. For the case when $f_{max} = f_c + \frac{B_{IF}}{2} = \nu B_{IF}$, then

$$B_{IF} = (\frac{2}{2\nu - 1})f_c. \tag{3.9}$$

Meanwhile, to avoid aliasing B_{IF} should be strictly band limited, and it should satisfy the following

$$B_{IF} = f_s/2. \tag{3.10}$$

In summary, three conditions should be met:

- Sampling frequency should be integer multiple of both the line frequency and the color subcarrier frequency.

- I.F. carrier frequency f_c should be selected such that, the upper edge frequency is an integer multiple of the bandwidth.
- Bandwidth of the I.F. signal should be selected to be exactly half the sampling frequency.

For an NTSC TV system, the ratio between the line frequency f_l and the color subcarrier f_{sc} is

$$\frac{f_{sc}}{f_l} = \frac{3579545}{15734.264} = \frac{455}{2}, \text{ i.e. } 2\, f_{sc} = 455\, f_l = K. \tag{3.11}$$

Therefore, a suitable value for the sampling frequency is: $f_s = 10$ x K $= 20$ x $f_{sc} = 4550$ x $f_l = 71.5909$ MHz $\simeq 71.6$ MHz. According to the preceding conditions the following values are calculated:

f_c(I.F. center frequency) $= 89.488625$ MHz $\simeq$ 89.5 MHz

B_{IF}(I.F. FM bandwidth) $= 35.79545$ MHz $\simeq$ 35.8 MHz

If the TV baseband frequency is assumed to be 4.2 MHz, then by using Carson's rule the FM peak frequency deviation Δf is ~ 13.7 MHz. From Equation 2.12 the FM improvement factor is ~ 39.2 dB. Therefore the minimum Carrier-to-Noise ratio (C/N) needed to meet the transmission standard of 56 dB is ~ 16.8 dB. Present FM/FDM systems requires about the same C/N [3,7].

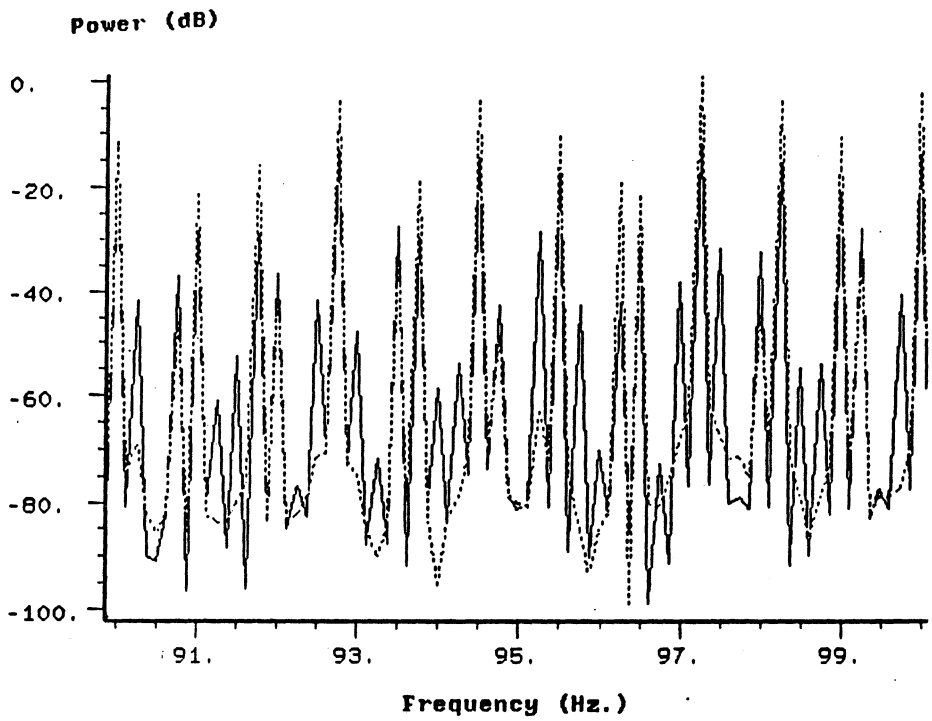

Figure 3.7 : Spectrum of a sampled FM signal with a sinusoidal frequency where f_s is not an integer multiple of the modulating frequencies f_s=100 Hz and the modulating frequencies are 2.75 and 4.5 Hz (.....) overlaid with the spectrum of the same signal after nonlinear distortion (___).

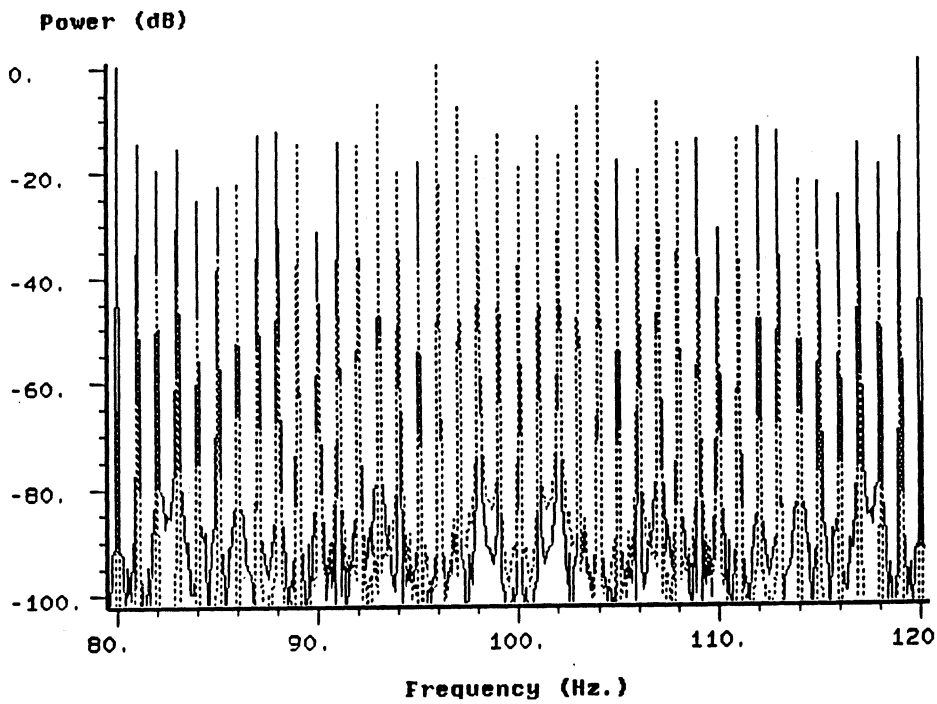

Figure 3.8 : Spectrum of a sampled FM signal with a sinusoidal frequency where f_s is an integer multiple of the modulating frequencies f_s=100 Hz and the modulating frequencies are 2 & 5 Hz (.....) overlaid with the spectrum of the same signal after nonlinear distortion (___).

CHAPTER 4

PERFORMANCE ANALYSIS

4.1 INTRODUCTION

The purpose of this chapter is to study the performance of the proposed system by analysis. Sources of distortion and noise are identified, and their values are calculated. Each distortion is categorized by whether it will yield a coherent or a non-coherent type of interference. Then, according to the maximum permissible distortion amounts, the expected performance of the proposed system is estimated. The same process is repeated for two of the present multi-channel TV transmission systems (FM/FDM and PCM/TDM). By comparing results, advantages and disadvantages of the proposed system are found.

4.2 COMPONENT PARAMETERS

For the purpose of performance evaluation, a light source, photo-detector, and receiver electronics are selected. These are the three major components in any multi-channel video system. One of them is usually the limiting factor for most multi-channel TV delivery networks. Since CATV links are usually short, effects of the fiber such as dispersion and nonlinear distortion are generally small and therefore not considered here.

As indicated, the motivation of this research is to avoid the inherent

nonlinear nature of laser diodes. It is essential to note that the performance of each specific broadband system depends mainly on the quality of components used for its implementation. If a perfectly linear laser diode, with very low *RIN*, is used for the purpose of the comparison, then the AM-VSB/FDM system may be identified as the best available system. That is due to its simplicity and compatibility with present CATV equipment. This misleading result is far from reality, because actual lasers are nonlinear devices. The same situation is valid for *RIN*. In an actual optical fiber link reflections may increase the *RIN* considerably above the intrinsic *RIN* of the laser. Therefore, comparison of the systems must be on the basis of actual representative component values, and the sensitivity of results to these component values must be studied as well.

4.2.1. LASER DIODE

A laser diode is an oscillator; to obtain oscillations one needs gain, feedback, and saturation [4]. To obtain gain, sufficient current should be injected into the device (above a threshold level I_{th}) so that a condition called population inversion exists in the active layer. Before holes and electrons spontaneously combine, an incident photon of light can stimulate the electron and the hole to emit their light energy synchronously with the existing field. Thus, the incident field grows in amplitude as it travels through the medium. To provide feedback, an optical cavity is formed as follows. For the direction front-to-back, perpendicular surfaces are cleaved at each end of the device. The interface between the semiconductor material and air produces an approximately 30% reflection. This reflection, when combined with the gain in the active layer, is adequate to result in a unity round-trip gain. In order for the device to operate, the population inversion must be confined to a small

volume of space to limit the injected current per unit area this is called the optical confinement factor Γ (unit less). The rate, at which electron-hole pairs are injected into the active region, and the photons are emitted, is described by two sets of differential equations called "rate equations". By solving these two rate equations for the steady state, it is found that the relationship between the photon density S_o and the bias current I_B is a linear relationship given by [23]

$$S_o \simeq \frac{\Gamma \tau_p}{\alpha} (I_B - I_{th}). \tag{4.1}$$

for $I_B \geq I_{th}$ where I_{th} is the threshold current, τ_p is the photon lifetime in seconds, and α is the volume of the active region multiplied by the electronic charge in C m^3 (Coulomb-meter^3).

To modulate the semiconductor laser, a current greater than the threshold current is applied (this current is called the bias current I_B), and the modulating signal $i_b(t)$ is added to it, resulting in an instantaneous current $I_b = I_B + i_b(t)$. Measurement and analysis have shown that lasers behave as a second order low pass filter with a bandwidth equal to a resonance frequency f_r (in Hz) given by

$$f_r = \frac{1}{2\pi} \cdot \left[\frac{S_o \, g_o}{\tau_p}\right]^{\frac{1}{2}}, \tag{4.2}$$

where g_o is the optical gain constant in $s^{-1}m^3$. Thus from Equations 1 and 2 we can write f_r

$$f_r = \frac{1}{2\pi} \cdot \left[\frac{\Gamma \, g_o}{\alpha}\right]^{\frac{1}{2}} \cdot (I_B - I_{th})^{\frac{1}{2}}. \tag{4.3}$$

A typical representative InGaAsP laser is selected to evaluate the performance of the three systems under consideration. As indicated, the laser selected here is representative, rather than the best that may be achieved. The characteristics of the laser are as follows [23]:

the optical gain constant $g_o = 2.4\text{x}10^{-12}$ $s^{-1}m^3$,

the bias current $I_B = 80$ mA,

the output power at this bias current = 4.5 mW

the threshold current $I_{th} = 45$ mA,

the optical confinement factor $\Gamma = 0.4$ Am^3s,

the volume of the active region x the electronic charge $\alpha = 2.2\text{x}10^{-35}C.m^3$.

For the above parameters values f_r is calculated to be 6.2 GHz. The lasers used by Olshansky *et al.* in their subcarrier multiplexed system experiments [16-18], have resonance frequencies in the range of 12-14 GHz. Typical lasers used for digital data transmission have a resonance frequency in the range of 2-3 GHz [4]. It is clear that the laser selected here has a resonance frequency better than lasers used for present digital communications, but poorer than the ones used for analog transmission.

Due to the limited bandwidth of the laser, the step response of the laser contains a damped oscillation at the relaxation frequency. The relaxation frequency damping factor *"a"* is found empirically to be [23]

$$a = \frac{\epsilon \Gamma}{\alpha} (I_B - I_{\text{th}}) \qquad \text{second}^{-1} \tag{4.4}$$

where ϵ is an empirical quantity called the gain compression. Its value for the selected laser is determined from measurements to be approximately $4.5\text{x}10^{-23}$ m^3. For the above values of I_B and I_{th}, we calculate $a = 2.9\text{x}10^{10}s^{-1}$.

In summary the specifications of the selected laser are [19]

- Resonance frequency f_r = 6.2 GHz,
- Relaxation frequency damping factor a = $2.9\text{x}10^{10}\text{second}^{-1}$,
- Gain compression damping coefficient ϵ =$4.5\text{x}10^{-23}\text{m}^3$,
- Optical gain constant g_o = $2.4\text{x}10^{-12}$ s^{-1}m^3,
- Photon lifetime τ_p = $1\text{x}10^{-12}$seconds.

4.2.2 PHOTODETECTOR

An optical detector provides a mechanism for converting optical power into electrical current. A simple approach to implementing an optical detector is to allow the incident optical power to illuminate a reversed biased *p-i-n* photo-diode, resulting in the generation of hole-electron pairs by absorbed photons. These pairs can, in turn, flow in the presence of an electric field to produce an observable reverse current. Very high frequency response (corresponding to low junction capacitances) and very good linearity are more readily obtained in detectors than in transmitters. Consequently, these factors will not be considered in the following analysis.

The performance of a detector is measured by many factors, the most important ones are the efficiency with which it converts optical power to electrical current (conversion efficiency), and the reverse saturation current without incident light (dark current).

The conversion efficiency is characterized by one of two equivalent measures. The first measure is the fraction of incident photons which produce electron-hole pairs. This is a number less than or equal to unity and is called

the quantum efficiency of the detector η_d. The second measure of conversion efficiency is the ratio of displacement current produced to incident optical power (amperes/watt). The displacement current is equal to the number of hole-electron pairs per second produced in the detector multiplied by the electron charge, e. The incident power is the number of photons per second incident upon the detector multiplied by the energy in a photon, hf (h is Planck's constant and f is the frequency of the incident light). The energy in a photon at 1 μm wavelength is about 2 x 10^{-19} J. The responsivity of the detector in amperes per watt is given by η_d x e/hf where η_d is the quantum efficiency. The ratio e/hf has the dimensions of ampere per watt (A/W) but numerically it is near unity (0.8 for 1 μm wavelength). Thus, numerically, the quantum efficiency (dimensionless) and responsivity (A/W) are similar. The *p-i-n* photo-diode selected for the application on hand has a quantum efficiency of 0.7 which corresponds to a responsivity of $\sim$ 0.56 A/W at 1.3 μm wavelength.

Another performance measure of a detector is the dark current. When an external reverse voltage is applied to the photo-diode, the total voltage across the depletion region is the applied reverse-bias voltage plus the junction contact potential [6]. A very small reverse saturation current due to leakage and thermally generated carriers will flow, this reverse saturation current is the "dark current". The *p-i-n* photodetector selected here has a dark current of 2 nA.

The bandwidth of the *p-i-n* photo-detector is not usually of concern. High-speed GaInAs *p-i-n* diodes with bandwidth up to 20 GHz [16] along with commercial low noise electrical amplifiers with 2-8 GHz bandwidths are readily available in the market. Also the nonlinearity of the photo-diode is negligible when compared to the average quality laser diodes.

In summary, for the application in hand, a *p-i-n* photodetector is selected with the following specifications:

- Responsivity = 0.56 A/W (equivalent to quantum efficiency of 0.7),
- Dark current = 2 nA.

Typical responsivity values varies from 0.5 to 0.7 A/W, and dark current values range from 1 nA to 100 nA.

4.2.3 RECEIVER ELECTRONICS

Since all systems under consideration are limited in the same way by the receiver's thermal noise, the selection of the receiver is not very critical in relative comparisons of the systems. Hence, a receiver containing *p-i-n* photodiode followed by a typical 50 Ω preamplifier with a noise figure of 1.5 dB is selected. As indicated in Section 2.2.3, receiver thermal noise spectral density $<i^2_{ckt}>$ in A^2/Hz is given by

$$<i^2_{ckt}> = \frac{4\ kTF_e}{50}. \tag{4.5}$$

Thus, the equivalent input thermal noise spectral density for the selected receiver at room temperature is found to be $5x10^{-22}A^2/Hz$. If a low noise receiver is used instead, with an APD detector and a state-of-the-art high-impedance GaAs MESFET amplifier, then all three systems will have better performance than what we calculated here. But the relative performance of the three systems should remain unchanged.

4.3 SPECTRAL EFFICIENCY

In FDM systems, harmonics and inter-modulation/cross-modulation distortions limit the use of the full bandwidth available. For example to avoid second harmonics, only one octave of the total transmission band is usually used. Furthermore, inter-modulation/cross-modulation distortion limits the number of channels to be transmitted. Furthermore, usually guard bands are left between channels to avoid adjacent channel interference. Similarly, in TDM systems, ISI forces the user to leave guard times between samples (pulses), limiting the number of channels to be transmitted. We define the spectral efficiency "η" to be

$$\eta = \frac{N\,W}{B_T}, \tag{4.6}$$

where N is the number of channels, W is the TV baseband bandwidth (~ 5 MHz), and B_T is the transmission bandwidth. The spectral efficiency η may be equal to 100% only if no spectrum spreading is applied to the signal, and no guard band (or time) are left between multiplexed channels. Usually, η is considerably less than 100%. Spread spectrum systems usually provide a tradeoff between η and the minimum required C/N for a given channel performance; the lower the spectrum efficiency η, the lower the minimum required C/N [29]. Since all of the three systems considered here require about the same C/N for a given baseband S/N, then η may be used to measure the spectral efficiency of each modulation scheme and compare the results.

An FM/FDM experiment reported by Olshansky *et al.* [16] used an 11 GHz bandwidth laser to transmit 60 TV channels. We calculate η for this experiment to be 3%.

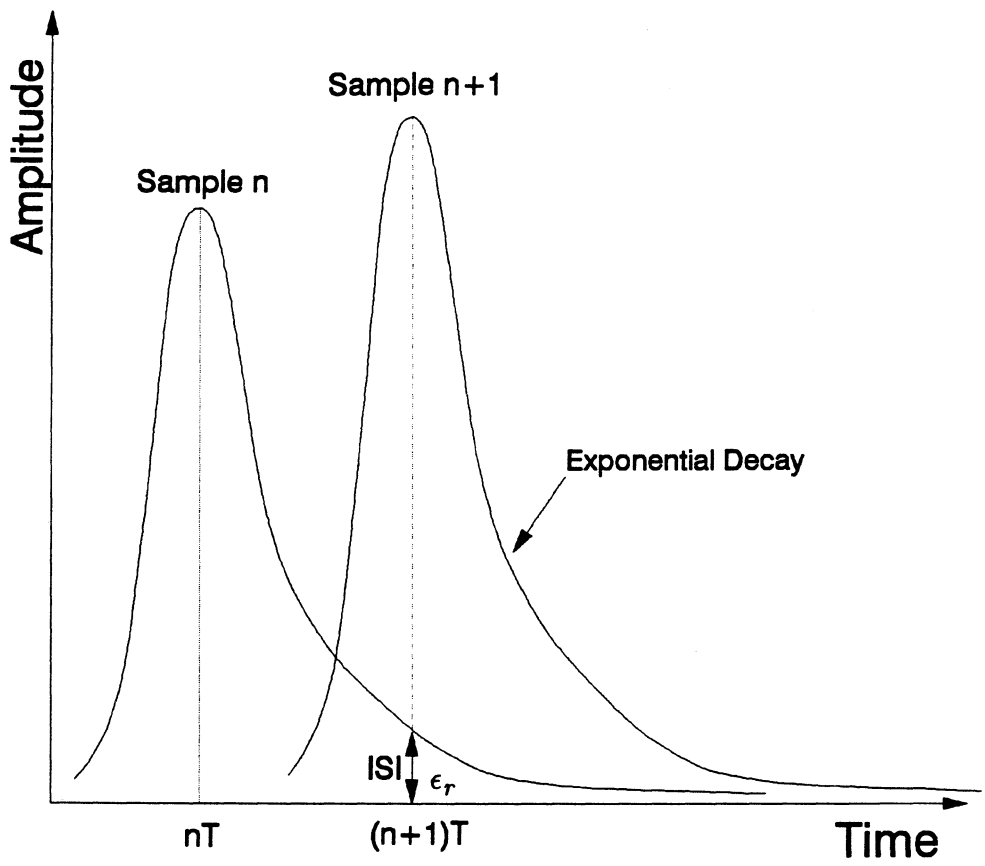

Figure 4.1: Inter-symbol interference as a result of the previous sample tail.

In TDM systems, there is no inter-modulation/cross-modulation, therefore more efficient spectrum utilization is possible. However, overlap between pulses gives rise to inter-channel crosstalk which in general is called inter-symbol interference (ISI). ISI can be decreased by increasing the transmission bandwidth, or by certain types of pulse shaping (Nyquist pulse shaping is an example). In this section the relationship between the ISI and the transmission bandwidth is determined if the applied samples are rectangular. ISI in the presence of pulse shaping and timing errors is studied in chapter 7.

As indicated above, the laser diode acts as a second order low pass filter [24]. The impulse response of such a filter is

$$h(t) = e^{-\delta.t}\ sin(\delta.t), \tag{4.7}$$

which represents a damped oscillation with a damping factor equal to δ. As illustrated in Figure 4.1, the tail of the n^{th} sample (or pulse) decays exponentially and distorts the (n^{th}+1) sample. Setting the damping factor δ equal to the damping factor "a" of the laser ($a = 2.9\text{x}10^{10}$ second^{-1}), and for the worst case condition of ISI, we assume that the magnitude of $sin(\delta.t) = 1$. For a sampled sinusoidal signal, with a magnitude = A, the average signal power is equal to

$$S = \frac{A^2}{2}\ \text{x}\ (\frac{\tau}{T}), \tag{4.8}$$

where τ is the sample duration, T is the time between samples, and $\frac{\tau}{T}$ is the duty factor of the sample. For exponential decay with a damping factor equal to a, the magnitude of the previous sample at time T is Ae^{-aT}. If the pulse period is considered to be too large compared to laser's fall time (i.e. the time at which a

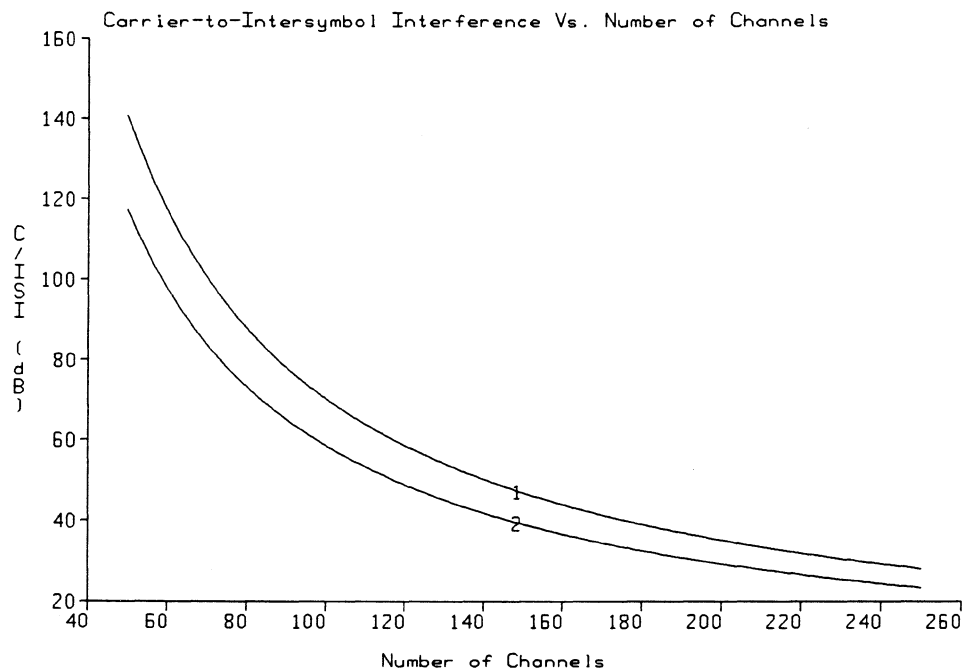

Figure 4.2: Carrier-to-ISI in dB vs number of channels for 1) FM/TDM system, and 2) PCM/TDM system.

pulse decays from 90% to 10%), then the distortion resulting from samples other than the previous sample may be ignored. Hence, the average power of the interference coming only from the previous sample is

$$ISI = \frac{A^2}{2} \text{ x } e^{-2aT_x} \left(\frac{\tau}{T}\right), \tag{4.9}$$

Therefore C/ISI can be calculated as

$$\frac{C}{ISI} = exp(2aT), \tag{4.10}$$

i.e.

$$\frac{C}{ISI} = exp\left(\frac{2.a}{N f_s}\right), \tag{4.11}$$

where f_s is the sampling rate in Hz,

N is the number of multiplexed channels.

For the PCM system the C/ISI may also be expressed as

$$\frac{C}{ISI} = exp\left(\frac{2.a}{N r_c}\right), \tag{4.12}$$

where r_c is the bit rate/channel. The *C/ISI*, as calculated from Equations 4.11 and 4.12, are shown in Figure 4.2 with $f_s =$ 71.6 MHz for FM/TDM and bit rate per TV channel $r_c = 85.9$ Mbit/s for PCM. As seen from the figure, the distortion due to ISI is completely negligible for any reasonable number of channels.

For digital systems satisfactory operation requires the C/N to be at least equal to 15.8 dB (FSK PCM). The ISI results in the degradation of the total C/N which in turn results in more bit errors. If C/ISI is set to be 30 dB, then the effect

on the overall performance is completely negligible. Limiting C/ISI to 30 dBc limits the maximum channel capacity to 190 channels. Then, the spectrum efficiency is limited to $\sim 15.3\%$ i.e. about five times as high as η for the FM/FDM system.

For the FM/TDM system, the ISI should not be considered as random Gaussian noise (as it was for the PCM system) but rather as a coherent distortion introduced by the adjacent channels. As indicated in Section 1.2.3, coherent distortion results in patterns often looking like moving diagonal bars, or as ghosts (if the interfering channels are synchronized). CATV target values for coherent distortions is less than 53 dBc, i.e. about 10 dB less than noise level. For trunk applications, or for high quality transmission, coherent distortions should be limited to values less than CATV target values, (20 dB below random noise [17]). Accordingly, ISI should be limited to 40 dBc. This limits the maximum channel capacity to ~ 150 channels. This corresponds to a spectrum efficiency of 12.1%, i.e about four times as high as η for the FM/FDM system.

4.4 NONLINEAR DISTORTION

Extensive study and research had been focused on the problem of nonlinear distortion in multi-channel fiber optic systems [5],[16-18],[24-28]. Many research and development labs are trying to improve the inherent nonlinear nature of laser diodes. In spite of significant success, present multi-channel optical fiber video systems are still limited by nonlinear distortion. In this section such distortions are analyzed and compared for the three systems under consideration. In the analysis, each system is loaded with 60 TV channels. Each channel has parameters as follows: FM bandwidth equals ~ 35.8 MHz; the FM/TDM sampling rate equals to

71.6 MHz; and the PCM pulse rate equals to 85.9 Mbit/s.

4.4.1. TDM SYSTEMS

The frequency spectrum of each sample (or pulse) is an infinite frequency band with shape dependent on the sample period, and shape. An approximate bandwidth of the sample spectrum can be determined from the sample duration.

A frequency band may be considered as the sum of infinite signals with discrete frequencies stacked adjacent to each other. If a frequency band is passed through a nonlinear device, the output will consists of the original frequency band plus distortion. The distortion will consists of harmonics and cross terms. For a signal with rectangular spectrum, harmonics distortion will have the tendency to shift some of the power from the low frequency side to higher frequency side (this explains why rise time increases with nonlinearity; i.e., pulse compression). On the other hand, cross terms have the tendency to return the infinitesimal power lost from the band in the cross terms, back to the band in distorted format. Second order cross terms have a maximum at the center of the band, while third order cross terms have their maximum value at the edges of the band [5]. These cross terms will not introduce a coherent type distortion as in the case of FDM systems. As long as these frequencies are not individually modulated, then no inter-modulation / cross-modulation distortion will be encountered. Thus, cross terms distortions may be ignored when compared to harmonic distortions. Therefore, equations given below (12 & 13) may be used to estimate the harmonic distortion in a band of frequencies; i.e., the dominant nonlinear distortions in the band are harmonic distortions.

Considering the laser to be represented as a memoryless nonlinearity, perturbation analysis has been applied [27],[28] to the rate equations to calculate harmonic levels for InGaAsP lasers. An expression for the second and third harmonic distortion (as a result of single tone) relative to the optical carrier intensity C are found respectively to be [28]

$$\frac{2HD}{C} = OMD \frac{f^2}{f_r^2\, g(2f)}, \tag{4.13}$$

$$\frac{3HD}{C} = \frac{3}{2}(OMD)^2 \frac{(\frac{f}{f_r})^4 + \frac{1}{2}(\frac{f}{f_r})^2}{g(2f)\, g(3f)}, \tag{4.14}$$

where f is the carrier frequency,

OMD is the optical modulation depth, (the OMD is defined as $I_{ac}/(I_B - I_{th})$, where I_{ac} is half the peak-to-peak amplitude of the modulating current, I_b is the bias current, and I_{th} is the laser's threshold current), and

$g(f)$ is the reciprocal of the small signal frequency response of the laser diode, given as follows:

$$H(f) = g(f)^{-1} = 1/\sqrt{[\,\{(\frac{f}{f_r})^2 - 1\}^2 + (\frac{2\pi\epsilon f}{g_o})^2\,]}, \tag{4.15}$$

where ϵ is the gain compression, and

g_o is the optical gain constant.

We notice that second order distortion is linearly proportional to the OMD, while third order harmonic distortion is proportional to the square of the OMD.

Furthermore, second order distortion is also proportional to the square of the ratio of the modulation frequency to the resonance frequency of the laser $(\frac{f}{f_r})$, while third order harmonic distortion is proportional to $(\frac{f}{f_r})^4$ (this explains why the resonance frequency of lasers used for present analog applications is always selected in the 10-20 GHz range). We conclude that third order distortions are more sensitive to *OMD* and to the laser's parameters. As indicated in Equations 4.13 and 4.14, the magnitude of these distortions are then further weighted by the response of laser to the resultant harmonic frequency *g(f)*. As indicated, distortion for such a spectrum results mainly from harmonic distortions. No inter-modulation / cross-modulation exists, since none of the infinite discrete frequency components (forming the sample/pulse spectrum) is individually modulated.

Inter-symbol interference (ISI) and harmonic distortion can theoretically be eliminated by using samples/pulses with Nyquist shaping. Specifically if we use samples with a raised cosine shaped spectrum given by [29]

$$P(f) = \left\{ \begin{array}{ll} \frac{1}{r} & |f| < \frac{r}{2} + \beta \\ \frac{1}{r} \cos^2 \frac{\pi}{4\beta} \left(|f| - \frac{r}{2} + \beta \right) & \frac{r}{2} - \beta \leq |f| \leq \frac{r}{2} + \beta \\ 0 & |f| > \frac{r}{2} + \beta \end{array} \right\}, \quad (4.16)$$

where *P(f)* is the power spectrum of the sample, r is the sample/pulse rate, and β is the excess bandwidth ($0 < \beta < \frac{\text{bit rate } r}{2}$). The case when $\beta = r/2$, is known as 100% rolloff. A plot of *P(f)* for three values of β is shown in Figure 4.3. When $\beta > 0$, the spectrum has a smooth rolloff, while for $\beta = 0$ it has a rectangle spectrum that extends to only $r/2$. From Parseval's theorem, energy in a sample may be written as [33]

$$E = \frac{1}{2\pi}\int_{-\infty}^{\infty} |P(\omega)|^2 d\omega, \tag{4.17}$$

where $\omega = 2\pi f$. For Nyquist shaped samples, the integral $\int_{-\infty}^{\infty} |P(\omega)|^2 d\omega$ is a constant independent of β [20]. Therefore, assuming that the noise is uniformly distributed, matched filters with different β's will pass an equal amount of noise. Therefore, different values of β should yield similar results. To simplify calculations we assume β to be zero in for the following analysis.

For a loading of 60 video channels, the pulse rate r for the PCM/TDM is 5.2 GHz, thus the spectrum of the pulse extends until $r/2 =$ 2.6 GHz. The FM/TDM has a sample rate of 4.3 GHz; therefore the spectrum of the sample extends until 2.15 GHz.

As indicated, the spectrum of each sample/pulse will suffer from second and third harmonic distortions. As shown in Equations 4.13 and 4.14, the magnitude of the harmonic distortion is a function of the frequency. The assumption of samples with a rectangular spectrum implies the use of optimum filtering. Thus, an ideal rectangular LPF (which matches the sample/pulse shape) should be placed at the receiver's front end, with a bandwidth equal to $\frac{r}{2}$. Laser generated harmonics are reduced by this front end optimum filter. This ideal LPF eliminates second harmonics caused by the upper half of the spectrum, as well as third harmonics caused by the upper two thirds of the spectrum. As shown in Figure 4.4, second order distortion, caused only by the lower half of the pulse/sample frequency spectrum, is received. The upper half (i.e. from $f = r/2$ until $f = r$) is eliminated by the matched filter (an ideal LPF). Similarly, third order distortion caused only by the first one third (1/3) of the spectrum is received. The upper two thirds is eliminated also by the

ideal LPF. Accordingly, an estimate of second order harmonic distortion is found by selecting the tone frequency of Equations 4.12 and 4.13 in the center of the band causing the harmonics, i.e. by selecting f of Equation 4.12 in the middle of the lower half of the sample/pulse spectrum (f equals to $\frac{r}{8}$, hence $f=$ 0.65 GHz for PCM/TDM, and $f=$ 0.54 GHz for the FM/TDM). Similarly, an estimate for third order harmonic distortion is found by substituting f of Equation 4.13 by $\frac{r}{12}$ (i.e. $f=$ 430 MHz for PCM/TDM and $f=$ 358 MHz for the FM/TDM). Furthermore, because the upper half of the second harmonic is not causing distortion, then the denominator of Equation 4.12 should be multiplied by a factor of two (only half of the carrier signal is causing distortion). Similarly the denominator of Equation 4.12 should be multiplied by a factor of three (only one third of the spectrum is causing distortion).

The validity of the above approximations will be verified later in Chapter 6 by simulations.

4.4.2. FDM SYSTEMS

In FDM systems, the channels are subject to all kinds of distortions: harmonic, cross-modulation, and inter-modulation. If only the band's upper octave is used then both second and third harmonic distortions are avoided. Also second order inter-modulation products (*IMP*) are eliminated. Consider a signal current i which consists of two sinusoids given by

$$i = I_a \sin(\omega_a t) + I_b \sin(\omega_b t), \tag{4.18}$$

to be applied to a laser with nonlinearity modeled by the power series

$$P_o = a_o + a_1 i + a_2 i^2 + a_3 i^3 + ..., \tag{4.19}$$

where P_o is the output optical power. Third order cross terms may be expressed as

$$CMD = a_3\{(\frac{3}{4} I_a^3 + \frac{3}{2} I_a I_b^2)\ sin(\omega_a\ t) + (\frac{3}{4} I_b^3 + \frac{3}{2} I_a^2 I_b)\ sin(\omega_b t), \tag{4.20}$$

$$\begin{aligned} IMP = & -\frac{3}{4} a_3 I_a I_b\{I_a\ sin(2\omega_a + \omega_b)\ t + I_a\ sin(-2\omega_a + \omega_b)\ t \\ & + I_b sin(\omega_a + 2\omega_b)\ t + I_b sin(\omega_a - 2\omega_b)\ t\}, \end{aligned} \tag{4.21}$$

where *CMD* is the cross-modulation distortion, and *IMP* is the inter-modulation products. *CMD* will overlay the original carriers. Thus, it may reduce the overall *C/N*. Usually, *IMP* is the dominant third order cross term distortion: this is because the number of *IMP* terms in the worst channel is proportional to N^2; furthermore, they result in a coherent distortion type which is very objectionable. The ratio of third *IMP* of two closely spaced tones to their optical carrier power *C* is given by [27-29]

$$\frac{IMP}{C} = (OMD)^2 \frac{\sqrt{\left((\frac{f}{f_r})^4 - \frac{1}{2}(\frac{f}{f_r})^2\right)^2 + \left(\frac{2\pi f^3 \tau_p}{f_r}\right)^2}}{g(f)\ g(2f)}, \tag{4.22}$$

where τ_p is the photon life time in seconds

f is the frequency of one of the two closely spaced tones

OMD is the r.m.s. optical modulation for the two tones.

The worst channel has $N^2/2$ inter-modulation products *(IMP)* terms and they add incoherently [16]. The magnitude of each is dependent on the frequency of

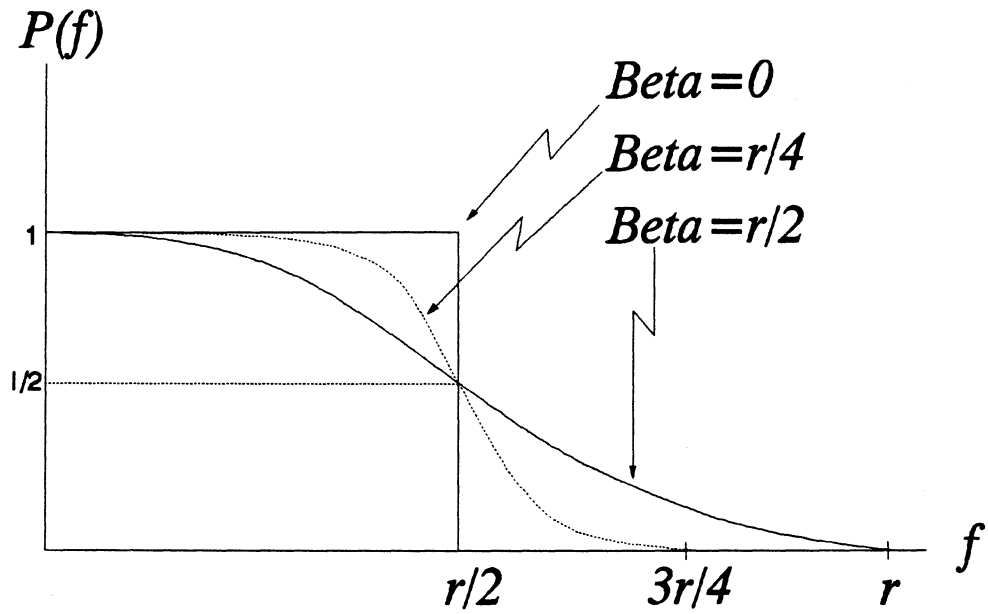

Figure 4.3: Power spectra of Nyquist shaped pulses,
where r is the pulse rate and β is the excess bandwidth.

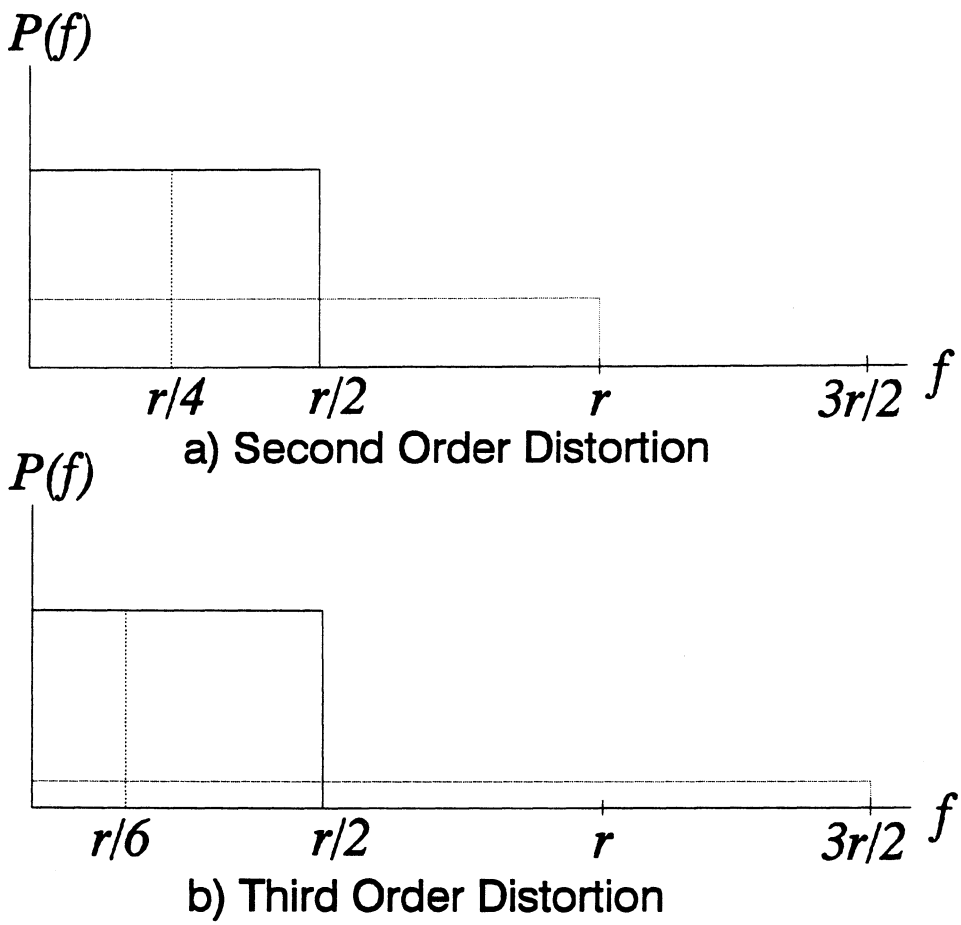

Figure 4.4: Power spectrum of the nonlinear distortion in TDM systems where r is the pulse rate.

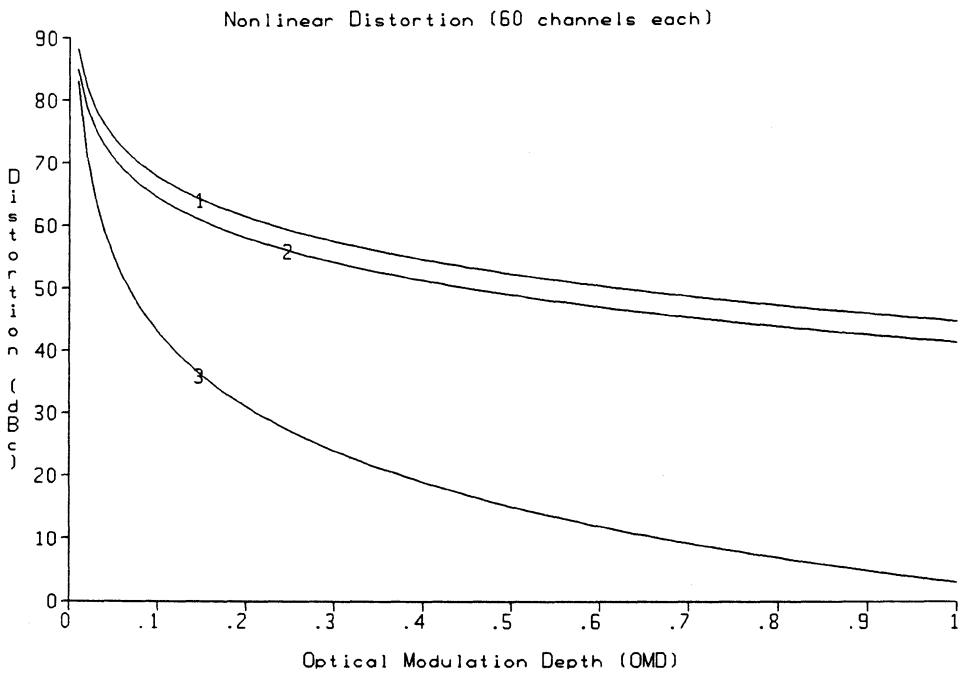

Figure 4.5: C/NLD in dB vs OMD

1) FM/TDM, 2) PCM/TDM, 3) FM/FDM.

the carriers causing it. Thus the level of *IMP* distortion at the band's lower edge is smaller than at the band's upper edge. As an average value, f is taken to be 4.65 GHz which is in the center of the upper octave.

For two incoherent interfering signals, x and y, the resultant interference is $\sqrt{x^2+y^2}$. If $x=y$, then the resultant interference is $x\sqrt{2}$. Similarly, the N *IMP*'s add incoherently. Then to get the total NLD Equation 4.17 should be multiplied by $\sqrt{N^2/2}$. Therefore, the total NLD in an FM/FDM system with N channels may be written as

$$\left(\frac{IMP}{C}\right)_T = \sqrt{\frac{N^2}{2}}\,(OMD)^2\,\frac{\sqrt{\left(\left(\frac{f}{f_r}\right)^4 - \frac{1}{2}\left(\frac{f}{f_r}\right)^2\right)^2 + \left(\frac{2\pi f^3 \tau_p}{f_r}\right)^2}}{\mathrm{g(f)\ g(2f)}} \qquad (4.23)$$

where *OMD* is the total r.m.s. optical modulation depth for the N channels such that [16] $OMD = OMD_{ch}\sqrt{N}$ (OMD_{ch} is the optical modulation depth per channel).

Total nonlinear distortion (NLD) versus *OMD* for both TDM and FDM systems is graphed in Figure 4.5. For all systems, NLD increases with increasing the *OMD*. In the FM/FDM system, the NLD is caused entirely by *IMP's* which are proportional to OMD^2. In the TDM systems, NLD is dominated by second order distortion which is linearly proportional to the *OMD*. Therefore, as seen from Figure 4.5, NLD increases in the FM/FDM system with a rate twice as much as in TDM systems.

For FM/TDM and PCM/TDM systems, because overall C/N could be as low as $\sim$16.5 dB, nonlinear distortion has no effect on the overall C/N even if the OMD is as high as 100%.

NLD in the FM/FDM is mainly *IMP's*, i.e. triple beats. Triple beats cause a coherent type picture impairments (see Section1.2.3) which is very objectionable

(similar to ISI in FM/TDM as in Section 4.2). As assumed in Section 4.2, coherent distortion should be limited to 20 dB below noise. Similarly, NLD should be limited to 60 dBc, which limits the total r.m.s OMD for the FM/FDM system to at most $\sim 12\%$. In the FM/FDM experiment performed by Olshansky *et al.* [16-17]the total r.m.s. OMD used was about 15%. This is because the laser they used had a higher bandwidth than the one we are using here.

4.5 OVER ALL IF CARRIER-TO-NOISE RATIO

As indicated in Section 2.2, for FDM subcarrier systems, IF C/N depends on the receiver's IF band-pass filter (BPF). In general, this bandwidth is called the IF noise equivalent bandwidth (B_n). For the FM/FDM system B_n is equal to $B_{IF} = 36$ MHz.

For the FM/TDM system, the LPF with a bandwidth equal to $r/2$ at the receiver's front end determine the amount of noise entering the receiver. Furthermore, this noise is reduced by the ratio τ/T_s at the receiver's sampler (duty factor or time slicing), where τ is the sample period, and $T_s = 1/f_s$ is the time between samples. For the PCM/TDM system, B_n is similar to the FM/TDM case, with $T_s = 1/nf_s$, were n is the number of bits per sample, and f_s is the baseband sampling frequency. Therefore IF noise equivalent bandwidth for the TDM systems is equal to

$$B_n = \frac{r \cdot \tau}{2 \cdot T_s}, \tag{4.24}$$

where $\tau = T_s/N$ (N is the number of channels).

IF noise equivalent bandwidth is calculated as follows:

$B_n = f_s/2 = 35.8$ MHz $\simeq 36$ MHz for FM/TDM,

$B_n = nf_s/2 = 43$ MHz for PCM/TDM,

$B_n = 36$ MHz for FM/FDM.

As indicated in chapter 2, the overall IF carrier-to-noise for any subcarrier multiplexed system may be written as [see Section 2.2 for details].

$$(C/N)^{-1} = (C/N)^{-1}_{RIN} + (C/N)^{-1}_{shot+dark+excess} + (C/N)^{-1}_{thermal} + (C/N)^{-1}_{NLD} \tag{4.25}$$

By replacing the noise band-width with B_n, each term can be rewritten as follows:

$(C/N)^{-1}_{RIN}$ is the carrier-to-noise ratio limitation caused by the laser's relative intensity noise

$$(C/N)^{-1}_{RIN} = \frac{RIN.\ B_n}{\frac{1}{2}\ OMD^2}, \tag{4.26}$$

where RIN is the laser intensity noise in W/Hz, (-130 dB/Hz)

B_n is the IF noise equivalent bandwidth in Hz, and

OMD is the optical modulation depth (90% for TDM systems & 12% for the FDM system.

$(C/N)^{-1}_{shot+dark+excess}$ is the carrier-to-noise ratio limitation caused by, shot noise, dark current, and excess noise.

$$(C/N)^{-1}_{shot+dark+excess} = \frac{2\ q.(I_{ph} + I_{dark})\ .\ B_n}{\frac{1}{2}\ OMD^2\ I^2_{ph}}, \tag{4.27}$$

where q is the electron charge (1.6×10^{-19}C),

I_{ph} is the received photodetector d.c. current (A), and

I_{dark} is the photodetector dark current (2 nA).

$(C/N)^{-1}_{thermal}$ is the carrier-to-noise ratio limitation caused by receiver's circuit thermal noise.

$$(C/N)^{-1}_{thermal} = \frac{<i^2_{ckt}> \cdot B_n}{\frac{1}{2} OMD^2 \cdot I^2_{ph}}, \tag{4.28}$$

$<i^2_{ckt}>$ is the receiver circuit input equivalent noise current spectral density (5×10^{-22}A^2/Hz).

$(C/N)^{-1}_{NLD}$ is the carrier-to-noise ratio limitation caused by laser's nonlinearities. As in Section 4.3 this term is limited to 40 dBc for the FM/FDM system and 45 dBc for both TDM systems.

As the result of Section 4.3, OMD should be limited to 12% for the FM/FDM system, while it could be as high as 100% for both TDM systems. The FM/TDM system carrier-to-noise ratio limitation of each noise is shown in Figure 4.6. As seen from the figure, for any reasonable operating region the main limiting factor is thermal noise. For a received optical power of 4.5 μW the gap between the thermal noise and shot noise is about 23 dB. This result will be compared later with simulation results in Chapter 6.

A plot of the overall C/N versus received optical power with OMD $= 12\%$ for the FDM system and OMD $= 90\%$ for TDM systems is shown in Figure 4.7. It is seen from the figure that the TDM systems have ~ 8.5 dB optical power budget

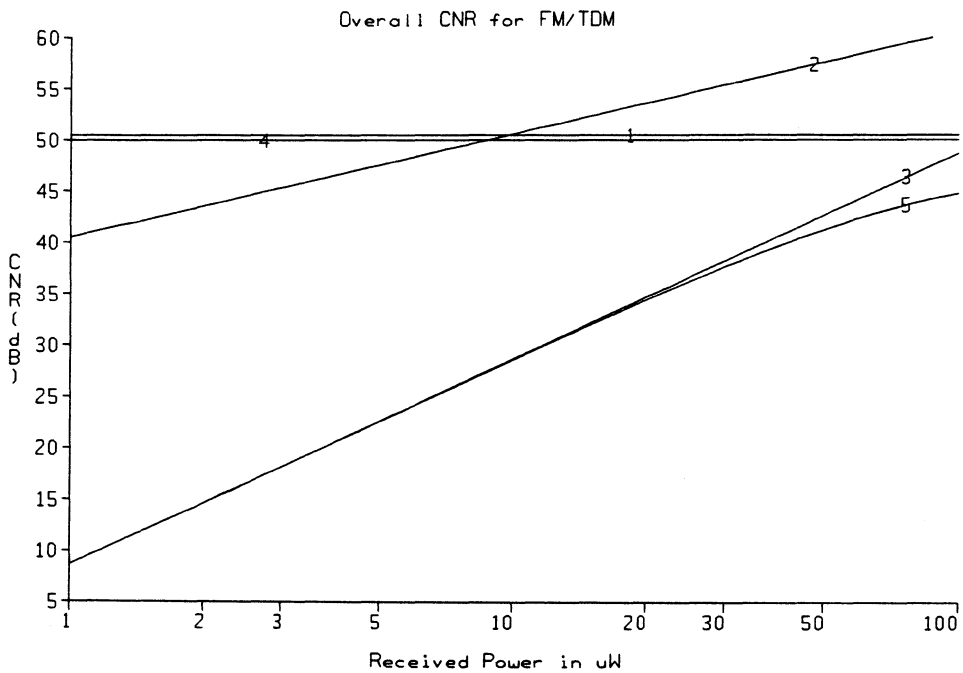

Figure 4.6: The FM/TDM system carrier-to-noise ratio limitations 1)*RIN* noise, 2) shot noise, 3) thermal noise, 4) *NLD*, and 5) overall C/N.

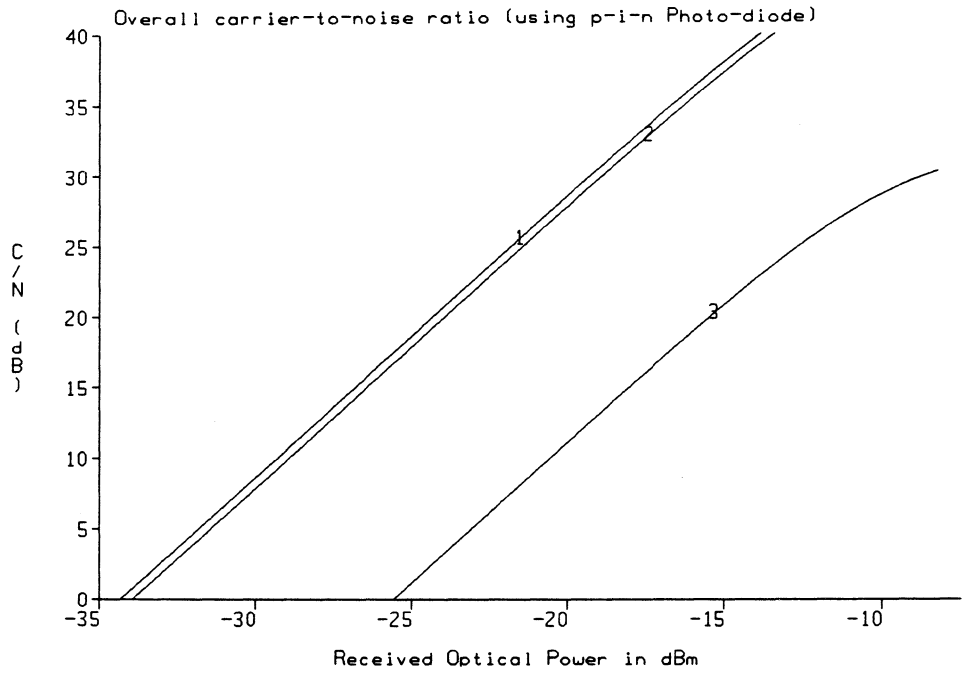

Figure 4.7: Overall IF carrier-to-noise in dB vs. received optical power in dBm 1) FM/TDM, 2) PCM/TDM & 3) FM/FDM.

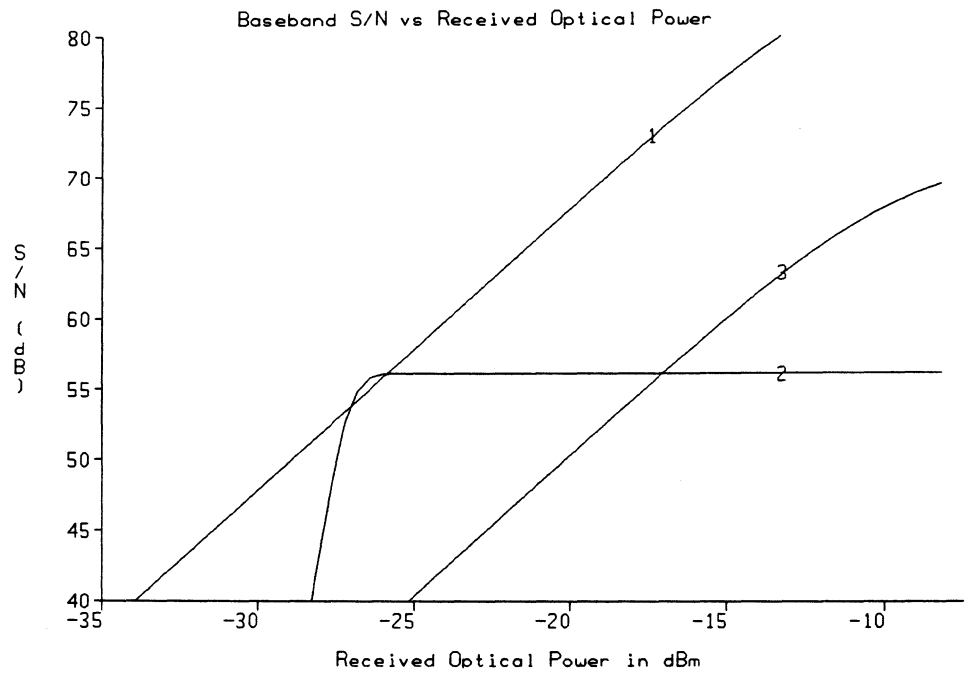

Figure 4.8: Weighted baseband signal-to-noise in dB vs. received optical power in dBm
1) FM/TDM, 2) PCM/TDM & 3) FM/FDM.

advantage over their FM/FDM system counterpart. This is essentially a result of the factor of 7.5 larger OMD. Other terms in the equations are comparable.

By using Equations 2.13 and 2.17, overall weighted signal-to-noise ratio (S/N) for the three systems PCM/TDM, FM/TDM, and FM/FDM are calculated and shown in Figure 4.8. It is obvious that both TDM systems have about the same S/N for small received power, but for larger received power the FM/TDM system is superior. Meanwhile, regardless of the received power, the FM/TDM system is always superior to the FM/FDM system. The S/N for the FM/TDM is about 17 dB better than for the FM/FDM system.

4.6 SUMMARY

In Section 4.2, spectral efficiency was studied and compared. The channel capacity is limited in the FM/FDM system because of nonlinear distortions which introduces triple beats. Similarly, in the FM/TDM system ISI introduces a similar type of interference (coherent distortion). The PCM/TDM system is the system which is least sensitive to ISI. As indicated, because the three systems under consideration require about the same C/N for satisfactory operation, the spectral efficiency (as defined in Section 4.4) is a good indication of how efficiently each system utilizes the total available bandwidth. For the three systems under consideration, the FM/FDM system has the lowest spectral efficiency ($\eta = 3\%$), next comes the FM/TDM system ($\eta = 12.1\%$), and the highest is the PCM/TDM system ($\eta = 15.3\%$).

In Section 4.3, nonlinear distortion for three systems is estimated. Nonlinear distortion generates coherent type distortion in the FM/FDM system,

thus it should be limited to 20 dB below the random noise level. This limits the OMD for the FM/FDM system to at most 12%. Since the laser diode is modeled with memoryless nonlinearities, then NLD does not increase the level of ISI between samples/pulses for TDM systems. Therefore, NLD in TDM systems is not from the coherent type distortion. From analysis, it was found that OMD for TDM systems may be as high as 100% with NLD less than 40 dBc (which is insignificant when compared to the overall C/N).

In Section 4.4, overall C/N and baseband S/N are calculated as a function of the received optical power. For any received C/N, TDM systems have roughly 8.5 dB higher optical power budget than the present FM/FDM system. With respect to picture quality, since S/N degradation in digital systems is not as graceful an in FM systems, large power margin is usually required to ensure satisfactory operation. In that range, the FM/TDM system has a slightly better S/N. Furthermore, the FM/TDM system has the advantage of being very flexible. S/N could be increased according to the application by adding optical amplifiers or by increasing the transmitted power. In digital systems, CODECs at the terminal sites need to be changed in order to improve to picture quality.

CHAPTER 5

SIMULATION MODELS

5.1 INTRODUCTION

To verify the analysis and the associated approximations several computer simulations were performed. The Block Oriented Systems Simulator[1] (BOSS^{TM}) was used to evaluate the performance of the proposed system. Specifically, simulations were used to obtain the nonlinear distortion in the IF band as a function of the *OMD*, and the baseband *S/N* as a function of the received optical power. The simulation results are in general consistent with the results of the approximate analysis presented in Chapter 4.

Furthermore, to probe the limits of the proposed system, two additional simulations were performed; one to estimate the baseband *S/N* as a function of the laser's nonlinearities, and the second to estimate baseband *S/N* when limited by nonlinearities, as a function of the IF bandwidth. Results of the simulations are given in the next chapter.

In this chapter simulation system modules and component modules are described. Simulation parameters are also justified and calculated. Components used in simulations (laser diode, *p-i-n* diode, etc.) have the same specifications as

[1]

the ones used for analysis. Also, noise sources used in the simulations have magnitudes and distributions same as the ones used for the analysis.

5.2 OVERVIEW OF THE BLOCK ORIENTED SYSTEMS SIMULATOR (BOSS^{TM})

BOSS provides a waveform level simulation of communications and signal processing systems. It consist of the following steps:

1. Representing the system in the form of a signal flow block diagram.
2. Generating samples of all input signals (waveforms).
3. Performing discrete-time signal processing operations according to the functional model of each block.
4. Storing the simulated waveforms and analyzing the stored waveforms to extract performance measures.

Monte Carlo techniques are used to handle random variations in signals and system parameters, and the simulations are run until enough samples have been accumulated to obtain satisfactorily valid estimates of performance measures.

The major components of the BOSS software package are written in LISP and run under the VMS operating system on the DEC VAX Station. BOSS is also available for the UNIX operating system on SUN 3 workstations. The simulation program to be executed is written within BOSS in FORTRAN based on the block diagram the user specifies. Thus, in part, BOSS acts as a translator which converts block diagrams into FORTRAN simulation programs.

BOSS assumes that all systems whether they are simple functional blocks such as modulators, or entire communications links can be described in a

hierarchical block diagram form. In order to simulate a system, the user must first construct a block diagram of the system. This is done by bringing existing modules from the library onto the workstation screen, and connecting them in the desired topology. A finished block diagram can be simulated immediately or used to build other models.

To start a simulation the user needs to recall the block diagram, attach probes at the desired points to record the simulated waveforms, set parameter values and direct BOSS to execute the simulation. Once the block diagram for the system to be simulated has been constructed, to accomplish any useful work it must be initialized. Simulation initialization consists of specifying the time between signal samples (DT), and the time length of the simulation run (STOP-TIME).

DT must be small enough to avoid aliasing for the signals being sampled. Ideally, 1/DT, which is the sampling rate, should be greater than twice the highest frequency present in the signals to be sampled. In practice many wave forms have infinite bandwidth (for example stream of samples, or pulses), and so DT is made small enough that the aliased power falling into the simulation bandwidth is small compared to the noise power in the same bandwidth. A sampling rate of 8 to 16 times the highest rate in the system is usually adequate for characterizing the waveform for simulation purposes. Lastly, all rates are internally rounded by BOSS from the entered value so that the corresponding period (1/rate) is an integer number of DT intervals. Therefore, for multi-rate simulations (when there is more than a single rate in the simulation), it is best if 1/DT is an integer multiple of all rates in the system, otherwise some round-off error may occur. If this is not possible, then STOP-TIME should be high enough such that $K/\mathrm{DT} = Mf$ where K and M are integer numbers. If, for example, the baseband

frequency used is $f_{baseband} = 1$ Hz, the FM frequency $f_C = 100$ Hz, and the sampling frequency is 80 Hz, then the best value for DT is $1x10^{-4}$ seconds, which gives

$1/DT=1000xf_{baseband} = 100xf_C = 125xf_S = 10000.$

The next best value is $DT = 1x10^{-3}$ which is an integer multiple of two of the frequencies and satisfies the second condition, i.e.

$1/DT = 1000\ f_{baseband} = 10f_C = 1000$, and $8/DT = 100f_S = 8000$ (in this example $K = 8$ and $M = 100$).

On the other hand, STOP-TIME should be set large enough to get good estimates of the quantities of interest. For discrete components (modulators, filters etc), STOP-TIME should be large enough such that these components exit the transient state before any measurements are taken. For noise and statistical models, STOP-TIME should be large enough to include enough bits to represent the noise or the distribution.

The results of a simulation are viewed using the post-processor component of BOSS. BOSS provides a variety of plots including time domain plots, frequency domain plots, and other displays (histograms, correlation plots etc).

It is possible to perform design iterations within BOSS by executing the simulations for different values of parameters. This is done using the parameter iteration option in BOSS. The results of multiple simulations can be viewed simultaneously for comparison.

Usually, the user needs to compromise between DT, STOP-TIME, and the execution time. A combination of small DT with a large STOP-TIME may be

accurate, but the execution time will be very long. In addition collected data size may be too large. The post-processor has limitation on the data size to be displayed which sets a limit on the size of the usable collected data. On the other hand, a combination of large DT with small STOP-TIME may take a small execution time but aliasing will reduce the accuracy of the result.

5.3 SIMULATION MODULES

As indicated above, four simulations are performed. The simulation system modules and component modules are described in this section. Each system is described in three steps. A simplified block diagram is first presented, then the details of the simulation are described, and finally simulation parameters are determined and justified.

5.3.1 IF NONLINEAR DISTORTION VS OPTICAL MODULATION DEPTH

The purpose of this simulation is twofold: to be able to compare various systems at IF as well as at baseband and to verify that the baseband performance may be calculated from IF performance (using the standard FM improvement factor). The simulation is used to calculate the IF nonlinear distortion in dBc as a function of *OMD*.

5.3.1.1 Simplified block diagram: As shown in Figure 5.1, the output of the sinusoidal generator representing the baseband signal is applied to an FM modulator, the output of which after filtering is sampled by a pulse train with a frequency equal to twice the FM signal bandwidth. The module following the sampler is a variable gain to adjust the *OMD*. After adding bias current, the

signal is then applied to a laser diode. The laser diode, which has characteristics as shown in Figure 5.2, generates nonlinear distortions (*NLD*) which are routed separately. Finally, the power of both the desired optical signal and the *NLD* are calculated and the *C/NLD* is estimated.

5.3.1.2 Details of the simulation: The actual simulated system is shown in Figure 5.3. The FM modulator generates a complex signal. However, the current applied to the laser diode has to be real. Therefore, the module "Real of complex" selects the real part of the complex signal, representing the current. The module after the sampler is an amplifier with a variable gain. By changing this gain the input signal maximum magnitude is changed, accordingly *OMD* is changed. The *OMD* can be calculated from the following relationship

$$OMD = \frac{\text{Maximum signal magnitude}}{I_B - I_{th}}. \tag{5.1}$$

The laser module shown in Figure 5.4, models the input current to optical power output characteristics above threshold. This module is represented by an AM-AM memoryless nonlinearity which is approximated by a power series given by [30]

$$P_o(t) = a_o + a_1 i(t) + a_2 i^2(t) + a_3 i^3(t) + \ldots., \tag{5.2}$$

where $P_o(t)$ is the output optical power in Watts,

$i(t)$ is the signal current applied to the laser diode in Amperes, and

a_o, a_1, a_2, and a_3 are the coefficients of the power series.

As seen from the laser's current-power characteristics shown in

Figure 5.2, the maximum allowable current swing is $I_M = I_B - I_{th}$, therefore the signal current $i(t)$ can be written as

$$i(t) = OMD \; . \; I_M \; . \; m(t), \tag{5.3}$$

where $m(t)$ is the normalized message signal such that $|m(t)|_{max} = 1$. For a sampled FM signal we get

$$i(t) = \; OMD \; . \; I_M \; . \sum_{n=-\infty}^{\infty} (cos \; (\omega_c t + \theta(t))).\delta(t - nT). \tag{5.4}$$

where ω_c is the carrier angular frequency, and $\theta(t)$ is the change in the instantaneous frequency due to the modulation. For a sinusoidal modulating frequency f_m, $\theta(t)$ can be written as

$$\theta(t) = \frac{\Delta f}{f_m} \, sin(\omega_m t). \tag{5.5}$$

The differential efficiency of the laser diode, a_1, is the slope of the $P - I$ characteristic line (in BOSS manuals they refer to it as the efficiency), hence,

$$a_1 = \frac{P_o}{I_B - I_{th}} \tag{5.6}$$

The laser diode selected in Section 4.2.1 has a bias point of $I_B = 80$ mA, $I_{th} = 45$ mA, and $P_o = 4.5$ mW. From the above equation we find $a_1 = 0.1286$ W/A.

As shown in Figure 5.4, the term $a_1 i(t)$ is routed separately and considered the desired signal. The sum of the other two terms is considered the

nonlinear distortion (i.e $a_2 i^2(t) + a_3 i^3(t)$). This is higher than the true nonlinear distortion. (the true nonlinear distortion is covered in more detail in Section 5.3.2.2.) We term this the over bounded distortion. The purpose of this simulation is to show that the over bounded distortion is small even when the *OMD* is large (simulation of the actual IF distortion is very difficult because of the overlap of the nonlinear distortion with the original signal which makes them difficult to separate.) From Equations 4.12 , 4.13, and 5.2, the ratio of the second harmonic-to-carrier, according to this model, is equal to

$$\left(\frac{2^{nd}\ Order\ Distortion}{C}\right)_{over\ bounded} = \frac{a_2.OMD.I_M}{a_1}, \tag{5.7}$$

and similarly, third harmonic-to-carrier is given by

$$\left(\frac{3^{rd}\ Order\ Distortion}{C}\right)_{over\ bounded} = \frac{a_3.OMD^2.I_M^2}{a_1}. \tag{5.8}$$

As indicated above, the above two equations do not represent the actual second and third order distortions in a real system. But Equations 5.7 & 5.8 are sufficient to calculate the coefficients a_2, a_3 for the module used in the simulation.

Following the laser is a Butterworth low pass filter (LPF) with half power point equal to $r/2$, where r is the sample rate, and an order of 10. In an actual system additional filtering is needed at both the transmitter and the receiver ends for Nyquist pulse shaping.

The IF nonlinear distortion relative to the carrier is then obtained by dividing the power of the desired signal, taken from output #1, by the power of the nonlinear distortion taken from output #2.

Each module in the system contributes some time delay. Thus there is a minimum execution time before the system reaches a stable condition (see Section 5.2). Therefore, a time delay should be applied before the beginning of measurements. The module "T_>=T_ON" turns on the signal-to-noise ratio meter ON after a given delay time. The module "= intgr" is a counter which keeps the module "SNR ratio" ON for a period of two baseband cycles before terminating the simulation. At the same instant at which the module "=intgr" triggers the module "terminate simulation", it triggers also a "sample and hold" circuit to sample the output C/N. This sample of the C/N is stored in the module "Tabular plot via iteration". The corresponding value for the *OMD* is also calculated and saved in the same module "Tabular plot via iteration". This process is repeated several times (BOSS limits this to a maximum of 10 times), resulting in a relationship between *OMD* and IF C/N (i.e. *OMD vs. NLD*).

5.3.1.3 System parameters: As indicated in Section 5.2, 1/DT should be an integer multiple of all rates used in the simulation. To facilitate such calculations it is easier to work with decimal base numbers. Thus, system parameters are changed slightly. Furthermore, frequencies are normalized by a factor of 10^6, i.e. 1 Hz in the simulated system is equivalent to 1 MHz in the actual system. Parameters of the simulated systems are

IF bandwidth = 40 Hz,

Sampling frequency f_s = 80 Hz,

IF center frequency = 100 Hz,

Baseband bandwidth = 5 Hz, and

Peak-to-peak frequency deviation = 10 Hz.

The above parameters meet most of the requirements for the FM/TDM system except its compatibility with existing NTSC systems, i.e. the sampling frequency in not an integer multiple of the line frequency and the color sub-carrier. The maximum frequency is 120 Hz which is an integer multiple of the IF bandwidth, also the sampling frequency is exactly twice the IF bandwidth. On the other hand, the IF bandwidth, and the peak-to-peak frequency deviation, are very close to present systems, which facilitates comparison with these systems.

From Equations 4.12 , 4.13, 5.7, and 5.8, for $a_1 = 0.1286$ W/A, and $OMD = 20\%$ we calculate $a_2 = 2.84757$ x 10^{-5} W/A^2 and $a_3 = 6.5087$ x 10^{-7} W/A^3.

The purpose of this simulation is to obtain *NLD* as a function of *OMD*. By changing the input signal magnitude the *OMD* will change accordingly. The laser chosen has $I_{th} = 45$ mA, while bias current $I_B = 80$ mA, hence input signal maximum magnitude of 35 mA is equivalent of $OMD = 100\%$. The power series nonlinear approximation given in Equation 5.2 is not valid for large *OMD* which may cause saturation or soft threshold distortion. Therefore, the results of the power series near 100% *OMD* may not considered accurate.

In the analysis the quantum efficiency of the photo-detector is assumed to be 0.7, the same value is taken for all simulations. Simulation system parameters are shown in table 5.1.

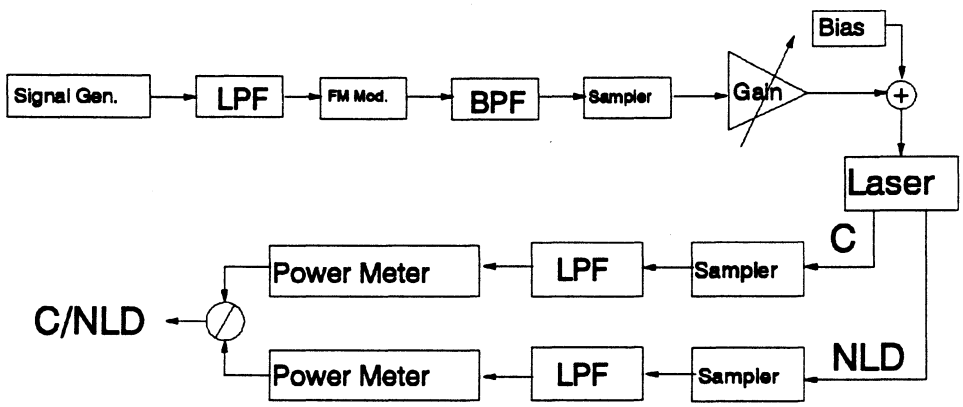

Figure 5.1: Simplified block diagram of the system

IF *NLD* vs. *OMD*.

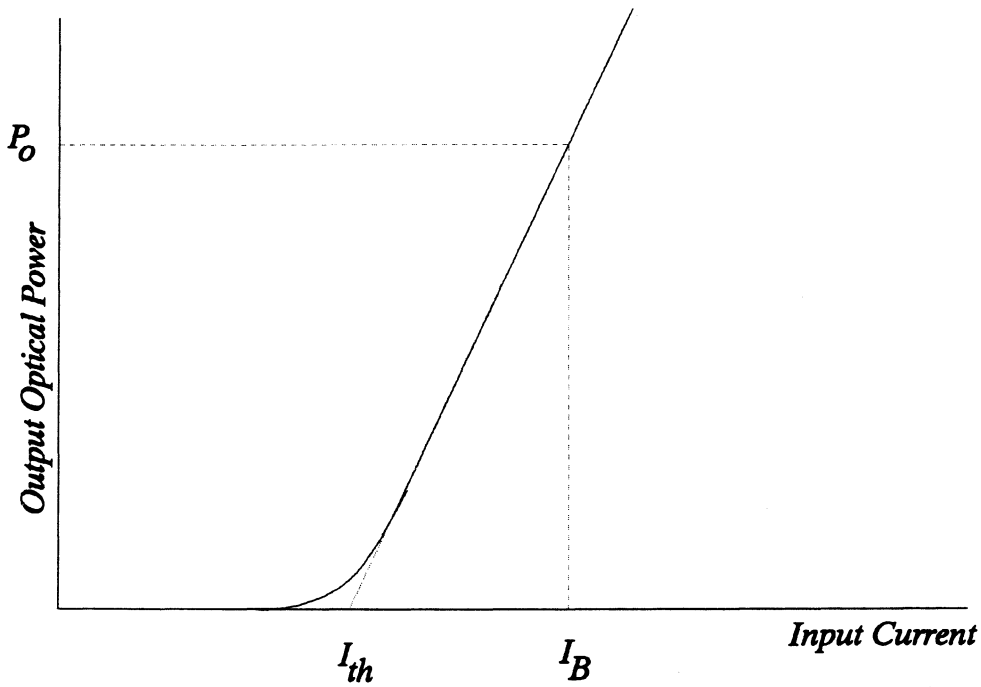

Figure 5.2: Input output characteristics of the laser.

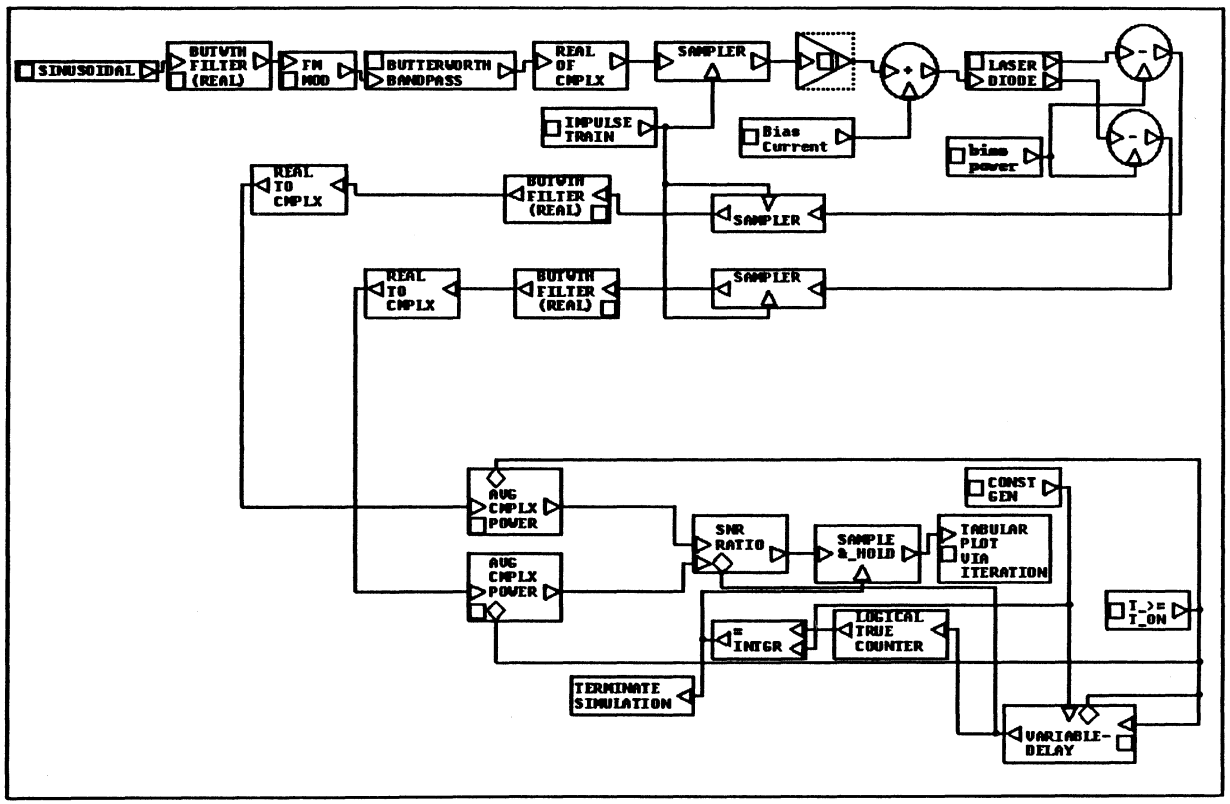

Figure 5.3: Detailed block diagram for the simulated system IF *NLD* vs *OMD*.

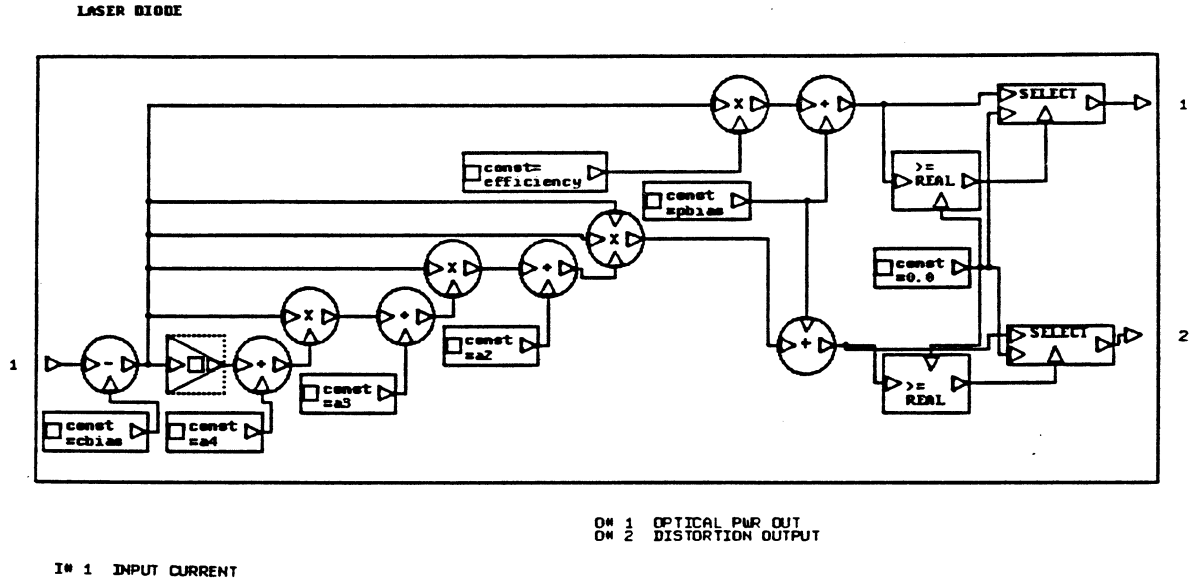

Figure 5.4: Block diagram for BOSS module "Laser Diode ".

STOP-TIME	= 14 seconds
DT	= 1.0 x 10^{-3} seconds
OPTICAL BIAS POWER	= 4.5 mW
TEST MODULATION INDEX	= 0.2
DIFFERENTIAL QUANTUM EFFICIENCY	= 0.1286 W/A
SECOND HARMONIC LEVEL	= 2.84757 x 10^{-5} W/A^2
THIRD HARMONIC LEVEL	= 6.5087 x 10^{-7} W/A^3
THRESHOLD CURRENT	= 45 mA
BIAS CURRENT	= 80 mA
INPUT SIGNAL MAGNITUDE	= 1 to 37 mA (10 steps)
BASEBAND FREQUENCY	= 1 Hz
SAMPLING FREQUENCY	= 80 Hz
FM CARRIER FREQUENCY	= 100 Hz
BANDPASS CENTER FREQUENCY	= 100 Hz
BANDPASS UPPER FREQUENCY EDGE	= 120 Hz
T-ON	= 8 seconds

Table 5.1: Simulation parameters for the system

IF *NLD* vs. *OMD*.

5.3.2 BASEBAND SIGNAL-TO-NOISE RATIO VS RECEIVED OPTICAL POWER

The principal simulation is to determine the baseband S/N as a function of received optical power in the presence of laser nonlinear distortion (with *OMD* equal to 90%) as well as all other noises (except relative intensity noise). The same system is used to generate the frequency spectrum of the signal at different points in the system for a particular received optical signal ($P_r = 4.5\ \mu$W). The results of these simulations are presented in the next chapter.

5.3.2.1 Simplified block diagram: Figure 5.5 is a simplified version of the actual simulated system. Similar to the previous simulation, the baseband sinusoid is generated by the signal generator, then it is frequency modulated and filtered. The signal is then sampled, followed by amplification to adjust the magnitude of the incoming signal to the desired *OMD* (90%). After adding the bias current, nonlinear distortion is then generated by the laser module which is approximated with a power series as given in Equation 5.2. The block "Optical loss" represents optical fiber loss. Hence, changing the optical loss changes the received optical power. Shot noise effects are added internally in the module "*p-i-n* photo-detector", and the receiver electronic thermal noise is added after the photo-detector. Thermal noise is represented by Gaussian a random noise generator with zero mean and variance proportional to the input noise current spectral density. This Gaussian noise is added to the sampled signal before the receiver's sampler. The signal is then sampled, filtered, and demodulated.

After demodulation the original sinusoid is filtered out and the

remainder of the received signal is considered to be noise and distortion. The S/N is then calculated by dividing the desired signal power by the noise power. This process is repeated for different received optical powers.

5.3.2.2 Details of the simulation: To recover the baseband signal, BOSS requires that the signal applied to the FM demodulator be in complex form. Therefore, as shown in Figure 5.6, the original FM signal is kept in complex form for all steps of the transmission channel.

The signal is first sampled by a complex sampler (which samples the magnitude and the phase), followed by the module "Real Coefficient Gain" which amplifies the magnitude of the incoming signal to the desired *OMD* (90%). Bias current is then added to both, the real part, and the imaginary part of the complex signal.

Nonlinear distortion is generated by the "Complex Laser" module shown in Figure 5.7. As seen from figure, both biasing current and biasing power are complex numbers with equal parts. Therefore nonlinear distortion is applied equally to both, real part, and imaginary parts. Substituting in Equation 5.2 with

$$i(t) = OMD \cdot I_M \cdot \sum_{n=-\infty}^{\infty} \left(e^{j(\omega_c t + \theta(t))} \right) . \delta(t - nT), \tag{5.9}$$

where OMD is the optical modulation depth,

I_M is the amplitude of the complex signal,

ω_c is the IF carrier radian frequency, and

$\theta(t)$ is the frequency modulation.

If we drop the term $\sum_{n=-\infty}^{\infty} \delta(t - nT)$ for convenience, then Equation 5.2 becomes

$$P_o = a'_o + a'_1 . OMD . I_M . e^{j(\omega_c t+\theta(t))} + a'_2 . (OMD.I_M)^2 . e^{j2(\omega_c t+\theta(t))}$$

$$+ a'_3 . (OMD. I_M)^3 . e^{j3(\omega_c t+\theta(t))} + \ldots\ldots , \qquad (5.10)$$

where a'_o, a'_1, a'_2, and a'_3 are the nonlinearity coefficients for the complex laser. By using Euler's identity we get

$$P_o = a'_o + \{a'_1.OMD.I_M . cos(\omega_c t+\theta(t)) + a'_2.(OMD.I_M)^2 . cos2(\omega_c t+\theta(t))$$

$$+ a'_3 . (OMD. I_M)^3 . cos3(\omega_c t+\theta(t)) + \ldots\ldots \}$$

$$+ j\{ a'_1 . OMD . I_M . sin(\omega_c t+\theta) + a'_2 . (OMD.I_M)^2 . sin2(\omega_c t+\theta)$$

$$+ a'_3 . (OMD. I_M)^3 . sin3(\omega_c t+\theta) + \ldots\ldots \}. \qquad (5.11)$$

Hence, both the real and the imaginary parts have second harmonic with a magnitude equal to $a'_2.(OMD.I_M)^2$; also both parts have third harmonic distortion with a magnitude equal to $a'_3.(OMD. I_M)^3$.

For a power series nonlinearity approximation with a real input signal, by substituting Equation 5.4 with coefficients up to a_3, in Equation 5.2 (again the term $\sum_{n=-\infty}^{\infty} \delta(t-nT)$ is dropped for convenience), and by collecting terms, we get

$$P_o = (a_o + \frac{a_2 OMD^2 I_M^2}{2}) + (a_1 OMD I_M + \frac{3}{4} a_3 OMD^3 I_M^3) cos(\omega_c t+\theta(t))$$

$$+ \frac{1}{2} a_2 . (OMD.I_M)^2 . cos2(\omega_c t+\theta(t))$$

$$+ \frac{1}{4}a_3.(OMD.\ I_M)^3.\ cos3(\omega_c t + \theta(t)) + \ \ldots\ldots, \tag{5.12}$$

By equating the coefficients of Equations 5.11 and 5.12 we get

$$a'_0 = a_0 + \frac{a_2 OMD^2 I_M^2}{2},\ a'_1 = a_1 + \frac{3}{4}a_3,\ a'_2 = \frac{1}{2}a_2, \text{ and } a'_3 = \frac{1}{4}a_3, \tag{5.13}$$

From the above equation we conclude the following: the fundamental coefficient for both lasers (the laser with complex input and the one with real input) is about the same ($a_1 \simeq a_1 + \frac{3}{4}a_3$); the second order coefficient for the complex laser is only half the one for the real laser; and the third order coefficient of the complex laser is one fourth the one for the real laser. These results are used later in Section 5.3.2.2 to calculate the simulation parameters.

The block "Optical Loss" represents optical fiber loss. The output of this module is simply equal to the input multiplied by a gain coefficient. By changing the gain coefficient the received optical power changes.

Similar to the complex laser module, the complex PIN photo-detector, shown in Figure 5.8 has two branches one for each part of the complex signal. Shot noise effects are simulated using a Poisson distributed random number added to each part separately in the block "PIN photo-detector". Hence, both components of the complex numbers are contaminated equally with noise (dark current and shot noise). Each branch of the complex photo-diode has an output current given by [30]

$$i(t) = \frac{q.\ n_p}{\Delta t}, \tag{5.14}$$

where q is the electronic charge,

n_p is the number of primary charge carriers generated in Δt seconds. The number of primary charge carriers n_p is modeled by a Poisson process, with an average number per Δt given by

$$\bar{N} = \frac{\eta}{hf} .P_i(t).\Delta t \ + \ n_d \ . \ \Delta t, \tag{5.15}$$

where $P_i(t)$ is the incident optical power,

η is the quantum efficiency,

h is Planck's constant,

f is the optical frequency, and

n_d is the number of dark charge carriers/second.

The exact number of primary charge carriers, n_p, is drawn from a Poisson distribution given by

$$P(n_p) = \frac{(\bar{N})^{n_p}.\ e^{-\bar{N}}}{n_p!}, \tag{5.16}$$

where $P(n_p)$ is the probability that n_p charge carriers are generated in a time interval Δt seconds.

The receiver electronic thermal noise is represented by a Gaussian random noise generator with zero mean, and variance proportional to the input noise current spectral density. Each time the simulation is executed (each DT seconds) a sample of this Gaussian noise is added to both parts of the complex signal.

After blocking the d.c. components, the signal is sampled, filtered and demodulated. After demodulation the original sinusoid (f=1 Hz) is filtered out and the contents of the band from 1.5 Hz to 5 Hz are treated as noise and distortion.

An ideal channel FM system (i.e. transmission channel without, nonlinear distortion, and sampling) is simulated simultaneously along with the FM/TDM system. To reduce computational errors particularly at high levels of S/N (note that BOSS uses single precision calculations), the distortion of the ideal channel FM system (N_i) is subtracted from the noise of the FM/TDM system (N_a). The difference ($N_d = N_a - N_i$) should be a closer estimation than N_a of the distortion of an actual system .

Baseband S/N is then calculated by dividing the demodulated signal power by the difference of the distortion N_d. The division and the log of the result is done in the module "SNR ratio". This calculation is repeated for different values of the "Optical loss", i.e. for different received optical powers. The results are discussed in the next chapter.

5.3.2.3 Simulation parameters:

- The simulation "Spectra" is used to display the magnitude signal spectrum at different points. To get the best results, DT should be selected to satisfy all the conditions mentioned in Section 5.2. Since this simulation is executed only once, the execution time is not vital. Thus, simulation sampling interval DT is selected to be 10^{-4} s.
- The second version of the simulation is to plot S/N vs. received optical power. This simulation should be repeated several times, furthermore it is not used to display signal spectra. Thus the high accuracy is compromised

with execution time. Therefore, as in the previous case, DT is selected to be equal to 10^{-3} s.

From Equation 5.14, we find expressions for second and third order harmonic distortions to be as follows:

$$\frac{2HD}{C} = \frac{\frac{1}{2}.a_2.OMD^2.I_M^2}{a_1.OMD.I_M + \frac{3}{4}a_3.\ OMD^3.I_M^3} \simeq \frac{1}{2}.\frac{a_2}{a_1}.OMD.I_M, \tag{5.17}$$

$$\frac{3HD}{C} = \frac{\frac{1}{4}.a_3.OMD^3.I_M^3}{a_1.\ OMD.I_M} = \frac{1}{4}.\frac{a_3}{a_1}.OMD^2.I_M^2, \tag{5.18}$$

For $OMD = 20\%$, and from Equations 4.12, 4.13, and the above equations, we calculate $a_2 = 5.695$ x 10^{-5} W/A^2 and $a_3 = 2.603$ x 10^{-6} W/A^3 (a_1 is already calculated to be 0.1286 W/A). The coefficients for the complex laser used in the simulations should be half what is found here. To be conservative we will use these coefficients for this simulation (the system performance is limited mainly by thermal noise).

Originally the input to the laser module should be in Watts, the output in μA, and the dark current in nA. To improve the accuracy of the module, all previous values are scaled by a value of 10^3. Hence the input is in milliwatt, dark current is in pA, and the output is in nA. Shot noise for the selected photo-diode is assumed to be 2 nA. Hence, the output power of the laser is written as 4.5 W (instead 4.5 x10^{-3}W), also the dark current is entered as 2000 nA (instead 2 nA as selected in Chapter 3).

Receiver thermal noise is represented by a Gaussian noise generator with a mean=0, and a variance *Var* should satisfy the basic identity:

Total thermal noise in the simulated channel =

Total thermal noise in actual channel.

This may be rewritten as follows

$$Var \,.\, B_s = < i_{ckt}^2 > \,.\, B_{IF} \,.\, K, \tag{5.19}$$

where Var is the variance of the noise in A^2/Hz (in the simulation),

B_s is the simulation bandwidth in Hz (40 Hz),

$< i_{ckt}^2 >$ is the noise density in A^2/Hz (5 x $10^{-22}A^2$/Hz),

B_{IF} is the IF bandwidth of the actual system (40 MHz), and

K is a scaling factor (convert the current from A^2 to nA^2 as indicated in the previous section i.e. $K = 10^{18}$).

The variance of the Gaussian random generator (Var) equivalent to $5x10^{-22}$ A^2/Hz is found to be equal to 500 A^2/Hz. This Gaussian noise is then added to both components of the complex signal. Simulation parameters for both systems simulated here are shown in Tables 5.2 and 5.3.

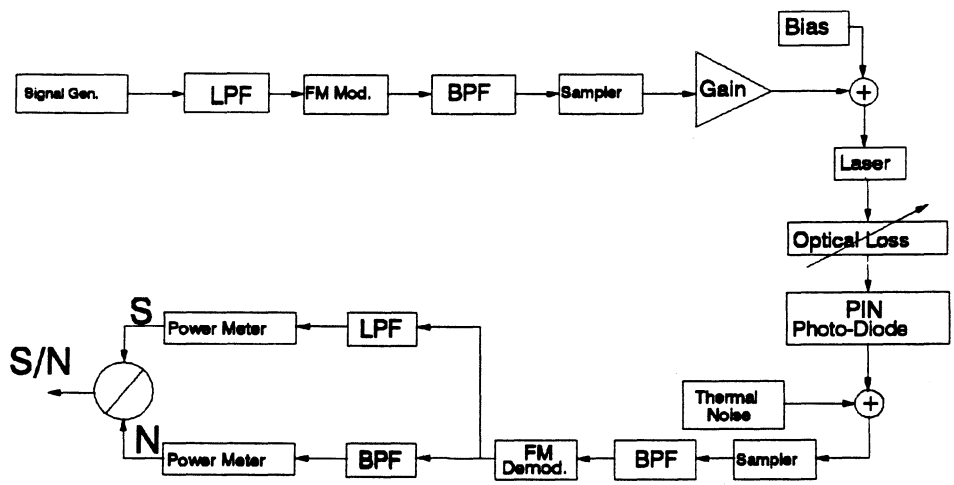

Figure 5.5: Simplified block diagram of the simulation system to calculate baseband S/N vs. received optical power.

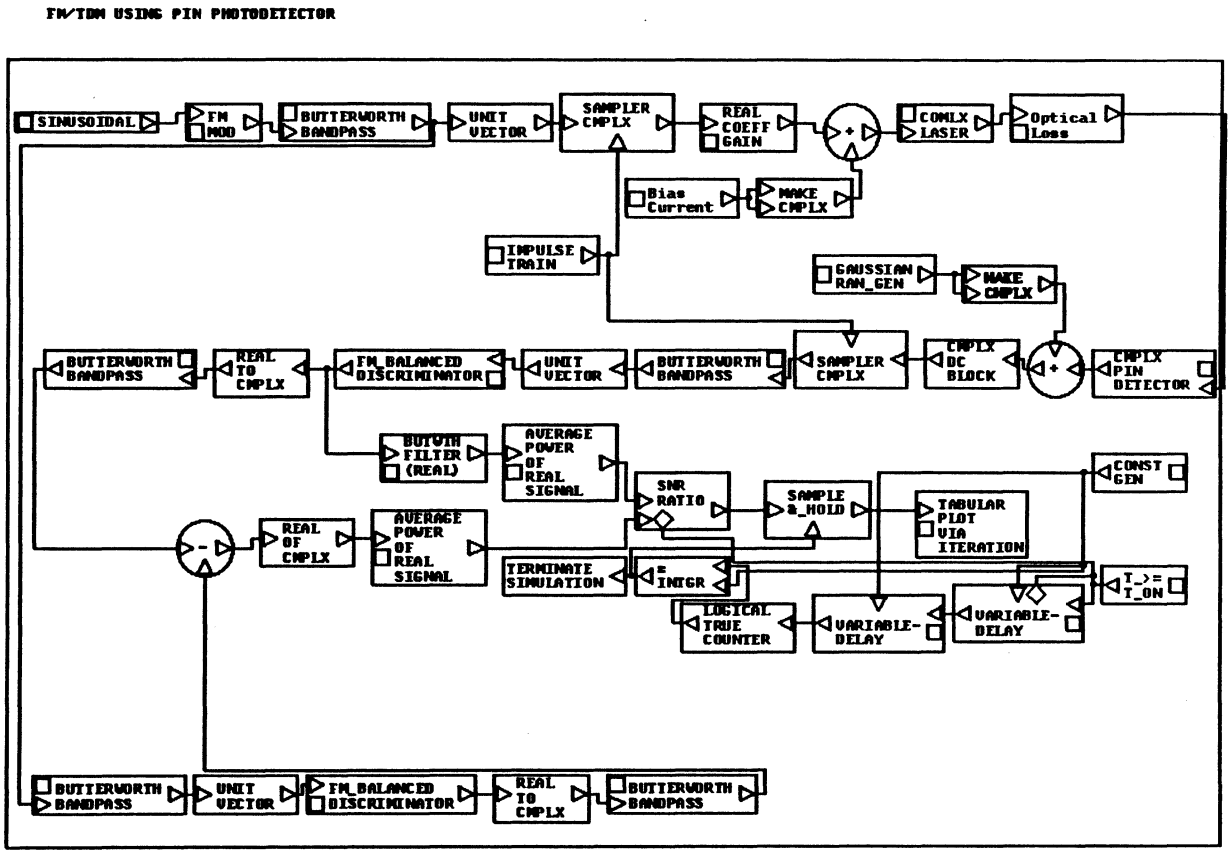

Figure 5.6: Detailed block diagram for the simulated system

Baseband S/N vs received optical power

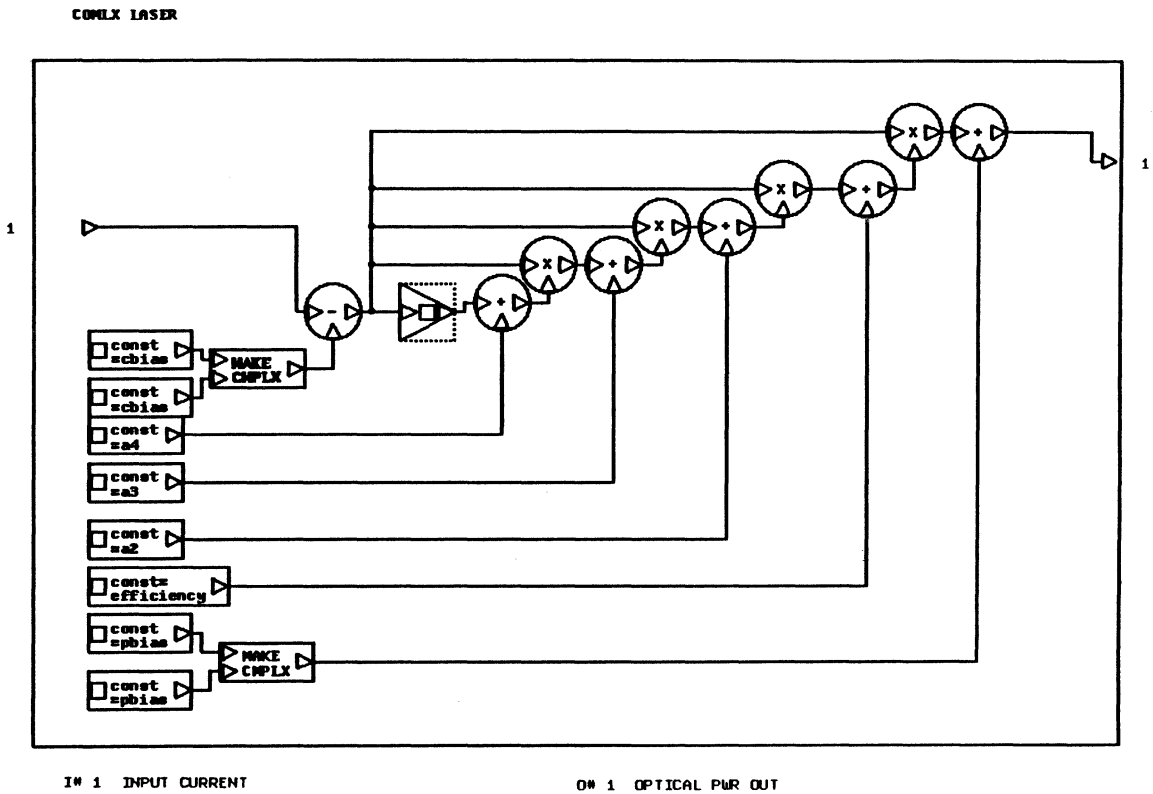

Figure 5.7: BOSS module "Complex Laser".

STOP-TIME	= 41 seconds
DT	= 1.0 x 10^{-4} seconds
OPTICAL BIAS POWER	= 4.5 mW
ATTENUATION FACTOR (fiber loss)	= 1x10^{-3}
TEST MODULATION INDEX	= 0.2
DIFFERENTIAL QUANTUM EFFICIENCY	= 0..1286 W/A
SECOND HARMONIC LEVEL	= 2.84757 x 10^{-5} W/A^2
THIRD HARMONIC LEVEL	= 6.5087 x 10^{-7} W/A^3
THRESHOLD CURRENT	= 45 mA
BIAS CURRENT	= 80 mA
INPUT SIGNAL MAGNITUDE	= 31.5 mA
BASEBAND FREQUENCY	= 1 Hz
SAMPLING FREQUENCY	= 80 Hz
FM CARRIER FREQUENCY	= 100 Hz
BANDPASS CENTER FREQUENCY	= 100 Hz
BANDPASS UPPER FREQUENCY EDGE	= 120 Hz
DARK CURRENT	= 2 nA
GAUSSIAN NOISE MEAN	= 0
GAUSSIAN NOISE VARIANCE	= 500 A^2/Hz
T-ON	= 35 seconds

Table 5.2: Simulation parameters for the system "Spectra".

STOP-TIME	= 31 seconds
DT	= 1.0 x 10^{-3} seconds
OPTICAL BIAS POWER	= 4.5 mW
TEST MODULATION INDEX	= 0.2
ATTENUATION FACTOR (fiber loss)	= 1x10^{-4} to 1x10^{-2} (22 steps)
DIFFERENTIAL QUANTUM EFFICIENCY	= 0.1286 W/A
SECOND HARMONIC LEVEL	= 2.84757 x 10^{-5} W/A^2
THIRD HARMONIC LEVEL	= 6.5087 x 10^{-7} W/A^3
THRESHOLD CURRENT	= 45 mA
BIAS CURRENT	= 80 mA
INPUT SIGNAL MAGNITUDE	= 31.5 mA
BASEBAND FREQUENCY	= 1 Hz
SAMPLING FREQUENCY	= 80 Hz
FM CARRIER FREQUENCY	= 100 Hz
BANDPASS CENTER FREQUENCY	= 100 Hz
BANDPASS UPPER FREQUENCY EDGE	= 120 Hz
DARK CURRENT	= 2 nA
GAUSSIAN NOISE MEAN	= 0
GAUSSIAN NOISE VARIANCE	= 500 A^2/Hz
T-ON	= 25 seconds

Table 5.3: Simulation parameters for the system

baseband S/N vs. received optical power

5.3.3 SIGNAL-TO-NOISE VS LASER'S NONLINEARITIES

This simulation is used to estimate baseband *S/N* vs. the degree of nonlinearities of the laser. The goal here is to find the limits of nonlinearities with which satisfactory operation may still be possible.

5.3.3.1 Simplified block diagram: A simplified system block diagram is shown in Figure 5.9. In this case, photodetector shot noise, dark current, and receiver thermal noise are not included, (assuming that *NLD* is the dominant distortion).

Similar to previous simulations, the baseband sinusoid is generated by the signal generator, then it is frequency modulated and filtered. The signal is then sampled, followed by amplification to adjust the magnitude of the incoming signal to the desired *OMD* (90%). After adding the bias current, nonlinear distortion is then generated by the laser module which is approximated with a power series as given in Equation 5.2. The ratio a_2/a_1 is varied from $10^{-5}A^{-1}$ to 0.3 A^{-1}, while a_3/a_2 is kept constant and equal to $10^{-2}A^{-1}$(this value is close to actual values of typical lasers). The coefficients a_4 and a_5 are assumed to be negligible.

After FM demodulation the original modulating tone is filtered out and the contents of the band from 1.5 Hz to 5 Hz are considered distortion resulting from the laser's nonlinearities. The *S/N* (which is limited by nonlinearities) is then calculated by dividing the signal power by the noise power for different values of a_2/a_1.

5.3.3.2 Details of the simulation: As indicated above, all sources of distortion other than nonlinearities are removed. Therefore, as shown in Figure 5.10, both the PIN photo-detector and the Gaussian random generator are removed. Removing the photo-detector eliminates shot noise, while removing the Gaussian random noise generator eliminates receiver electronic thermal noise.

Similar to the previous simulation system, after FM demodulation the original modulating tone is filtered out and the contents of the band from 1.5 Hz to 5 Hz are considered the nonlinear distortion. Also, to reduce computational errors, an ideal channel FM system is simulated simultaneously along with the FM/TDM system and the distortion of the ideal channel FM system is subtracted from the noise and distortion of the FM/TDM system. The results are discussed in the next chapter.

5.3.3.3 Simulation parameters: All simulation parameters here are similar to the simulation parameters of the previous system. The only difference is that the coefficients a_1, a_2, a_3 etc. are entered as harmonic levels, measured relative to the fundamental in dB, rather than polynomial coefficients (see Appendix). The ratio $\frac{a_2}{a_1}$ is varied from -50 dB to -5 dB , while $\frac{a_3}{a_2}$ is kept constant equal to -20 dB (equivalent to the ratio a_2/a_1 is varied from 10^{-5}A^{-1} to 0.3 A^{-1}, while a_3/a_2 is kept constant equal to 10^{-2}A^{-1}). Simulation parameters are shown in Table 5.4.

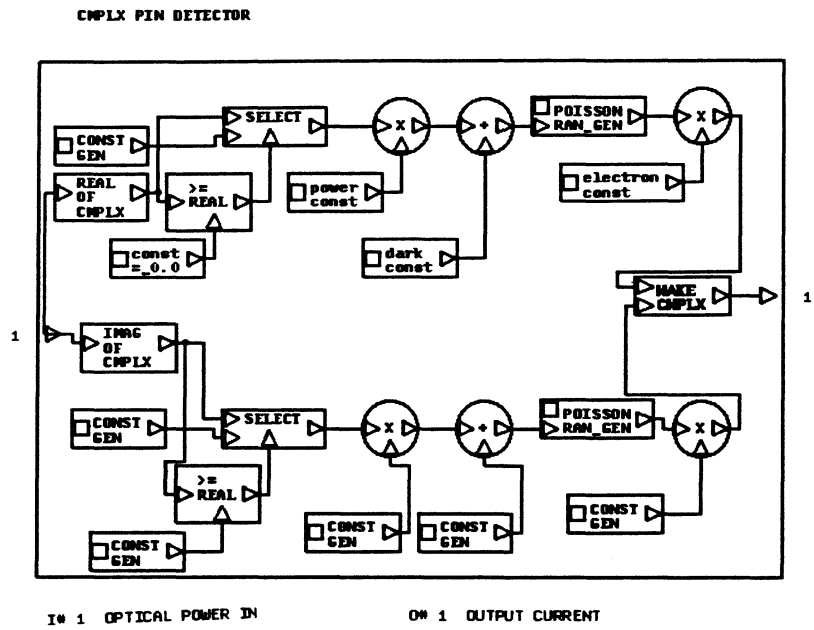

Figure 5.8: BOSS module "Complex PIN"

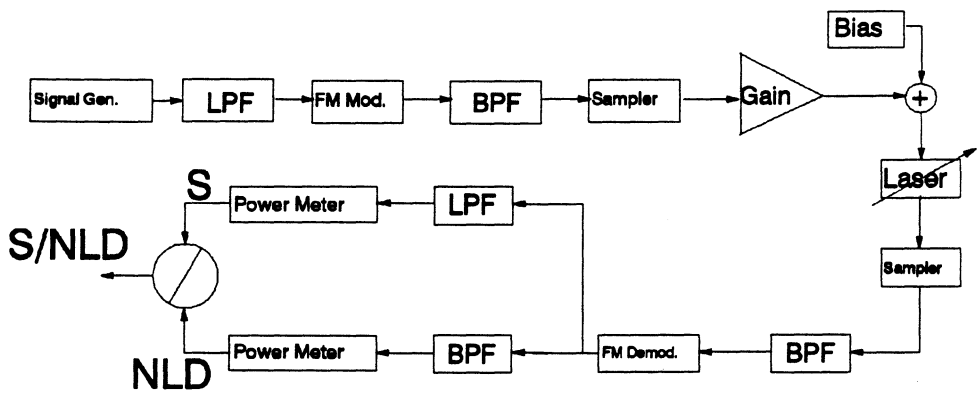

Figure 5.9: Simplified block diagram for the simulated system Baseband S/N vs. laser nonlinearities.

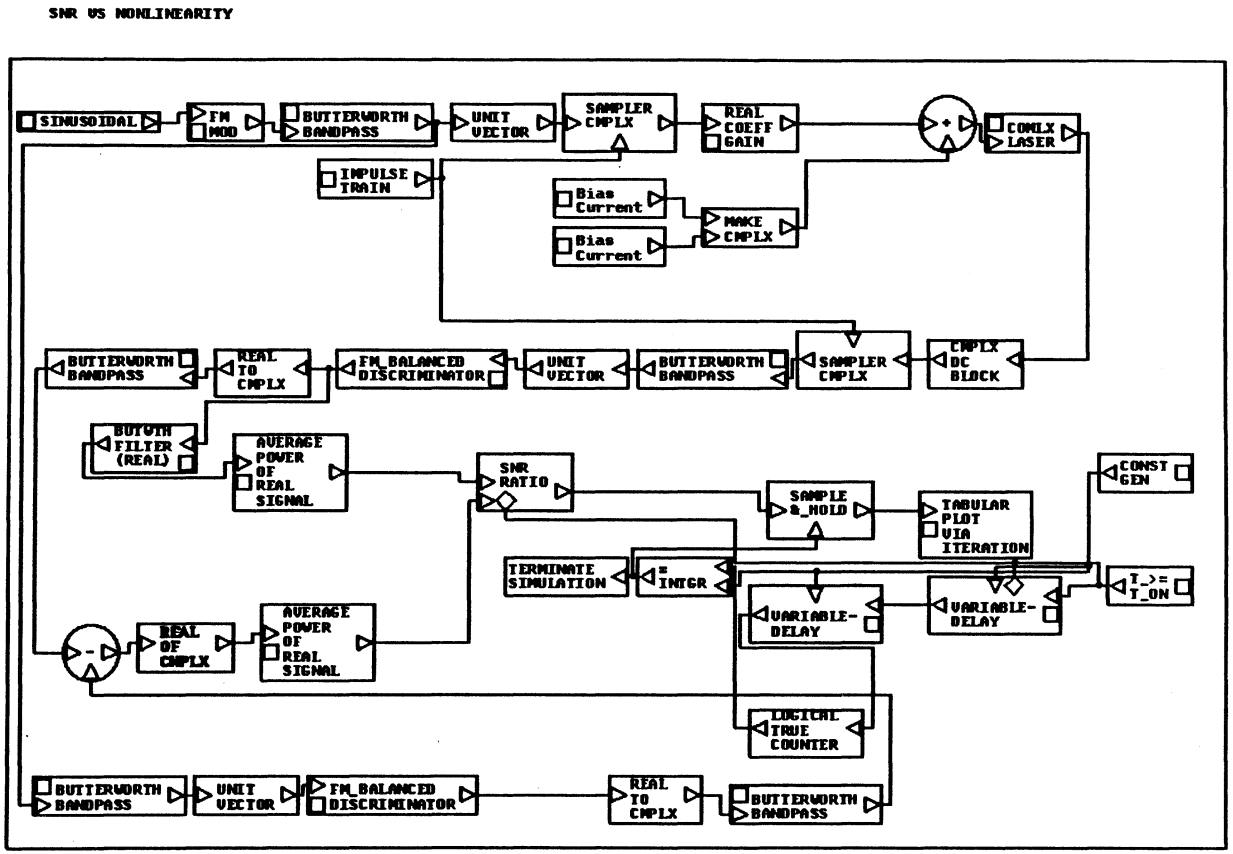

Figure 5.10: Detailed block diagram for the simulated system

Baseband S/N vs laser nonlinearities.

STOP-TIME	= 41 seconds
DT	= 1.0 x 10^{-3} seconds
OPTICAL BIAS POWER	= 4.5 mW
TEST MODULATION INDEX	= 0.2
DIFFERENTIAL QUANTUM EFFICIENCY	= 0.1286 W/A
SECOND HARMONIC LEVEL	= -50 to -5 dB (10 steps)
THIRD HARMONIC LEVEL	= -20 dB
SECOND HARMONIC LEVEL	= -20 dB
THRESHOLD CURRENT	= 45 mA
BIAS CURRENT	= 80 mA
INPUT SIGNAL MAGNITUDE	= 31.5 mA
BASEBAND FREQUENCY	= 1 Hz
SAMPLING FREQUENCY	= 80 Hz
FM CARRIER FREQUENCY	= 100 Hz
BANDPASS CENTER FREQUENCY	= 100 Hz
BANDPASS UPPER FREQUENCY EDGE	= 120 Hz
T-ON	= 35 seconds

Table 5.4: Simulation parameters for the system

Signal-to-Noise vs. Laser's Nonlinearities.

5.3.4 SIGNAL-TO-NOISE VS IF BANDWIDTH

As indicated in Section 3.4.2, second order and third order nonlinear distortion for a sampled system in the frequency domain is the convolution of the signal with it self twice and three times respectively (Equations 3.7 & 3.8). Therefore, second order distortion is symmetric around the center-band and has its peak magnitudes at the edges of the band, while third order distortion has its peaks at the center of the band and is also symmetric around the center of the band. Usually, second order distortion is larger than third order distortion ($a_2 \gg a_3$). Therefore, for high nonlinear distortion levels, it is expected that if the IF bandwidth is reduced the performance of the system may be improved somewhat (although further narrowing of the bandwidth increases the FM distortion, see results in Chapter 6). The purpose of this simulation is to verify this by determining the S/N (when limited by nonlinear distortion) as a function of the IF bandwidth. This is repeated for different levels of nonlinearities.

5.3.4.1 Simplified block diagram: In this system the *OMD* is fixed, as well as the laser nonlinearity levels. The ratio of the second order distortion coefficient with respect to laser efficiency $(\frac{a_2}{a_1})$ is entered in dB (the ratio actually has units of A^{-1}), while a_3/a_2 is kept constant equal to $10^{-2}A^{-1}$. The coefficients a_4 and a_5 are assumed to be negligible. The bandwidths of the two BPF's at both the transmitter and the receiver are varied.

Because of the nature of the noise (shot, and thermal noise are assumed to be uniformly distributed over the IF bandwidth), it is obvious that reducing the bandwidth will reduce the noise in the received signal. Therefore, noise is not included in this system, and only nonlinear distortion is considered.

Similar to the previous simulation system, after FM demodulation the original modulating tone is filtered out and the contents of the band from 1.5 Hz to 5 Hz are considered distortion resulting from the laser's nonlinearities. The *S/N* (which is limited by nonlinearities) is then calculated by dividing the signal power by the noise power for different values of the IF bandwidth. This process is repeated for different values of $\frac{a_2}{a_1}$.

5.3.4.2 Details of the simulation: Due to the need to recover the baseband signal at the receiver, the FM signal is kept in complex form for all the stages of the transmission channel. Therefore, the complex laser module is used followed by a d.c. block. Recovering the baseband signal and calculating the *S/N* is achieved in a way similar to the method described in Section 5.2.3.2.

5.3.4.3 Simulation parameters: This simulation is executed four times (for four levels of nonlinearities; thus the ratio $\frac{a_2}{a_1}$ is changed four times in steps of 10 dB ($10^{-1}A^{-1}$). The range is from $\frac{a_2}{a_1} = 10^{-1}A^{-1}(-10$ dB), to $\frac{a_2}{a_1} = 10^{-4}A^{-1}(-40$ dB)). The bandwidth of the BPF's are reduced from 40 Hz to 20 Hz in ten steps. The S/N is then calculated for each bandwidth. The value of a_3 is kept 20 dB below a_2 ($\frac{a_3}{a_2} = 10^{-2}A^{-1}$). The *OMD* is kept about 90% for all four simulations. The four simulation parameters are shown in table 5.5.

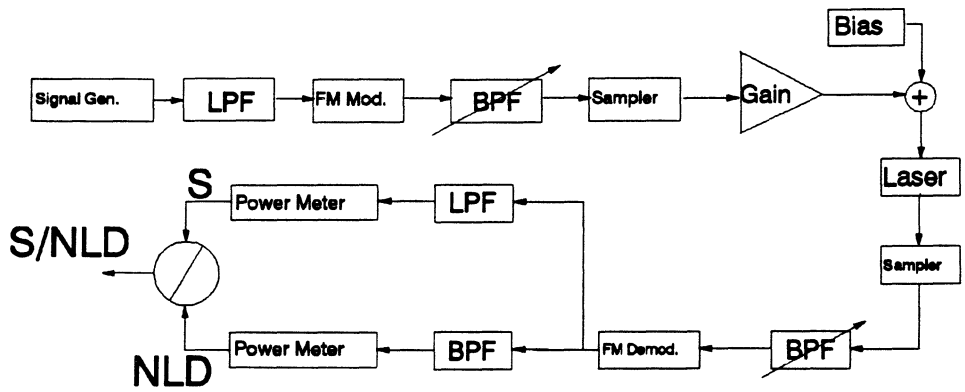

Figure 5.11: Simplified block diagram for the simulated system

Baseband S/N vs. IF bandwidth.

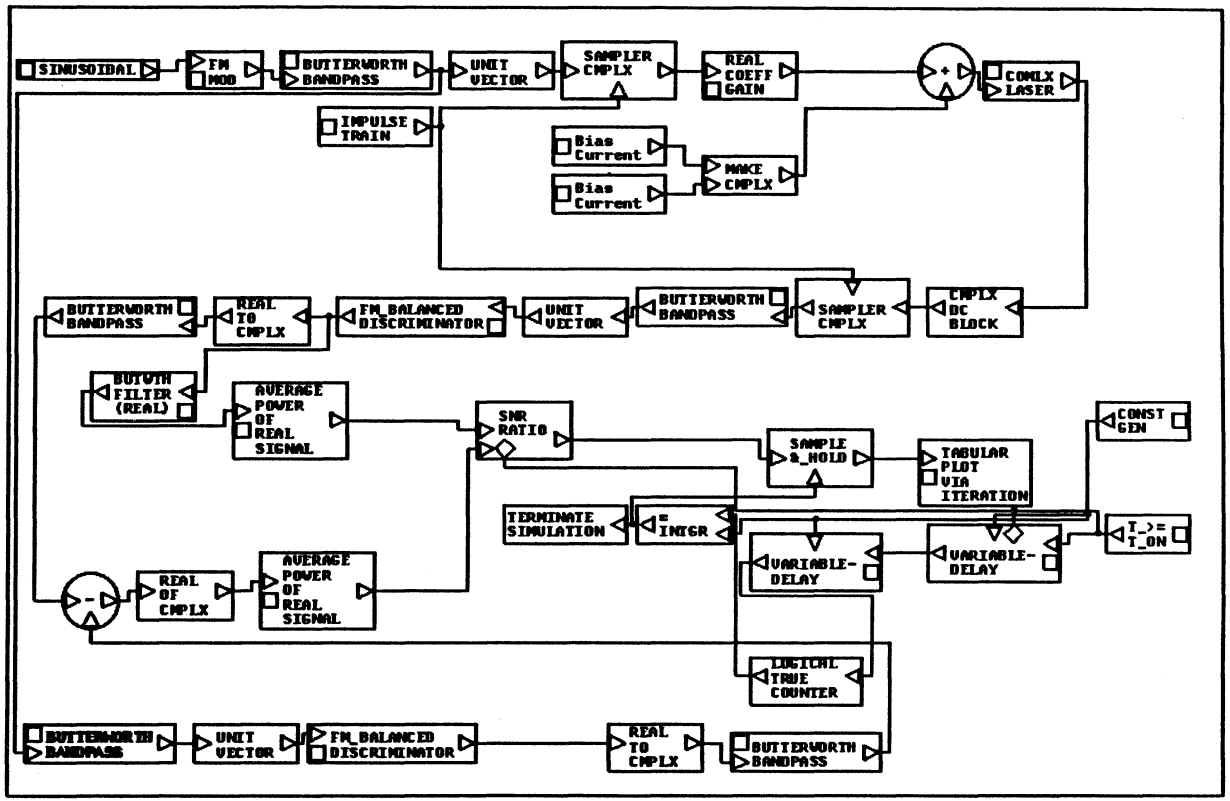

Figure 5.12: Detailed block diagram for the simulated system

Baseband S/N vs IF bandwidth.

STOP-TIME	= 20 seconds
DT	= 1.0 x 10^{-3} seconds
OPTICAL BIAS POWER	= 4.5 mW
TEST MODULATION INDEX	= 0.2
DIFFERENTIAL QUANTUM EFFICIENCY	= 0.1286 W/A
SECOND HARMONIC LEVEL	= $-10, -20, -30$, and -40 dB
THIRD HARMONIC LEVEL	= -20 dB
SECOND HARMONIC LEVEL	= -20 dB
THRESHOLD CURRENT	= 45 mA
BIAS CURRENT	= 80 mA
INPUT SIGNAL MAGNITUDE	= 31.5 mA
BASEBAND FREQUENCY	= 1 Hz
SAMPLING FREQUENCY	= 80 Hz
FM CARRIER FREQUENCY	= 100 Hz
BANDPASS CENTER FREQUENCY	= 100 Hz
BANDPASS UPPER FREQUENCY EDGE	= 120 Hz to 111 Hz (10 steps)

Table 5.5: Simulation parameters for the system

Baseband S/N vs. IF bandwidth.

CHAPTER 6

SIMULATION RESULTS

6.1 INTRODUCTION

In Chapter 4, analysis is used to evaluate the performance of the proposed system compared to presently used FM/FDM and PCM/TDM systems. In the previous chapter several simulation modules are suggested, not only to verify the analysis but also to find the limits for laser nonlinearities under which satisfactory performance is possible. Finally, a simulation module is also suggested to investigate the effect of the bandwidth on the overall S/N under heavy nonlinear distortion.

In this chapter the results of these simulations are presented and explained. Whenever possible they are compared to analytical results. The results shown below verify the conclusions we have reached in Chapter 4. They agree with analysis not only in trend but also in their values. Furthermore, simulations indicate that the proposed system may still be usable under more severe by nonlinear distortion conditions than those assumed initially for the analysis.

6.2 SIMULATION RESULTS

In this section simulation results are presented and compared to analytical results when applicable.

6.2.1 IF NONLINEAR DISTORTION VS. OPTICAL MODULATION DEPTH

The first simulation is to plot the IF C/N vs. *OMD* when the dominant distortion is the nonlinear distortion. As indicated in Chapter 5, the *OMD* of the laser is varied by varying the input signal magnitude while all other parameters are kept constant. The simulation results of the first system are shown in Figure 6.1. It is clear that these results have the same shape as the analytical results. In Figure 6.2, simulation results are plotted on the same graph with the analytical results. As seen from the figure, simulation results match more closely the curve for the PCM/TDM system (curve #2). This may be explained as follows: the simulation bandwidth was taken to be 40 MHz instead of 35.8 MHz (which is the value used for the analysis) to obtain the integer relation needed in the simulation. Therefore the simulation is expected to give slightly poorer performance than the analytical results. There is a better agreement with the PCM/TDM result because the bandwidth there is 43 MHz which is closer to the simulated bandwidth than the FM/TDM bandwidth.

The analysis and simulation indicates that the OMD could be 100% and satisfactory performance achieved. To be more realistic, and to avoid clipping distortions, we assume that the *OMD* in the FM/TDM system may be at most 90% instead of 100%. This *OMD* value is used for the following simulations.

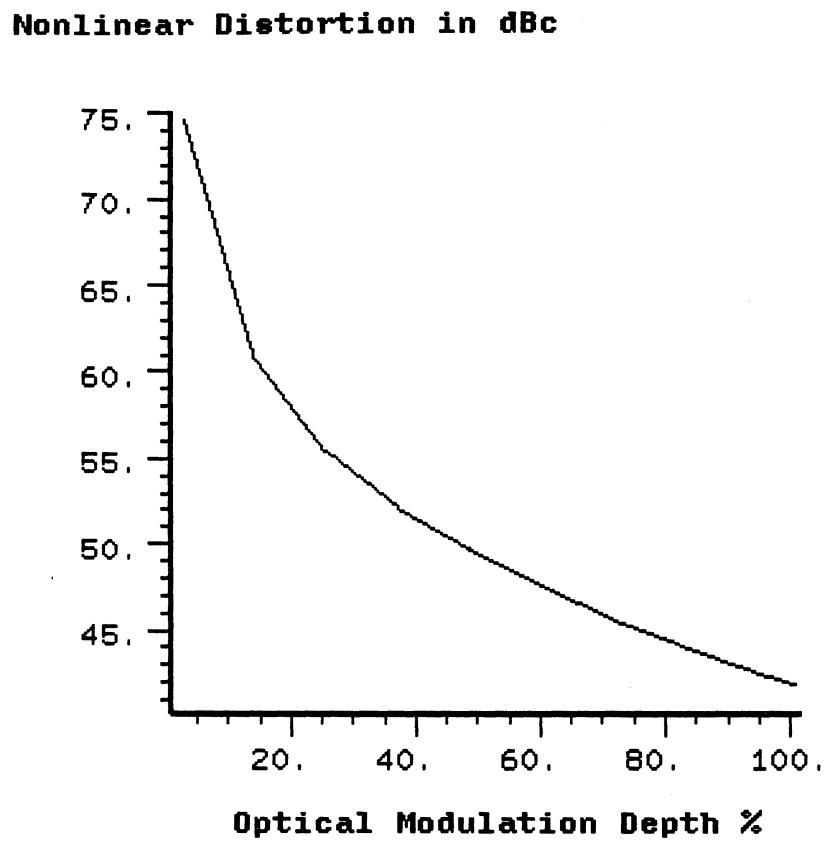

Figure 6.1: Simulation results for *NLD* in dB vs. *OMD%* for the FM/TDM system.

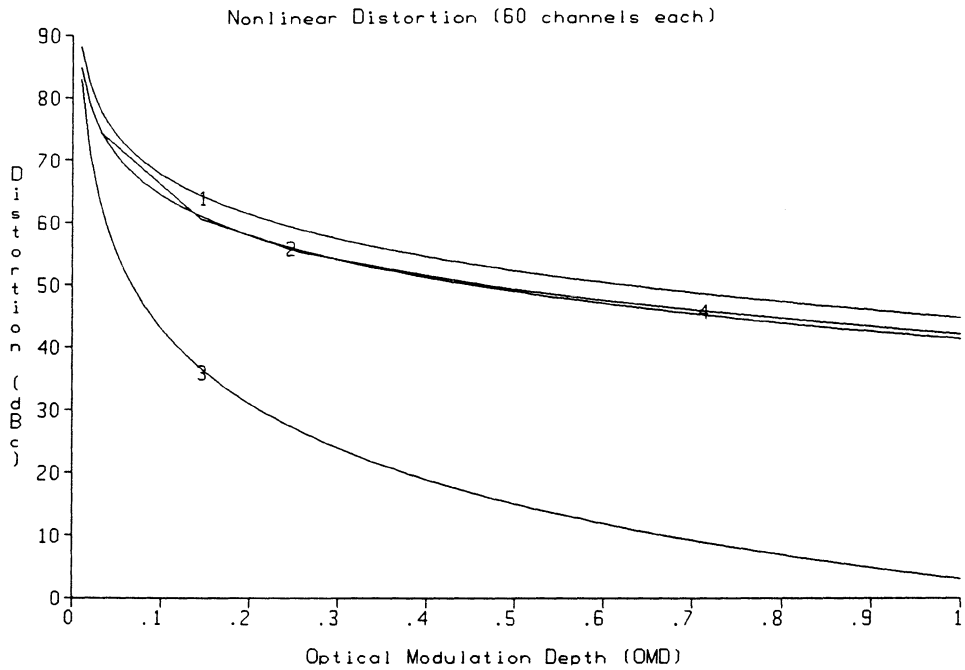

Figure 6.2: Simulation and analysis results for *NLD* in dB vs *OMD%* analytical results for (1) FM/TDM, (2) PCM/TDM, (3) FM/FDM, and simulation result for (4) FM/TDM system.

6.2.2 BASEBAND S/N VS. RECEIVED OPTICAL POWER

This simulation is divided into two parts; the first is to probe different test points and display the corresponding frequency response of the FM/FDM system, and the second is to estimate baseband S/N as a function of the received optical power. In both simulations, the exact values of the laser's nonlinearities, and all other noises are included (except *RIN* which is usually negligible compared to other noise sources in normal operating range).

6.2.2.1 FM/TDM System: The output optical power emitted by the laser diode is taken to be to be 4.5 mW (see Section 4.2.1). If the optical loss is 30 dB (factor of 10^{-3}), then the received optical power is 4.5 μW. In the first simulation the received optical power is assumed to be 4.5 μW. Test points for the displayed waveforms are shown on the simplified simulation block diagram of Figure 6.3. The next nine figures illustrate the power spectrum of the signal at different points of the simulated system. The input signal was a single sinusoid with frequency equal to 1 Hz.

- The power spectrum of the FM signal at *TP 1* is displayed in Figure 6.4. Note that the separation of the harmonics is equal to the modulating frequency which is 1 Hz (integer submultiple of the sampling frequency which is 80 Hz).
- The power spectrum of the sampled signal at *TP 2* is displayed in Figure 6.5. As seen from the figure there is no aliasing and the spectrum of the sampled signal (within the bandwidth of the original signal) is a replica of the original FM signal.
- The power spectrum of the sampled signal after laser's nonlinear distortion (*TP* 3) is shown in Figure 6.6. We can see from the figure that the nonlinear

distortion harmonics lie exactly on the harmonics of the original components with magnitudes greater at the edges than in the center. This is due to the fact that the dominant distortion (second order distortion) has its peaks at the edges of the band.

- The power spectrum of the output electrical current of the *p-i-n* diode (*TP* 4) with only shot noise and dark current is shown in Figure 6.7. As seen from the figure, shot noise and dark current are distorting the signal with an average level about 45 dB below the level of the carrier which is consistent with the analysis. This conclusion is further verified in section 6.2.4.
- The power spectrum of the output electrical current of the *p-i-n* diode with dark current, shot noise, and thermal noise (*TP* 5) is shown in Figure 6.8. As in the analysis (shown in Figure 4.6), the level of the thermal noise is about 20 dB higher than the level of shot noise.
- The power spectrum of the sampler output (*TP* 6) is shown in Figure 6.9. We notice that the noise level at the output of this sampler is about 18 dB less than the noise level at its input. As indicated in Section 4.5, the effective noise bandwidth is reduced by the ratio $\frac{\tau}{T_s} = \frac{1}{N}$ where τ in the sample duration, T_s is the sampling period, and N is the number of channels. When calculating the Gaussian noise generator spectral density "*Var*" (Section 5.2.2.3) we assumed a bandwidth of 40 Hz (with a scaling factor of 10^6) which is very close to the value of 36 MHz used in the analysis. In the analysis, the drop in the noise level equals to 10 x log(60) = 17.8 dB which is in very close agreement with the simulation.
- The power spectrum of the input baseband signal is shown in Figure 6.10. The spectrum consists of a single frequency component at 1 Hz.
- The power spectrum of the received baseband signal (*TP* 9) is shown in

Figure 6.11. The spectrum consists of harmonics which are the result of the nonlinearities, and white noise which is the result of other noise (mainly thermal noise).

- The power spectrum of the noise is shown in Figure 6.12. We notice that the band from 0 to 1.5 Hz is filtered out. The remainder of the band is considered as noise and distortion. The distortion consists of harmonics of the original applied tone which is the result of nonlinearities, and white noise which is due to mainly the receiver thermal noise. The white noise should be flat over the bandwidth of the signal, but this is not the case shown in Figure 6.12. The limited size of the memory of the BOSS post-processor (maximum of 8192 samples) limits the integration time in a displayed frequency response. If this time is extended to infinity, then the white noise in the base band should be flat.

6.2.2.2 Received Baseband S/N vs. Received Optical Power: In this simulation the *OMD* is fixed to 90% while the received optical power is varied (by varying the optical loss). As shown in Figure 6.13, the results have the same shape as the analytical results. In Figure 6.14 both simulation results and analytical results are shown on the same graph. We observe that the simulated curve is about 6 dB below the calculated curve. This is due to the fact that the calculated S/N is the weighted S/N; i.e., there is an extra 6 dB which accounts for the non-uniform response of the human eye to white noise in the video signal. When we account for this 6 dB the two curves match more closely.

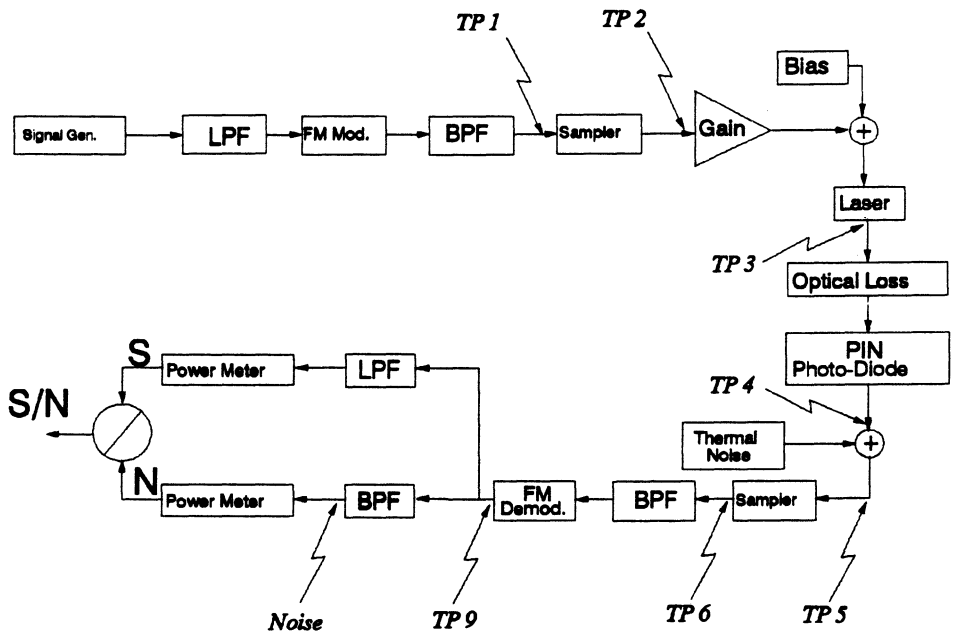

Figure 6.3: Simplified block diagram for the simulation system used to display the spectra at the indicated test points.

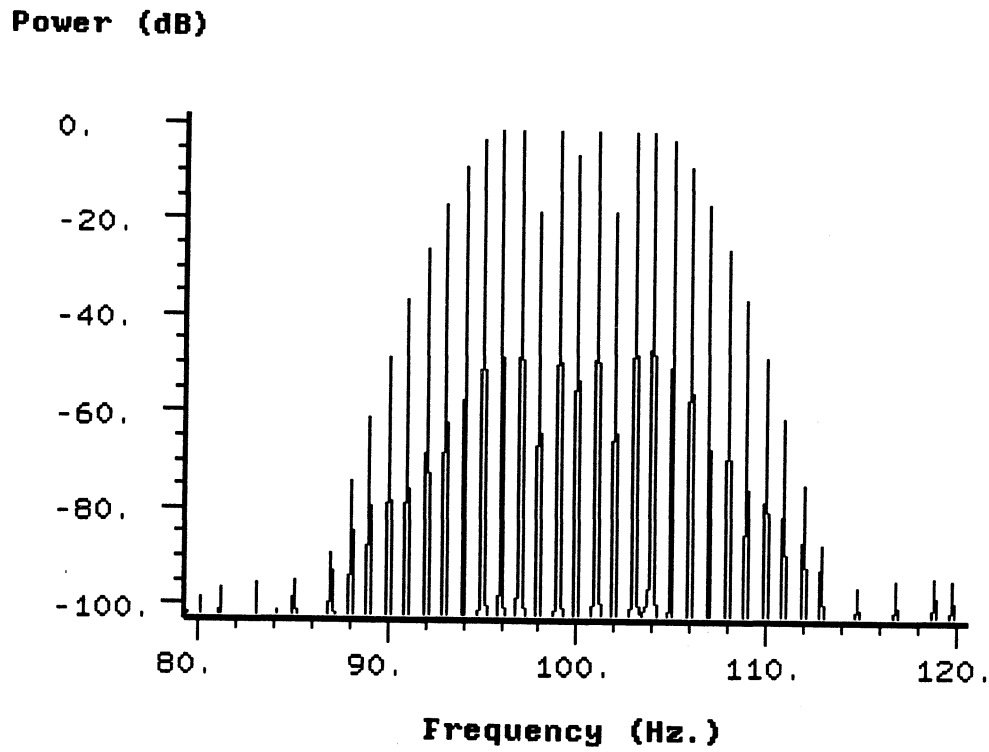

Figure 6.4: Power spectrum of the FM signal (TP 1).

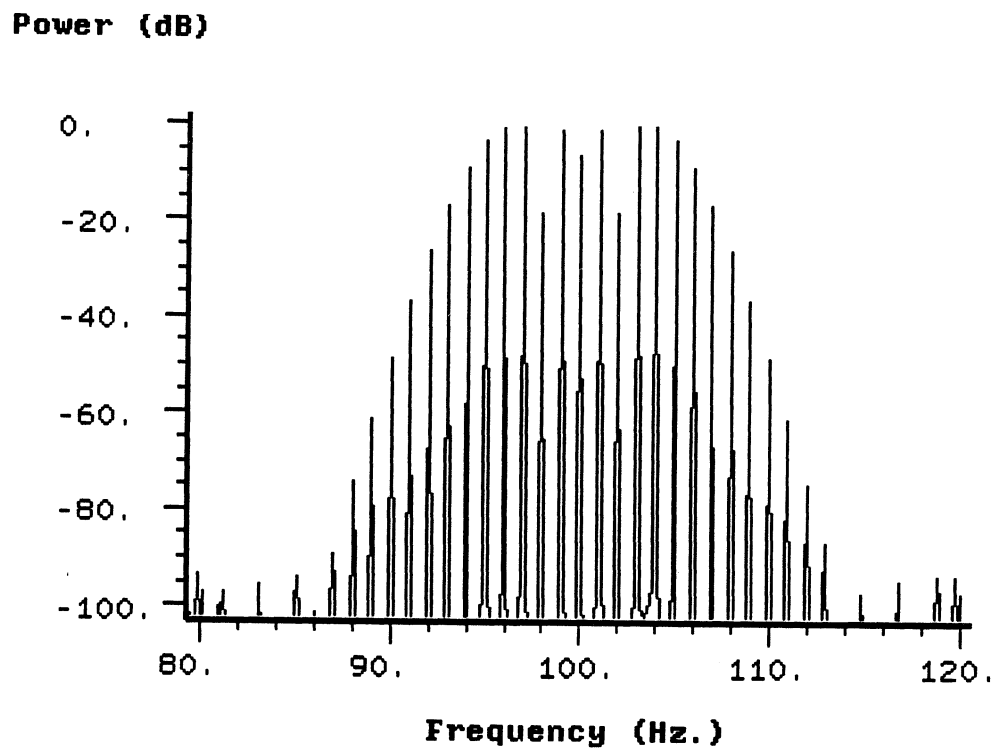

Figure 6.5: Power spectrum of the sampled FM signal (TP 2).

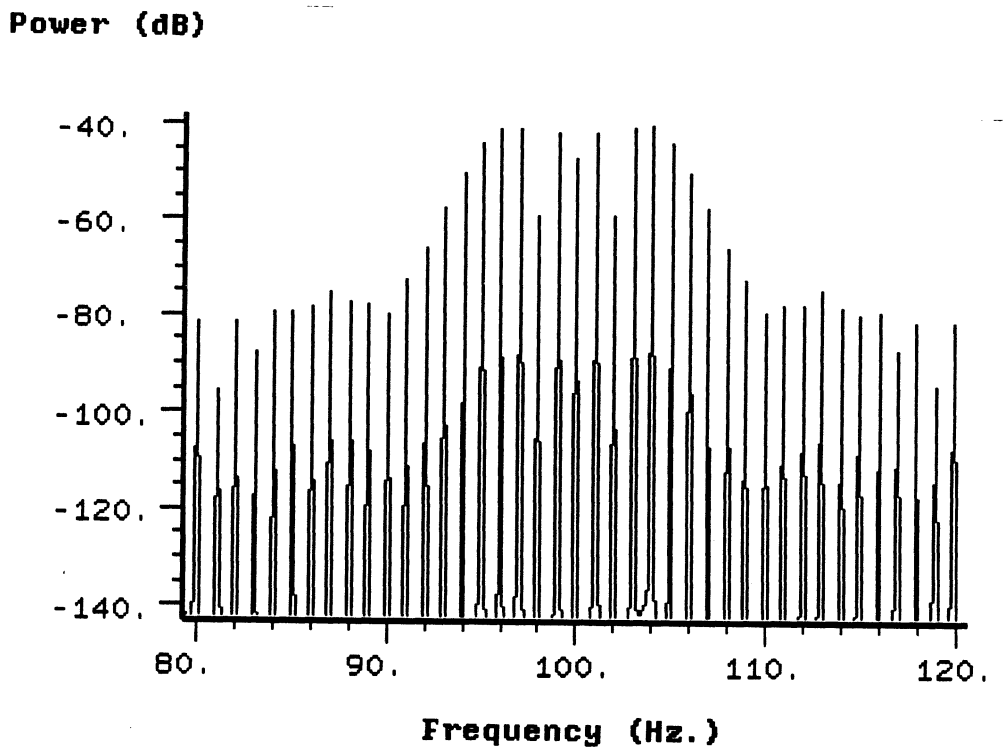

Figure 6.6: Power spectrum of the received optical signal after the nonlinear distortion (TP 3).

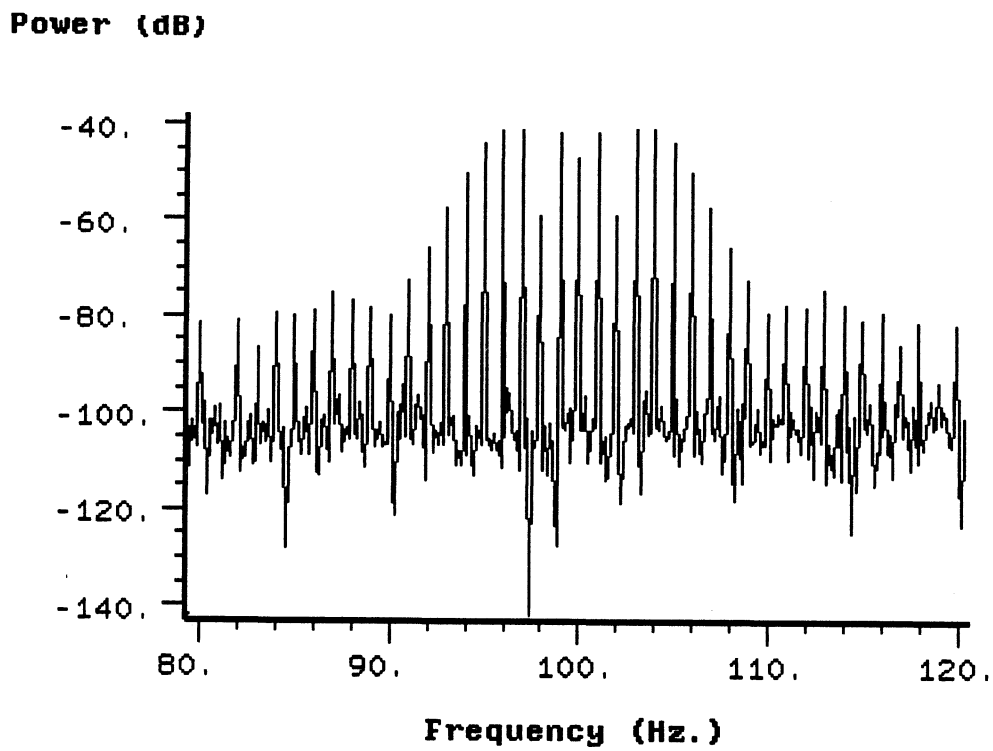

Figure 6.7: Power spectrum of the received electrical signal + nonlinear distortion + dark current + shot noise (TP4).

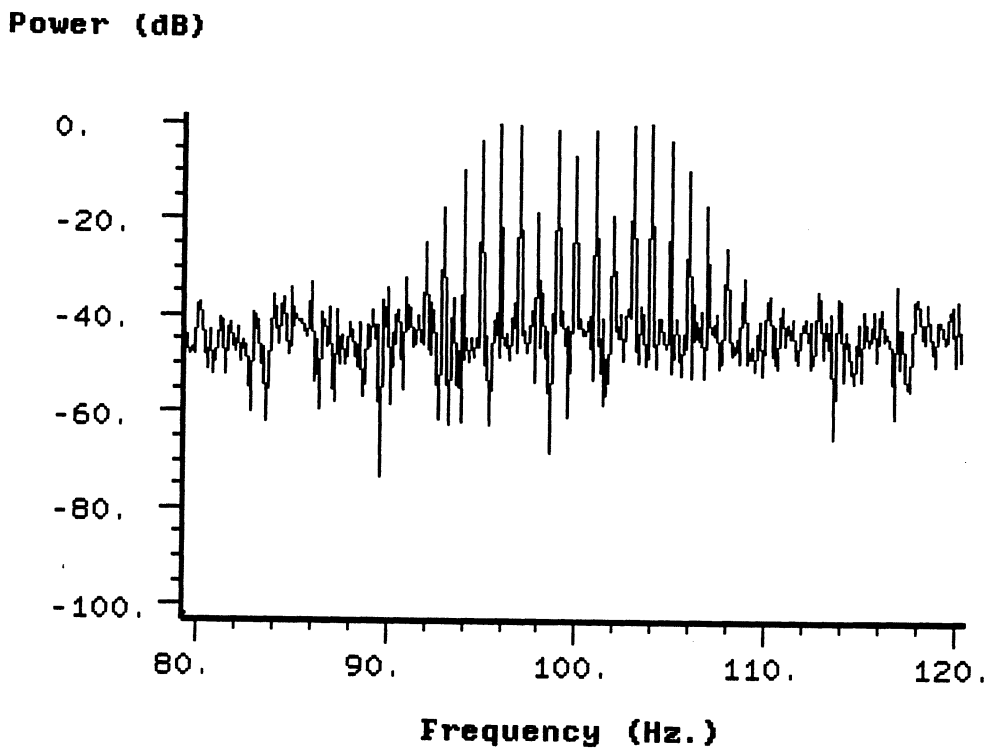

Figure 6.8: Power spectrum of the received sampled signal + all noises (nonlinear distortion, dark current, shot noise, and thermal noise) before receiver's side sampler (TP 5).

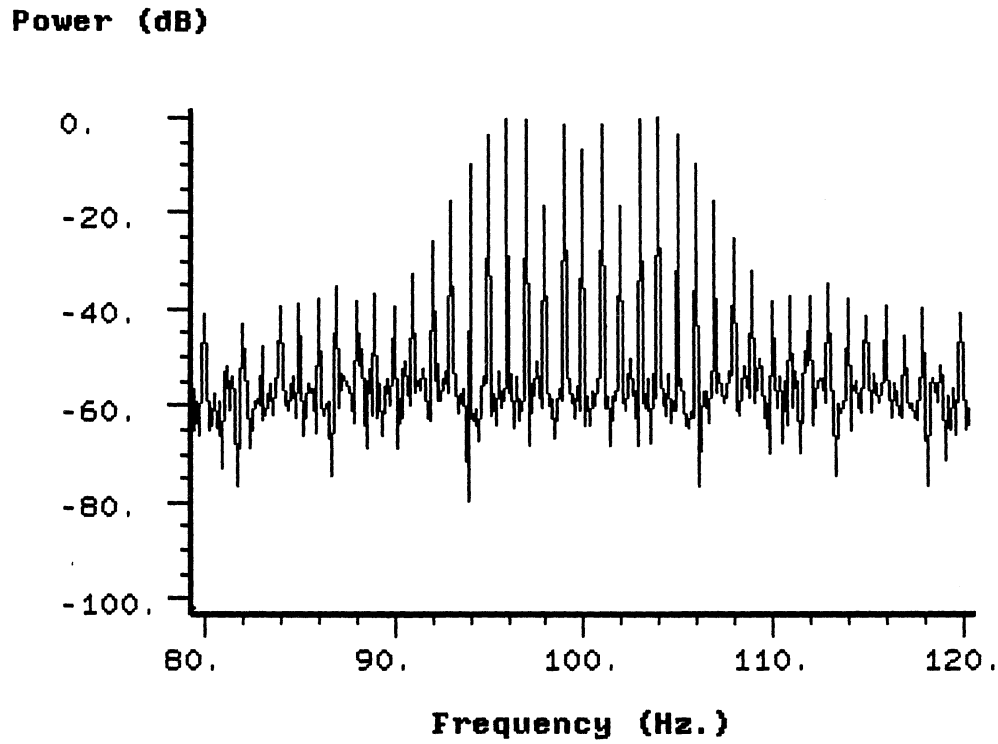

Figure 6.9: Power spectrum of the received signal after the receiver's side sampler (TP 6).

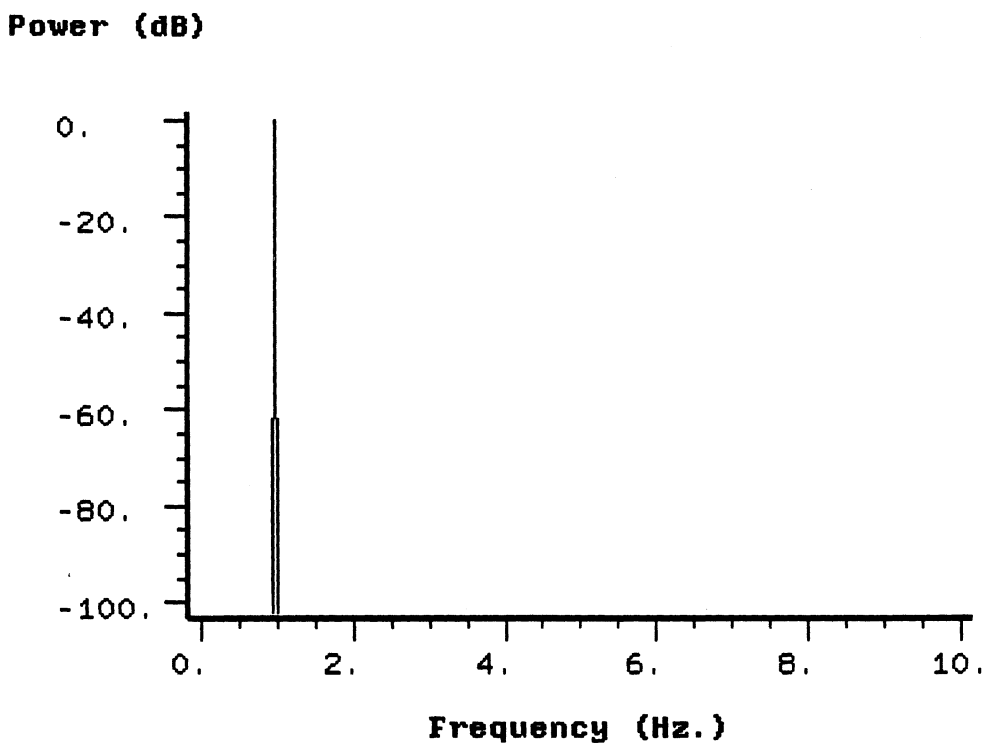

Figure 6.10: Power spectrum of the input baseband signal.

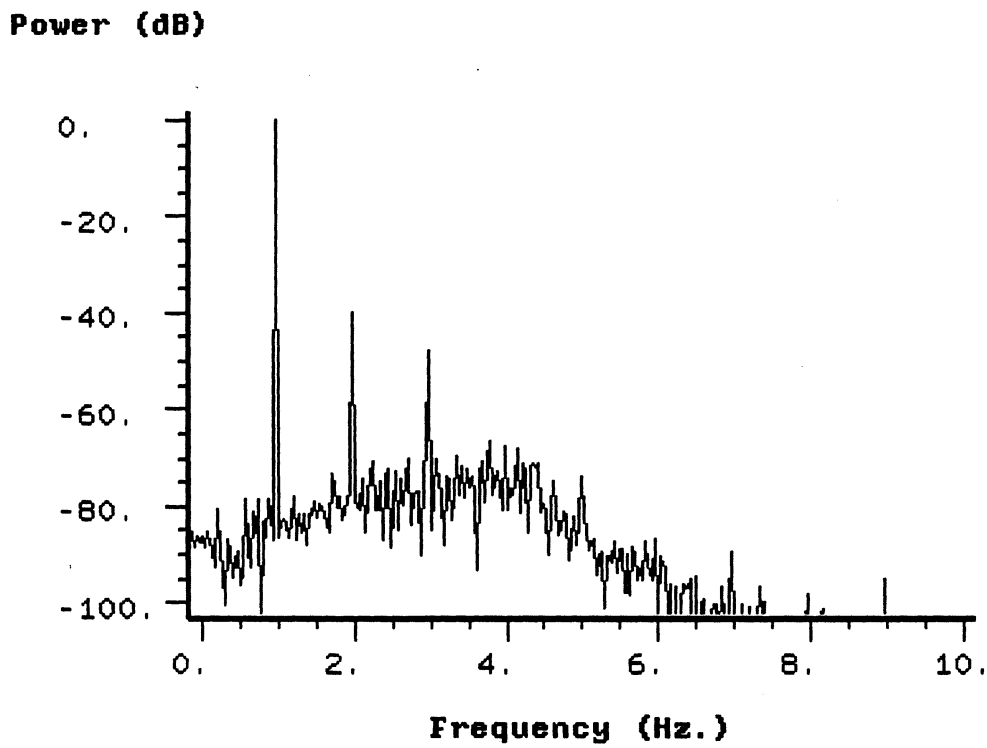

Figure 6.11: Power spectrum of the output baseband signal.

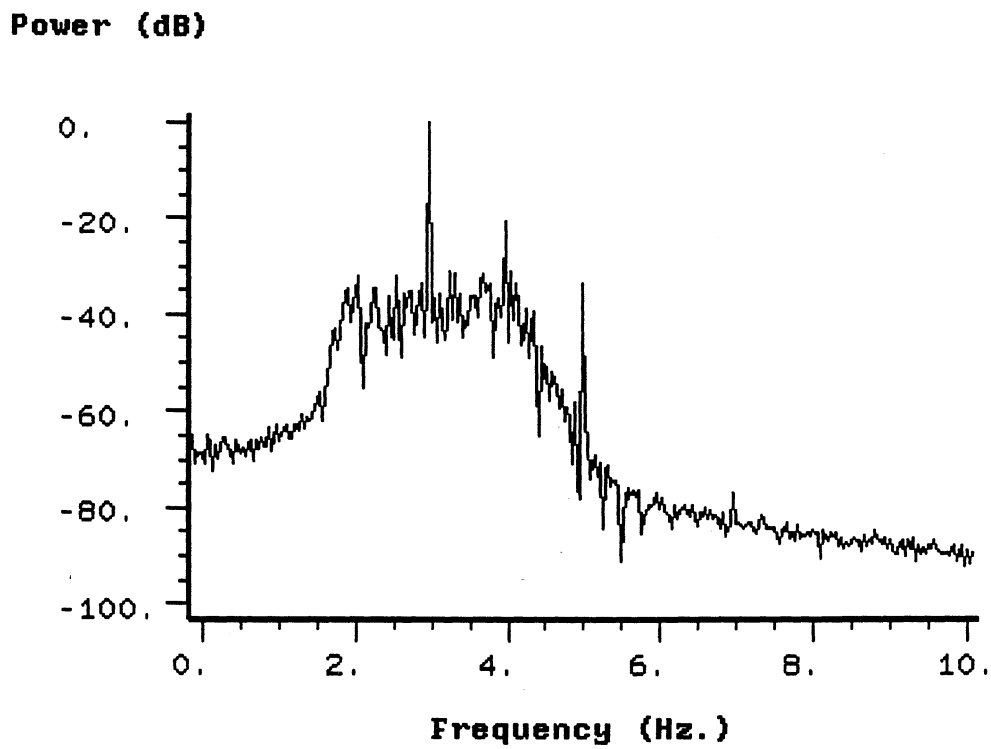

Figure 6.12: Power spectrum of the noise and distortion in the received baseband signal.

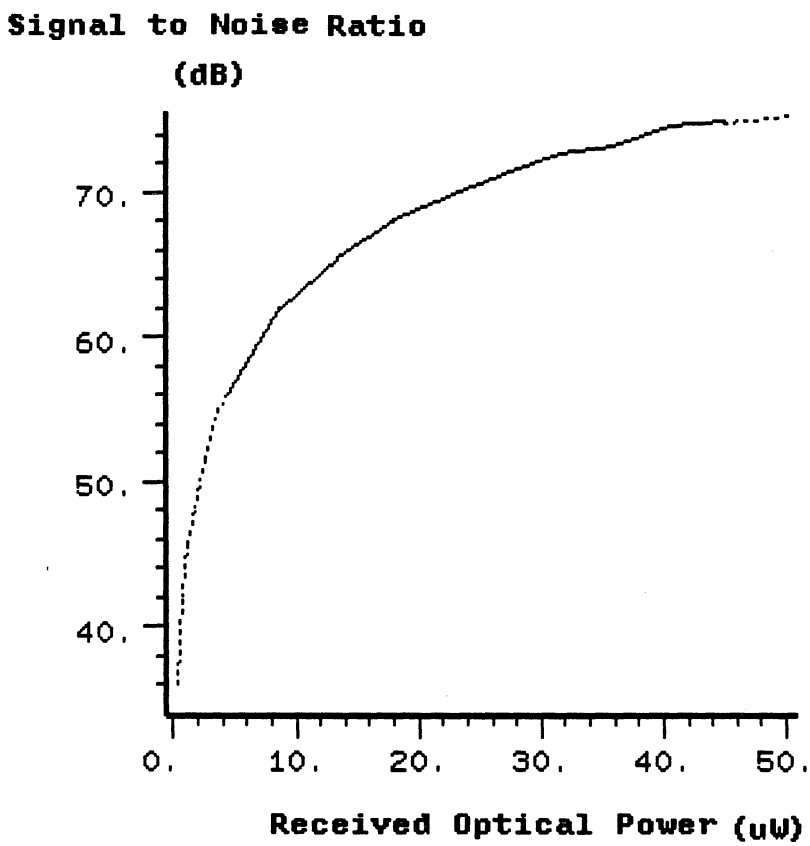

Figure 6.13: Baseband S/N in dB vs. received optical power in mW (simulation results).

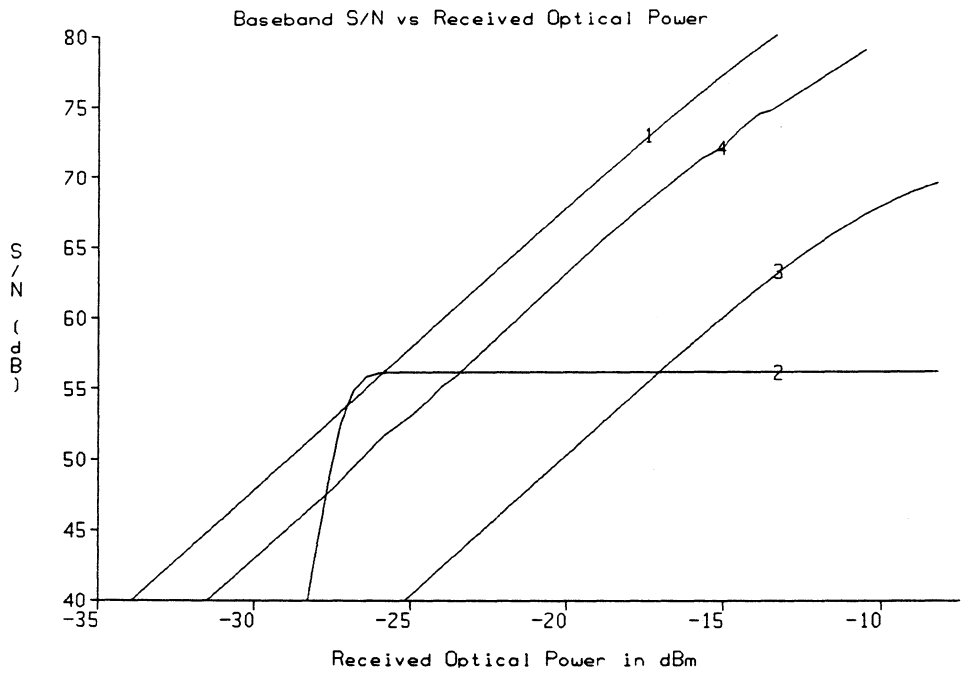

Figure 6.14: Baseband S/N in dB vs. received optical power in dBm analytical results for (1) FM/TDM, (2) PCM/TDM and (3) FM/TDM and simulation results for (4) FM/TDM system.

6.2.3 BASEBAND S/N VS LASER NONLINEARITY

In this simulation, the coefficients of the power series representing the nonlinearities are varied, while *OMD* is kept constant. The simulation results, shown in Figure 6.15, indicate for smaller values of a_2/a_1 *NLD* is negligible compared to the FM modulation/demodulation distortion, and thus it has no effect on the detected S/N until a_2/a_1 reaches a level of $\sim 10^{-3}$ A^{-1}, then the S/N starts to deteriorate. For $a_2/a_1 < 1.2\text{x}10^{-1}$ A^{-1} second harmonic distortion is the dominant distortion. For larger nonlinear distortion values, third order distortion becomes more significant. This explains the increase in the slope of the curve at the points 10^{-3} and $1.2\text{x}10^{-1}$ A^{-1}.

From the graph, the ratio a_2/a_1 could be as large as $10^{-3}A^{-1}$ without affecting the overall *S/N*. Note that the "typical" laser used in the analysis and simulations in the previous chapters had a_1=0.1286, a_2=5.595x10^{-5} and a_3=2.603x10^{-6}, i.e. a_2/a_1=4.4x$10^{-4}A^{-1}$ and a_3/a_1=2x$10^{-5}A^{-2}$. Thus, even considerably poorer lasers could be used in the proposed system. Hence, for a_1 equal to 0.1282, a_2 could be as large as $1.28\text{x}10^{-4}$ without affecting the overall *C/N* (i.e. very high S/N is achievable, limited by other noises). Furthermore, a_2 and a_3, may be as high as $1.3\text{x}10^{-3}$ W/A^2 and $1.3\text{x}10^{-5}$ W/A^3 respectively while still achieving the desired S/N (studio quality) with OMD equals to 90% (note here that *NLD* is one of the limiting factors to the overall C/N in addition to other noise sources). For the experiment reported by Olshansky et al. the coefficients of the laser used at OMD equals to 14% are $a_2 = 1\text{x}10^{-5}W/A^2$ and $a_3 = 1.7\text{x}10^{-8}W/A^3$ respectively. The bandwidth used in this experiment was less than one octave, thus there were no second order distortions. One may notice that because only third order distortions lie within the transmission

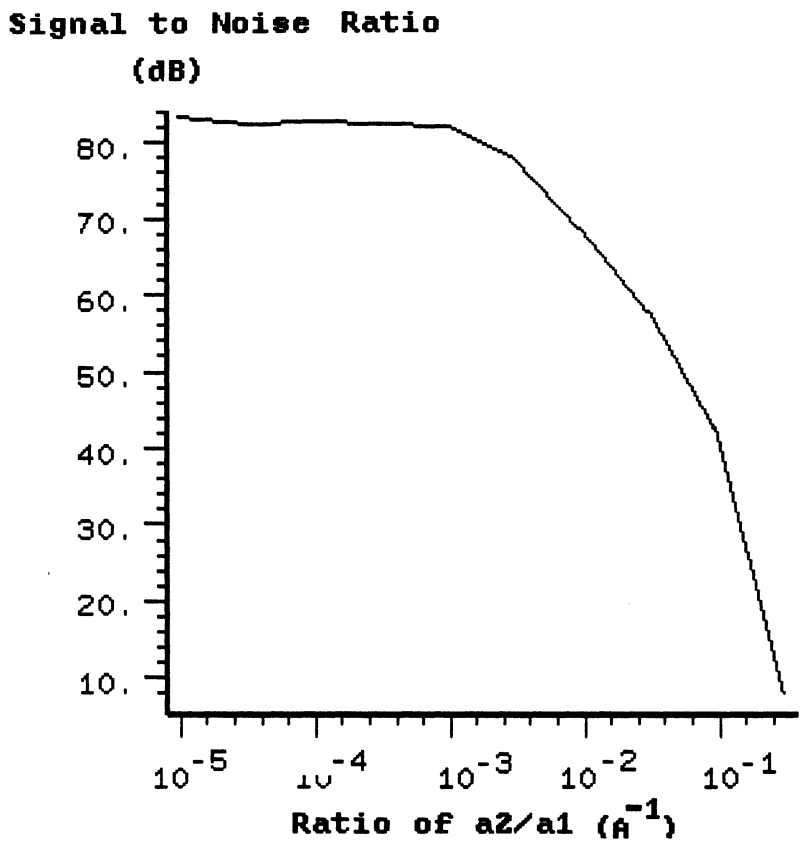

Figure 6.15: Baseband S/N in dB vs. Nonlinear Distortion for the FM/TDM System (Simulation result)

band, a_3 for the laser used is very small.

This simulation indicates that the proposed modulation scheme (FM/TDM) may result in relatively good performance by using lower cost optical components which are definitely not suitable for any present subcarrier multiplexed analog system.

6.2.4 BASEBAND S/N VS IF BANDWIDTH

This last simulation is to determine the effect of the IF bandwidth on the baseband *S/N* when the nonlinear distortion is dominant. For a given nonlinearity, the bandwidth of both IF BPF's (before and after the transmission channel) is varied from 20 Hz to 40 Hz. This process is repeated four times, curve #1 is for $a_2/a_1 = 10^{-1}$ A^{-1}, curve #2 is for $a_2/a_1 = 10^{-2}$ A^{-1}, curve #3 is for $a_2/a_1 = 10^{-3}$ A^{-1}, and curve #4 is for $a_2/a_1 = 10^{-4}$ A^{-1}. As seen in Figure 6.16, for small nonlinear distortion the best possible *S/N* is achieved with the widest bandwidth possible (~ 38 Hz for curve #1). But by increasing the nonlinear distortion, the maximum possible *S/N* may be achieved only if the IF bandwidth is reduced. As example, the maximum possible *S/N* for case #2 is about 1 dB less than case #1 with 4 Hz narrower bandwidth. For case #4 the maximum possible S/N is ~ 26 dB less than its counterpart of case #1 with a bandwidth of 14 Hz narrower than case #1.

If the noise were flat over the IF bandwidth then reducing the bandwidth by a given factor would increases the S/N by the same factor (assuming that most of the FM signal power is concentrated in the center of the IF band). For example reducing the bandwidth by a factor of 10% increases the S/N by the same factor (the noise entering the receiver is reduced).

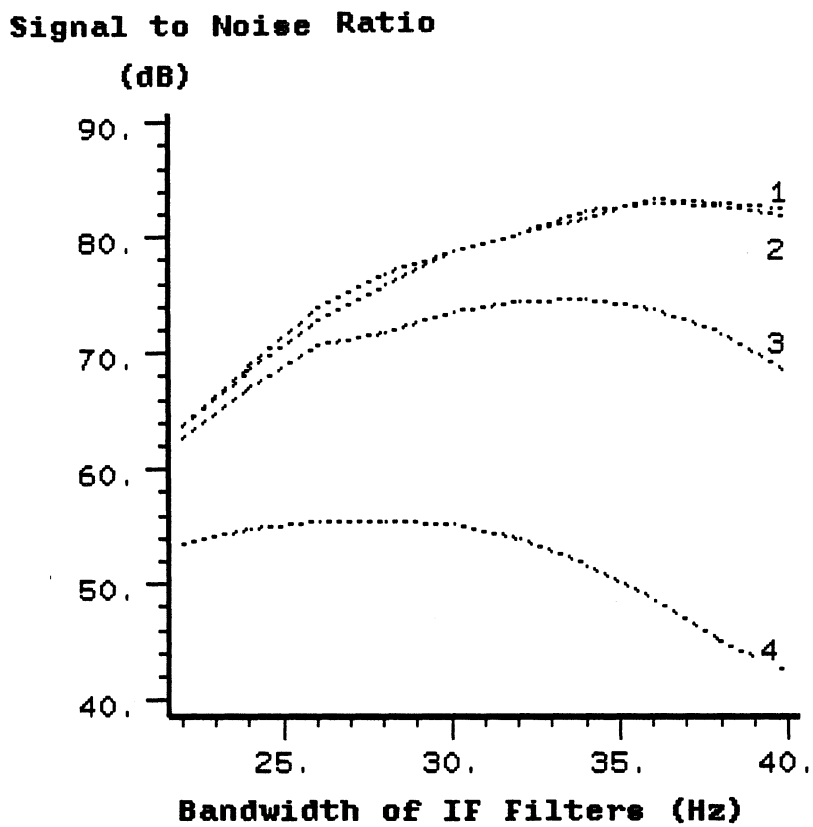

Figure 6.16: Baseband S/N in dB vs. IF bandwidth in Hz for (curve #1) $a_2/a_1 = 10^{-4}\text{A}^{-1}$, (curve #2) $a_2/a_1 = 10^{-3}\text{A}^{-1}$, (curve #3) $a_2/a_1 = 10^{-2}\text{A}^{-1}$, and (curve #4) $a_2/a_1 = 10^{-1}\text{A}^{-1}$

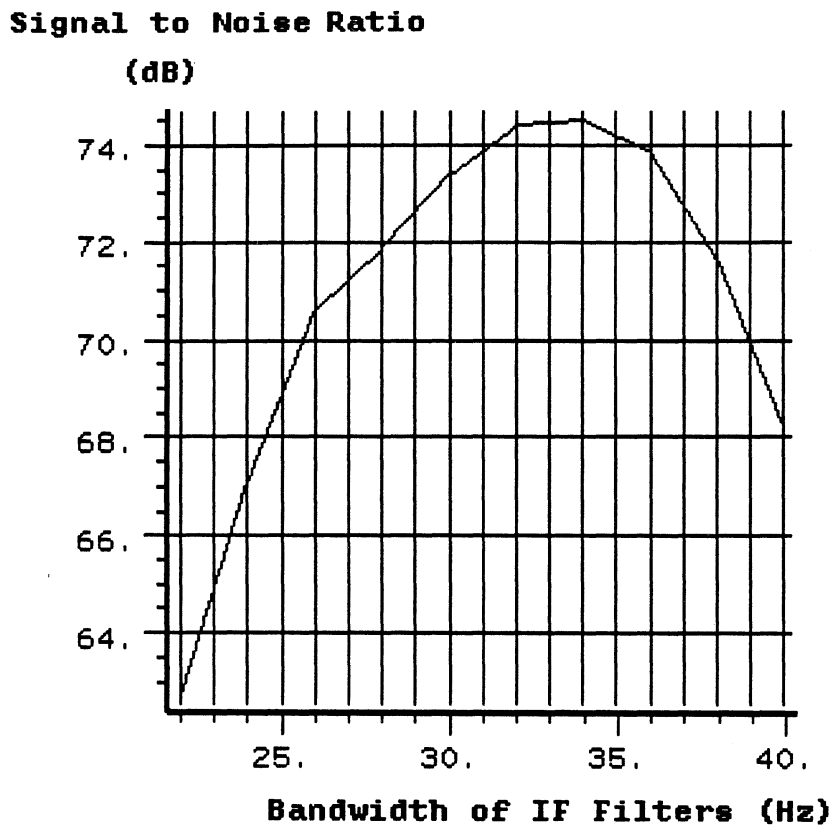

Figure 6.17: Baseband S/N in dB vs. IF bandwidth in Hz for $a_2/a_1 = 10^{-2}\mathrm{A}^{-1}$.

A more detailed graph for curve #3 is shown in Figure 6.17. As seen from the graph, a 6 Hz reduction (equivalent to 0.7 dB reduction) in the bandwidth results in a 6 dB improvement in the S/N. Thus, the improvement in the S/N is much more than the reduction in the IF bandwidth. This simulation verifies that the dominant second order distortion is not flat over the bandwidth but rather has peaks at the edges of the band. As the simulation suggests, these peaks may be avoided by reducing the IF bandwidth. The degree of bandwidth reduction is a function of the level of the nonlinear distortion.

6.3 SUMMARY

In this chapter, simulations are used to verify approximate analytical results and to find the limit at which a satisfactory operation is possible even with heavy nonlinear distortions. Moreover, the last simulation investigated the effects of the IF bandwidth on improving the overall *S/N* in the presence of high nonlinear distortions.

In the first simulation, the IF nonlinear distortion is estimated vs. *OMD*. Similar to analytical results we found that the *OMD* may be as high as 100% with negligible nonlinear distortion. To be more realistic and to avoid clipping effects, *OMD* of only 90% is used for the rest of the simulations.

The second simulation included all sources of noise. First the signal is probed and tested at different points of the system. The power spectrum of the signal at these points is examined, and the values of noise are found to be similar to the analytical values used in Chapter 4. By calculating the *S/N* for different received optical powers, a plot of the baseband *S/N* vs. received optical power is

found. The results agreed with analytical results given in Chapter 4.

The third simulation is to find the limits of nonlinearities under which the system may still gives acceptable received signal quality. The received baseband S/N is estimated as a function of laser's nonlinearities. The results indicate that lasers with considerably larger nonlinearities may be used.

Finally the effect of the IF bandwidth on the received baseband S/N is simulated. This simulation is repeated four times with different nonlinear distortions. The results indicate that the higher the level of nonlinear distortion the smaller the IF bandwidth should be. That is to say, nonlinear distortion is higher at the edges than in the center of the band.

CHAPTER 7

TIMING AND JITTER EFFECTS

7.1. INTRODUCTION

In time division multiplexed systems, it is essential that the receiver obtain accurate timing information indicating the proper time instants to operate the sampling device which selects the desired channel. In the FM/TDM system the problem is especially acute and the timing error must be held to a small fraction of the sample repetition interval for satisfactory performance. In general it is more desirable to extract the timing information from the signal itself, rather than transmitting a separate timing signal. For such self-timed receivers, the received signal is fed into timing recovery circuit which produces a "timing wave" which ideally has some periodic attribute, such as uniformly spaced zero crossings.

It is possible that the timing circuit might be simply a narrow-band filter tuned to a harmonic of the sample repetition rate. If the samples are raised cosine shaped, the spectrum vanishes at the sample rate r ($r = Nf_s$ where N is the number of channels, and f_s is the sampling rate). Hence it is essential that a nonlinear device, such as a square-law device or a full-wave rectifier, be inserted before the narrow-band filter. A block diagram of the timing recovery circuit is shown in Figure 7.1.

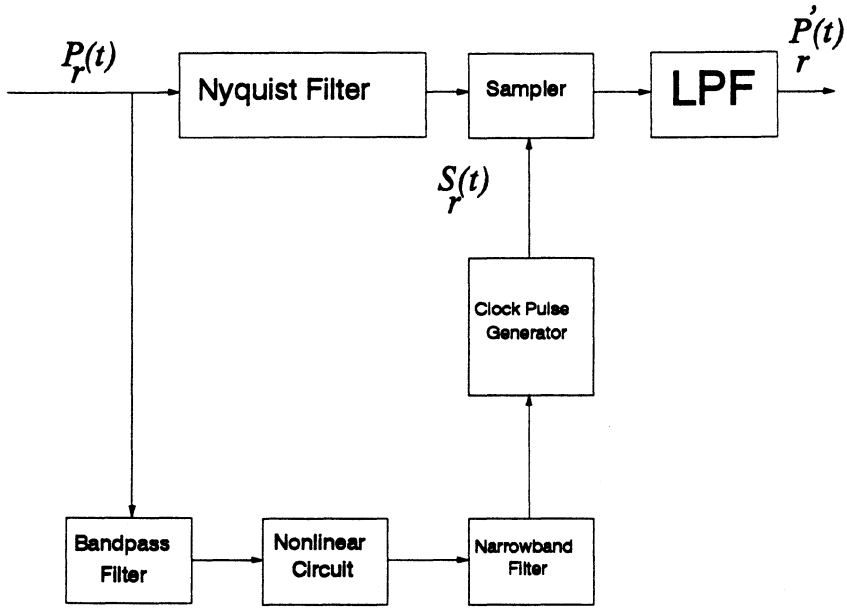

Figure 7.1 : Block diagram of the timing recovery circuit.

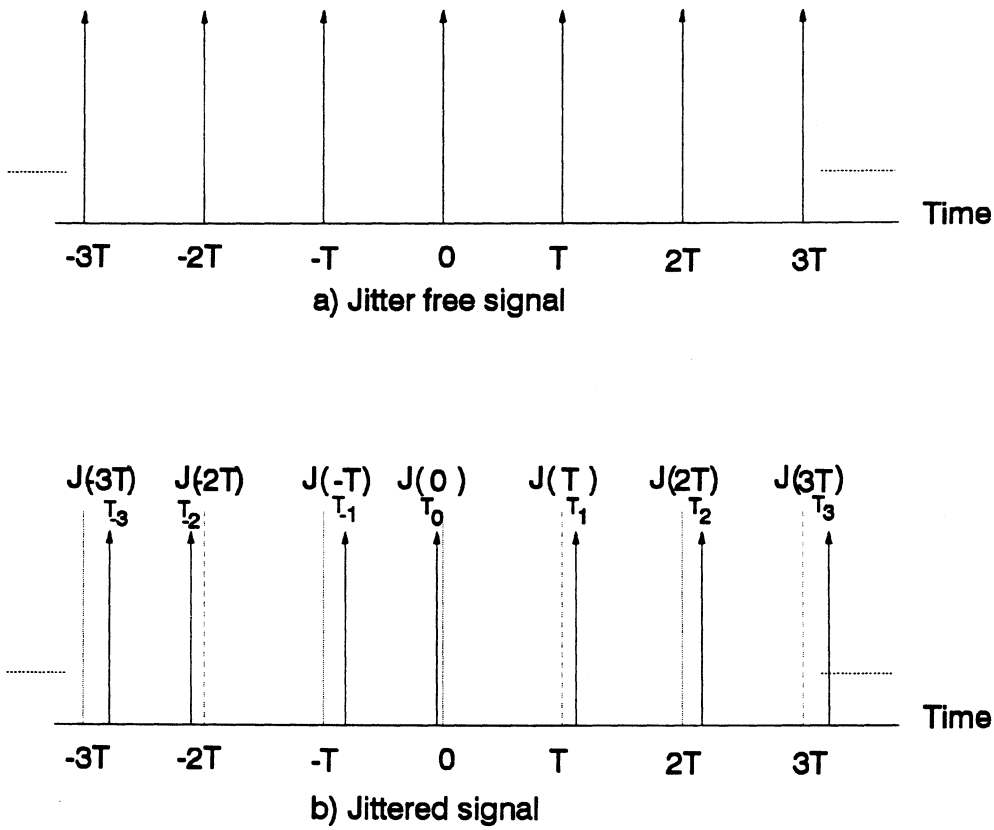

Figure 7.2 : Illustration of jitter.

In an ideal FM/TDM system, the samples would arrive at times that are integer multiples of the sample rate $T = 1/r$. However in a real system, samples may arrive at times that differ from integer multiples of T. This error in timing is called jitter. To illustrate jitter, Figure 7.2a shows a train of unit impulses initially spaced equally in time; after either transmission or reception these unit impulses become spaced slightly irregularly in time as shown in Figure 7.2b (occurring at times T_n). The time deviations from integer multiples of T from a discrete time T_n (the time at which the sample is taken), is a continuous amplitude sequence $J(nT) = nT - T_n$. This sequence is the fundamental description of jitter [35-37]; $J(nT)$ has dimensions of time in amplitude and is positive for a given pulse that arrives earlier than time nT. $J(nT)$ may be converted to units of degrees by defining T to equal to 360°. Therefore a jitter amplitude of T seconds is 360°.

The amount of timing jitter depends both on the shape of the data sample and the particular sequence of sample amplitudes [36]. In the following analysis we assume, raised cosine shaped samples. For the worst case condition, we also assume that the samples polarity is alternating (any positive sample is followed by a negative sample and visa versa) with an average value = $2A/\pi$ where A is the maximum sample magnitude (average amplitude of sinusoid samples $= \frac{A}{\pi}\int_0^{\pi} sin(x)dx = \frac{\pi}{2}$). The alternating sequence tends to give rise to the maximum inter-symbol interference which in turn results in the worst jitter penalty.

7.2 TIMING AND JITTER EFFECTS ON TRANSMISSION QUALITY

From chapter 2 the demultiplexed received sampled FM signal can be written as

$$f_{s_i}(t) = \sum_{n=-\infty}^{\infty} f_i(nT).q(t-nT) \tag{7.1}$$

where $f_i(nT)$ is the value i^{th} channel at time equals nT in volts,

T is the duration between samples in seconds,

$q(t)$ is the impulse response of the shaping filter, and

$f_{s_i}(t)$ is the sampling rate for the i_{th} channel.

For raised cosine shaped samples, $q(t)$ is given by [36]

$$q(t) = \frac{sin(\pi.t/T)}{\pi.t/T} \cdot \frac{cos(\pi.t/T)}{1-4\ t^2/T^2} \tag{7.2}$$

Timing error and jitter are due to timing inaccuracies at both the transmitter and the receiver. Assume that the received signal has a jitter $J_T(t)$, which may be due to the transmitter circuitry, the transmission channel, or the internal stages of the receiver. Then the received signal $P_r(t)$ may be written as

$$P_r(t) = \sum_{n=-\infty}^{\infty} f(nT)\ .\ q(t-nT-J_T(nT)) + \eta_r(t) \tag{7.3}$$

where $\eta_r(t)$ is the total received noise (RIN+shot+thermal+NLD) as in Chapter 3. If the jitter introduced by the timing recovery circuitry is $J_R(t)$, then the timing signal $S_r(t)$ is given by

$$S_r(t) = B\ sin\left(\frac{2\pi}{T}\ (t-J_R(t)-\Delta\tau)\right) \tag{7.4}$$

where $\Delta\tau$ is a phase delay caused by the timing recovery circuitry. The sampled received signal $P'_r\ (t)$ can then be written as

$$P'_r\ (t) = \left\{\left(P_r(t)+\eta_r(t)\right) . \sum_{m=-\infty}^{\infty} \delta\,(t - mT - J_R(mT) - \tau)\right\} * p(t) \qquad (7.5)$$

where τ is the total static phase offset and is equal to $\Delta\tau$ + time delay due to the physical separation of the time recovery circuit and the receiver sampler, $\delta\,(t)$ is the delta function, $*$ denotes convolution, and $p(t)$ is the impulse response of the receiver shaping filter (LPF). By moving the quantity $\left(\mathrm{P_r(t)}+\eta_\mathrm{r}(\mathrm{t})\right)$ within the summation we obtain

$$P'_r\ (t) = \left\{\left[\sum_n \left(f(nT)\ \ q(t - nT - J_\mathrm{T}(nT)\right) + \eta_r(t)\right)\right] .$$

$$\sum_m \delta\,(t - mT - J_R(mT) - \tau)\Big\} * p(t) \qquad (7.6)$$

i.e.

$$P'_r\ (t) = \sum_m \left\{\sum_n \Big(f(nT)\ q(mT - nT + J_R(mT) - J_T(nT) + \tau)\ +\ \eta_r(t_m)\right)$$

$$. \delta\,(t - mT - J_R(mT) - \tau)\Big\} * p(t) \qquad (7.7)$$

where $t_m = mT + J_R(mT) + \tau$. Changing indices to k=$m - n$ and extracting the k=0 term we obtain

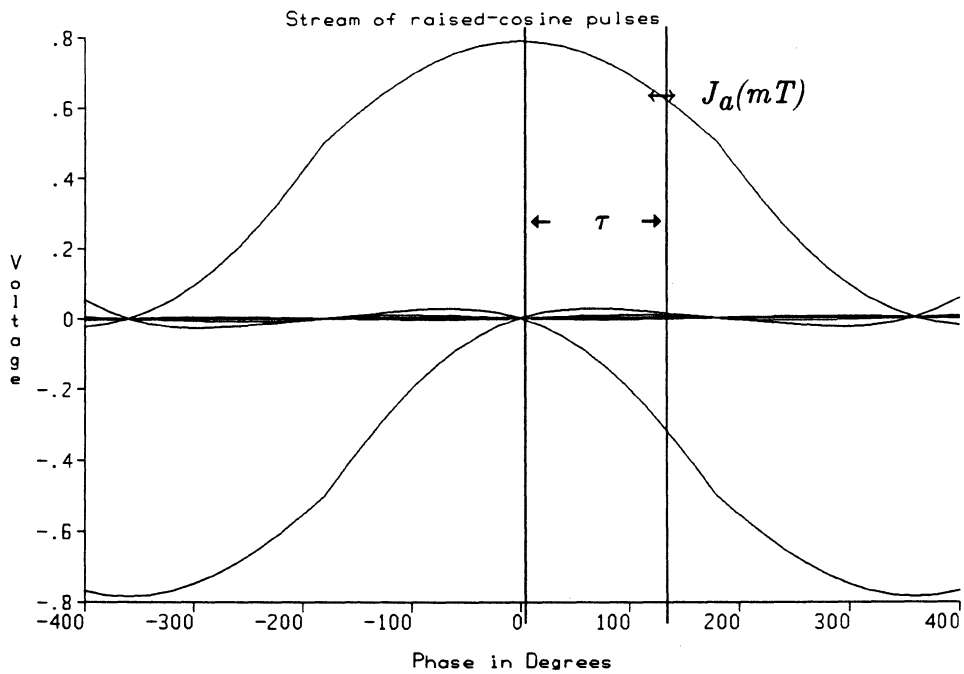

Figure 7.3 : Sequence of raised cosine samples.

$$P'_r(t) = \sum_m \Big\{ f(mT)\, q(J_R(mT) - J_T(mT) + \tau) + \sum_{k \neq 0} f(kT)\, q(kT + J_R(mT) - J_T((m-k)T) + \tau) + (\eta_r(t_m)) \cdot \delta(t - mT - J_R(mT) - \tau) \Big\} + p(t) \tag{7.8}$$

Since $J_T(t)$ is a slowly varying low-pass stochastic process, then for small values of $|k|$

$$J_T(m-k)T \simeq J_T(mT) \tag{7.9}$$

We now define the alignment jitter at the receiver sampling circuit as

$$J_a(mT) = J_R(mT) - J_T(mT) \tag{7.10}$$

Both the static offset τ and the alignment jitter $J_a(mT)$ affect performance. This is illustrated in Figure 7.3 where a sequence of raised cosine samples is shown. If both the sampling static phase offset $\tau = 0^\circ$ and $J_a(mT) = 0^\circ$ then the magnitude of the desired sample is maximum while the ISI value is zero. If either τ or $J_a(mT)$ (or both) is unequal to zero then the received sample is not sampled at the maximum magnitude location while the ISI magnitude is greater than zero. Therefore Equation 7.8 may be rewritten as

$$P'_r(t) = \left\{ \sum_m \left\{ f(mT) \cdot q(J_a(mT)+\tau) + \sum_{k \neq 0} f(kT) \cdot q(kT + J_a(mT)+\tau) \right. \right.$$

$$\left. \left. + \eta_r(t_m) \right\} \cdot \delta(t - mT - J_R(mT) - \tau) \right\} + p(t) \qquad (7.11)$$

where the first quantity $f(mT) \cdot q(J_a(mT)+\tau)$ is the value of the present sample at a time instant equal to $J_a(mT)+\tau$ (total timing error), $\sum_{k \neq 0} f(kT) \cdot q(kT+J_a(mT)+\tau)$ is the ISI, and $\eta_r(t_m)$ is the noise. If the total timing error is equal to zero, then the magnitude of $q(0)$ is maximum (equal to unity for normalized signal). Hence the magnitude of the desired sample is equal to $f(mT)$ which is the desired signal. When the timing error is unequal to zero, the magnitude of the desired signal will be reduced by a factor less than unity reducing the carrier level (for timing jitter it also may add distortion; see Section 7.4). The second quantity $\sum_{k \neq 0} f(kT) \cdot q(kT + J_a(mT)+\tau)$ is the inter-symbol-interference (ISI) where each term in the summation corresponds to the ISI introduced by the k^{th} adjacent sample. If the timing error $(J_a(mT)+\tau) = 0$, then the value of $\sum_{k \neq 0} f(kT) \cdot q(kT)$ is equal to zero and no ISI exists; otherwise the presence of the ISI will increase the effective overall noise and distortion level. The combined effect, of reducing the carrier level and increasing the noise degrades the overall C/N.

7.3 STATIC PHASE OFFSET TRANSMISSION PENALTY

Transmission penalty is defined as the extra C/N needed for a given baseband signal-to-noise ratio when compared with the zero jitter and static phase offset case. In this section the transmission penalty is examined by assuming that

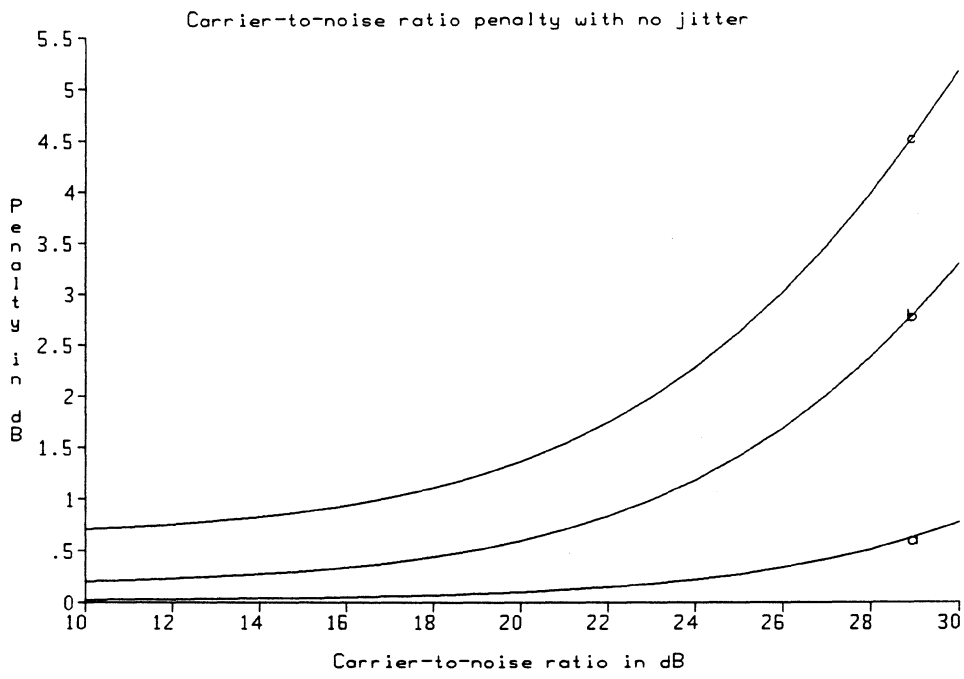

Figure 7.4 : Transmission penalty in dB vs carrier-to-noise in dB,

the alignment jitter $J_a(mT) = 0$

a) τ=10°, b) τ=30° & c) τ=60°

the alignment jitter is zero.

As a result of the static phase offset τ, the desired sample magnitude is reduced by a factor equal to $q(\tau)$ while the ISI terms ($|\sum_{k \neq 0} f(kT)\ q(kT+\tau)|$) are added to the noise. The samples are sinusoidal signal samples, hence the samples average power is $A^2/2$ (duty factor does not affect results since it comes into the numerator and denominator the same way). As indicated we will assume that samples with average value $=A/\pi$ alternate in polarity. Therefore C/N for a normalized samples may be written as

$$\frac{C}{N} = \frac{\frac{1}{2}\, q^2(\tau)}{\left(|\sum_{k \neq 0} \frac{2(-1)^k}{\pi}\ q(kT+\tau)| + \eta_\tau(t_m) \right)^2} \tag{7.12}$$

This relationship is shown in Figure 7.4 for various values of τ (expressed in degrees) and for k=8 adjacent samples affecting the current sample level. Figure 7.4 shows that if the static phase offset is 60°, (i.e. $\frac{1}{6}$ of a time slot) then the transmission penalty is ~ 1 dB. Therefore the minimum C/N required for studio quality transmission should be ~ 19.3 dB instead 18.3 dB. Therefore, with no alignment jitter the effect of static phase on transmission performance is small for reasonable C/N (up to studio quality transmission).

For higher quality transmission, the requirements for static phase offset is more stringent. This may be explained as follows; if the power of the signal at zero offset is P watts, and the reduction due to static offset is p watts, and the IF noise is n watts. Then the new signal-to-noise ratio is $(P-p)/n$. Thus, the static offset penalty is p/n. It is clear that this ratio is larger if n is smaller. Therefore phase

offset errors should be minimized if high quality transmission is desirable.

7.4 STATIC PHASE OFFSET AND JITTER TRANSMISSION PENALTY

In the presence of alignment jitter, the static phase offset is much more serious. This can be shown by assuming $J_a(mT)$ has a Gaussian distribution, with zero mean and standard deviation equal to $\frac{1}{6}$ the peak-to-peak alignment jitter. This distribution approximates the distribution of the alignment jitter in digital fiber optics links [36].

Similar to the static phase offset, the effects of the jitter are to reduce the desired signal, to increase the magnitude error, and to increase ISI. The dominant distortion in this case is the magnitude error, which results from the error in the sample value when compared with the zero jitter case. Furthermore the jitter introduces a distortion as a result of ISI. All these sources of noise and distortion add incoherently reducing the final *C/N*. According to the aforementioned factors, the C/N may be written as

$$\frac{C}{N} = \frac{< \frac{1}{2} q^2(J_a(mT)+\tau) >}{\left(\mid \mathcal{E}_m + \mathcal{E}_{ISI} \mid + \eta_r(t_m) \right)^2} \tag{7.13}$$

where $< \frac{1}{2} q^2(J_a(mT)+\tau) >$ is the desired signal average power,

$\mathcal{E}_m = q(J_a(m-1)T)+\tau) - q(J_a(mT)+\tau)$ is the error as a result of the magnitude difference between the previous and present sample values,

$\mathcal{E}_{ISI} = q(\sum_{k \neq 0} \frac{2(-1)^k}{\pi} q(kT + J_a(mT)+\tau)$ is the ISI and $\eta_r(t_m)$ is the noise.

The Gaussian distributed points $J_a(mT)$ are generated by converting a set

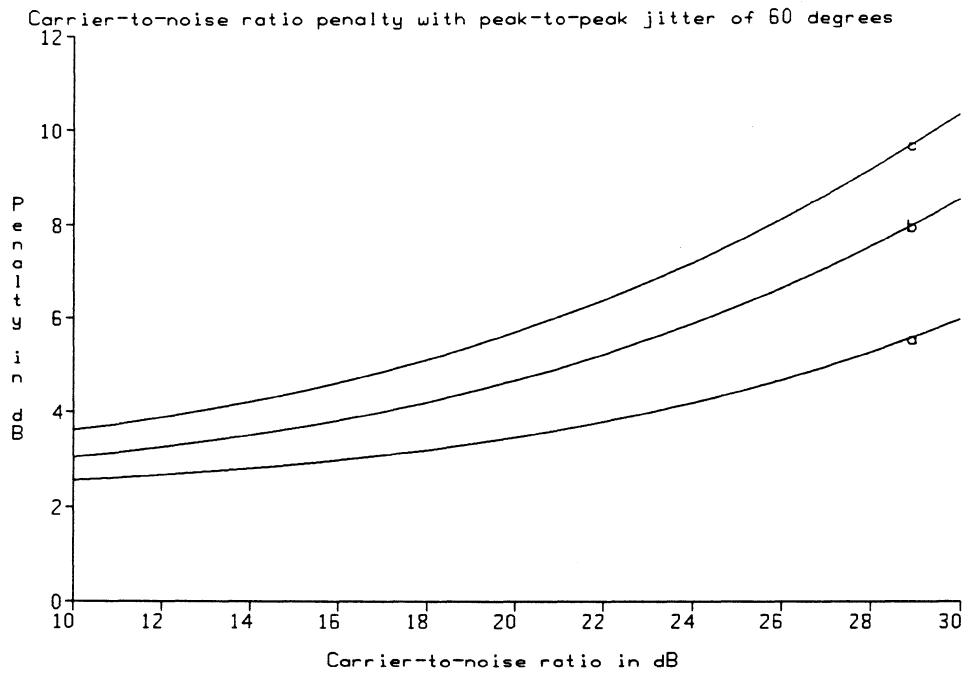

Figure 7.5 : Transmission penalty in dB vs carrier-to-noise in dB,

the alignment jitter $J_a(mT) = 60^\circ$

a) τ=10°, b) τ=30° & c) τ=60°

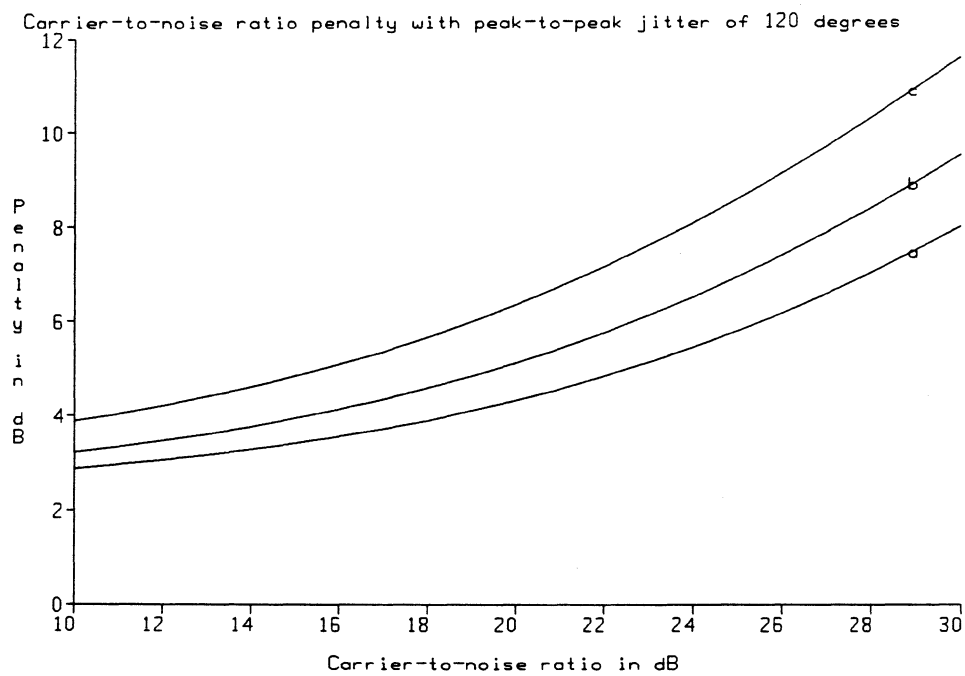

Figure 7.6 : Transmission penalty in dB vs carrier-to-noise in dB,

the alignment jitter $J_a(mT) = 120^\circ$

a) τ=10°, b) τ=30° & c) τ=60°

of random numbers to a normally distributed random numbers by using the the following relationship

$$F(x) = \frac{1}{2} + \frac{1}{2}\, erf\,(\frac{x-m}{\sqrt{2}\,\sigma}) \tag{7.14}$$

where $F(x)$ is the Gaussian cumulative distribution function,

x is the Gaussian distributed random number,

m is the mean,

σ is the standard deviation,

$erf(x)$ denotes the error function which is defined as

$$erf(x) = \frac{2}{\sqrt{\pi}} \int_0^x e^{-t^2} dt \tag{7.15}$$

By using Monte Carlo techniques, Equation 7.13 is plotted in Figure 7.5 (by using TK Solver software package) where the transmission penalty vs C/N for peak-to-peak alignment jitter of 60° with static phase offset of 10°, 30° and 60°, is shown. In Figure 7.6 the peak-to-peak alignment jitter is 120°. It is readily seen that the transmission penalty is largest when the largest combination of alignment jitter and static phase offset is present. This shows that the system is less tolerant to alignment jitter when static phase offset is present. Therefore static phase offset must be minimized in order to minimize the effect alignment jitter has on the transmission penalty.

Also it is seen that the transmission penalty increases with increasing the C/N. This phenomenon may be explained as follows: for a given phase offset and peak-to-peak jitter the jitter noise is constant regardless of the input C/N. This

noise becomes the main limiting noise in the absence of other noise (high C/N). For low C/N the magnitude of jitter noise may be less than the noise already existing with the signal therefore its effect may be small. Therefore timing errors should be minimized if high quality transmission is desirable.

7.5 SUMMARY

In this chapter timing and jitter effects are investigated. Timing errors may result from static phase offset or from from alignment jitter (or a combination of both). As shown in Section 7.3, in the absence of jitter, the FM/TDM system has a high tolerance for the static phase delay. For example, the static phase offset may be as high as 60° with only ~ 1 dB of penalty (for studio quality transmission). This may be explained as follows: static phase offset affects only the amplitude of the signal (the phase may change but not the frequency). The penalty results from the fact that the magnitude of the signal has been reduced by the phase offset while the noise level remains unchanged, which reduces the C/N (the received signal is not sampled at its peak magnitude). The resultant effect is as if the noise level has been increased by the factor of the transmission penalty. Therefore, the baseband S/N is expected to drop by the same value; i.e., the baseband S/N will suffer from an equal noise penalty.

In the presence of jitter, the transmission penalty is largest when the largest combination of alignment jitter and static phase offset is present. Thus, the system is less tolerant to static phase in the presence of jitter. Equivalently, one may conclude that the system is less tolerant to jitter in the presence of static phase offset. This is due to the fact that the slope of the sample increases by increasing

the offset. Therefore, a certain peak-to-peak jitter causes more distortion when the offset is larger. Because jitter distribution is a Gaussian process, the noise resulting from the jitter will be approximately also Gaussian distributed with zero mean (assuming that the jitter peak-to-peak is very small). This jitter noise adds incoherently to the transmission noise already in the IF band (which is Gaussian also). Thus, similar to the previous case, the penalty to the detected baseband S/N is the same amount as to the IF signal.

For both cases (static offset with no jitter and static offset with jitter), the penalty is larger for higher C/N. Therefore the higher the quality the more stringent the requirements for the timing errors will be.

CHAPTER 8

CONCLUSIONS AND RECOMMENDATIONS

In this dissertation a new compound modulation technique for multi-channel analog video transmission over fiber is presented. The performance of the proposed system is analyzed and compared to the performance of present analog and digital systems. The analysis results are verified by simulations.

In present analog FDM systems, laser nonlinearities result in coherent type impairments (composite triple beats), which limit the capacity and optical modulation depth that may be obtained with such systems. Coherent impairments may occur also in the FM/TDM system, but they result from ISI, which is a function of the laser's bandwidth and the number of channels transmitted. An average quality laser can carry up to 150 video channels with no significant ISI. More likely, the number of channels to be transmitted may be limited by the available terminal technology (e.g. the high speed multiplexer) rather than by the optical components.

Comparing simulation results with analytical and experimental results indicates that the proposed FM/TDM system has considerable better nonlinear distortion than that of FM/FDM systems, (depends on the laser OMD and the quality of the laser) and is similar to that of PCM/TDM systems. This permits the use of considerably larger optical modulation depth (as high as in digital systems), which results in a very large power budget (as large as present PCM/TDM systems).

With respect to picture quality, since S/N degradation in digital systems is

not as graceful as in FM systems, a large power margin is usually required to ensure satisfactory operation. In that range, the FM/TDM system has better S/N than the PCM/TDM system. Furthermore, the FM/TDM system has the advantage of being very flexible. S/N could be increased according to the application by adding optical amplifiers or by increasing the transmitted optical power. In the PCM/TDM system, CODECs at the terminals need to be changed in order to improve picture quality.

For a given S/N, the proposed system has roughly 8.5 dB higher optical power budget than the present FM/FDM system. Also the detected S/N for any given received optical power for the proposed system is about 17 dB better than present FM/FDM systems. Therefore less demanding optical components may be used for the FM/TDM than for present analog systems.

Timing accuracy and jitter distortions are also studied for the proposed system. Similar to digital systems, the transmission penalty is largest when the largest combination of alignment jitter and static phase offset is present. The factor which causes jitter to grow in digital systems is the presence of regenerators, since each regenerator contributes to timing errors. In the proposed system, there are no regenerators (only optical amplifiers need be used). Thus, timing errors are expected not to be as serious as in long haul digital systems.

Although TV transmission (including HDTV) may well evolve to be digital, but for present NTSC analog TV signals the proposed system may have advantages for high performance multi-channel delivery. It would be desirable to implement the system to verify both the analytical and simulation results. Therefore, it is highly recommended to pursue experimentations of this new technique here on campus. In addition to the optical components and optical test equipment needed

for the experiment, electrical test equipment is still needed, mostly for baseband video measurements (for example random noise measuring set, video waveform monitor / vector scope, video signal generator, etc). Furthermore, an FM modulator / demodulator, sampler, and short pulse generator are also needed.

Finally, it should be also noted that the FM technique may be combined with PCM to enable very high S/N to be achieved with a moderate number of quantization bits. Although higher S/N can be achieved in digital systems by increasing the number of bits of quantization, this may be impractical. For a limited number of bits of quantization and transmission bandwidth, significantly larger baseband S/N is achieved by using FM before sampling than that obtained by over-sampling. More research and experiments are also needed for this application.

BIBLIOGRAPHY

[1] Ciciora W.S., "An Introduction to Cable Televiosion in the United States", *IEEE LCS Magazine*, Vol. 1, No. 1, Feb. 1990, pp19-25.

[2] D. Robinson and d. Grubb III, " A High-Quality Switched FM Video System", *IEEE LCS Magazine*, Vol. 1, No. 1, Feb. 1990, pp53-59.

[3] David Large, "Tapped Fiber vs Fiber Reinforeced Coaxial CATV Systems", *IEEE LCS Magazine*, Vol. 1, No. 1, Feb. 1990, pp12-18.

[4] S. Personick, "Fiber Optics Technology and Applications", Plenum Press 1985.

[5] W. Way, "Subcarrier Multiplexed Lightwave Systems Design Considerations for Subscriber Loop Application", *IEEE J. Lightwave Technol.,* Nov. 1989, pp1806-1818.

[6] W. B. Jones, "Introduction to Optical Fiber Communication Systems", *HRW Inc.,* 1988.

[7] B. Arnold, "Third Order Intermodulation Products in a CATV System", *IEEE Transactions on Cable Television*, Vol. CATV-2, No 2, April 1977, pp 67-79.

[8] T. Darcie *et al*, "Fiber Optic Device Technology for Broadband Analog Video Systems", *IEEE LCS Magazine*, Vol. 1, No. 1, Feb. 1990, pp46-51.

[9] T. Darcie and G. Bodeep, "Lightwave Subcarrier CATV Transmission Sytems", *IEEE Transactions on Microwave Therory and Techniques*, Vol 38, No 5, May 1990, pp524-533.

[10] J. Schlafer and R. Lauer, "Microwave Packaging of Optoelectronic Componenets", *IEEE Transactions on Microwave Therory and Techniques*, Vol 38, No 5, May 1990, pp518-523.

[11] J. Lipson *et al*, "High-Fidelity Lightwave Transmission of Multiple AM-VSB NTSC Signals", *IEEE Transactions on Microwave Therory and Techniques,* Vol 38, No 5, May 1990, pp483-493

[12] T. E. Darcie *et al,* "Wide-Band Lightwave Distribution System Using Subcarrier Multiplexing", *IEEE J. Lightwave Technol.,* June 1989, pp997-1005.

[13] D. Grubb III, "AM Fiber-Optic Trunks", *Communications Technology Publications Corp.*, 50 S Steele Suite 700, Denver, CO 80209.

[14] T. Pratt and C. W. Bostian, "Satellite Communications", *Wiley & Sons Inc.,* 1986.

[15] W. C. Brinkerhuff and I. M. Levi, "A Point-to-Multipoint Fiber Optic CATV Transport System For the City of Cleveland, Ohio", *NCTA Tech. Papers,* 1988, pp58-66.

[16] R. Olshansky and V. A. Lanzisera, "60 Channel FM Video Subcarrier Multiplexed Optical Communication System", *Electron. Lett.*,Vol 23, 1987, pp1196-1197.

[17] R. Olshansky, V. A. Lanzisera and P. M. Hill, "Subcarrier Multiplexed Lightwave Systems for Broadband Distribution" *IEEE J. Lightwave Technol.*, Sep 89 , pp1329-1342.

[18] R. Olshansky, V. A. Lanzisera and P. M. Hill, "Simultaneous Transmission of 100 Mbit/s at Baseband and 60 FM Video Channels for a Wide-Band Optical Communication Network", *Elctron. Lett.*, 1988, Vol 24 pp1234-1235.

[19] J. E. Bowers *et al*, "Long Distance Fiber-Optic Transmission of C-Band Microwave Signals to and From Satellite Antenna", *IEEE J. Lightwave Technol.*, Dec. 1987, pp1733-1441.

[20] W. D. Gregg, "Analog & Digital Communications", *Wiley & Sons Inc.*, 1977.

[21] F. Stremler, "Introduction to Communications Systems", *Second edition, Addison-Wesley Publishing Co.*, 1982.

[22] Benson K.B., "Television Engineering Handbook", *McGraw-Hill*, 1985.

[23] R. Tucker and I. Kamino, "High-Frequency Characteristics of Directly Modulated InGaAsP Ridge Waveguide and Buried Heterostructure Lasers", *IEEE J.Lightwave Technol.*, Aug. 1984, pp385-393.

[24] K. Stubkjaer and M. Danielsen, "Nonlinearities of GaAlAs Lasers", *IEEE J. Lightwave Technol.*, May 1980, pp531-537.

[25] D. Chan and T. M. Yuen, "System Analysis and Design for a Fiber-Optic VSB-FDM System for Video Trunking", *IEEE Trans. on Comm.*, July 1977, pp680-686.

[26] J. C. Daly, "Fiber Optic Intermodulation Distortion", *IEEE Trans. on Comm.*, Aug. 1982, pp1954-1958.

[27] K. Lau and A. Yariv, "Intermodulation Distortion in a Directly Modulated Semiconductor Injection Laser", *Appl. Phys. Lett.*, Nov. 1984, pp1034-1036.

[28] T. Darcie and R. Tucker, "Intermodulation and Harmonic Distortion in InGaAsP Lasers", *Electronics Lett.*, Vol 21 Aug. 1985, pp665-666.

[29] A. Carlson, " Communication Systems", *McGraw-Hill Third Edition*, 1986.

[30] Shanmugan K. S. and Townsend J. K., "Simulation Modules for Optical Communications Systems Analysis", *STAR Corp.*, July, 1987.

[31] Verdeyen J. T., "Laser Electronics", *Prentice-Hall Second Edition*, 1989.

[32] Oppenheim A. and Willsky A., "Signals and Systems", *Prentice-Hall*, 1983.

[33] Poularikis A. and Seely S., "Signals and Systems", *PWS Publishers*, 1985.

[34] BOSS^{TM}, "User's Guide", *Third printing*, November 1989.

[35] Franks L. and Bubrouski J., "Statistical Propresties of Timming Jitter in a PAM Timming Recovery Scheme", *IEEE Trans. on Comm.*, Vol. Com-22, No. 7, July 1974, pp913-920.

[36] Patrick T. and Varma E., "Jitter in Digital Transmission Systems", *Artech House, Inc.*, 1989.

[37] Mengali U. and Pirani G., "Jitter Accumilation in PAM Systems", *IEEE Trans. on Comm.*, Vol. Com-28, No. 8, August 1980 pp1172-1183.

APPENDIX

In the following appendix all simulation module documentations used in the simulations mentioned in Chapters 5 and 6 are given. This enables any future continuation for the project if so desired. The modules presented are:

1. FM/TDM using PIN diode,
2. SNR vs OMD,
3. SNR vs Nonlinearities,
4. Complex Laser,
5. Laser Diode (real signal),
6. Complex Sampler,
7. Complex PIN Detector,
8. SNR Ratio.

MODULE NAME: FM/TDM USING PIN PHOTODETECTOR
GROUP: SYSTEM
DATABASE: DUA0:[USERS.ALFRED.TEST]
AUTHOR: ALFRED
CREATION DATE: 21-Nov-1991 13:08:45

DESCRIPTION:

This module is to estimate baseband signal-to-noise for a given optical received power. Optical modulation depth may be varied if so desired. Nonlinear distortion, shot noise dark curren, and thermal noise are included. Baseband signal is assumed to be 0-5 Hz. FM carrier is 100 Hz, and FM bandwidth is 40 HZ. The baseband tone should be less than 1.5 Hz. The contents of the band from 1.5 to 5 Hz is considered noise. The time T-ON should be at least 2 baseband cycles less than the STOP-TIME to ensure satisfactory measurements.

REVISIONS:

Author : ALFRED
Date : 1-Dec-1991 17:28:12
Description:

Edited 1-Dec-1991 17:28:12, No Edit Description Entered.

Author : ALFRED
Date : 21-Nov-1991 13:08:45
Description:

21-Nov-1991 13:08:56
Module CREATION.

INPUT SIGNALS: (none)

OUTPUT SIGNALS: (none)

PARAMETERS:
STOP-TIME Type: REAL
Lower Limit: 3.0e-39
Upper Limit: 1.7e38

Specifes the maximum value of time for the simulation (in seconds).
The simulation clock runs from time=0.0 to time=STOP-TIME
in steps of DT, all in seconds.

DT Type: REAL
Lower Limit: 3.0e-39
Upper Limit: 1.7e38

Time between discrete simulation signal samples (in seconds).
DT must be small enough to satisfy the Nyquist Sampling Theorem for all signals at all points in the simulation.

NOTE:
If the specified period or rate of a periodic function results
in a period that is not a multiple of DT, then BOSS will round
the period to the nearest value that IS a multiple of DT.
For example, if DT=0.125(sec) and a rate was specified as rate=1.4(hz) which corresponds to a period of T=0.714(sec) which is 5.7*DT , then BOSS will round this period to be 6.0*DT and thus the effective rate will be 1.333(hz).

Because of this, the choice for DT can affect the periods of the periodic signals in the simulation.

QUANTUM EFFICIENCY Type: REAL
Lower Limit: 0.0
Upper Limit: 1.0

The quantum efficiency of the pin diode.

VARIANCE Type: REAL
Lower Limit: 0.0
Upper Limit: 1.7e38

This parameter specifies the variance of the Gaussian distribution.

BASEBAND FREQUENCY Type: REAL
Lower Limit: -1.7e38
Upper Limit: 1.7e38

The frequency of the generated sinuaoidal tone in Hertz.

DARK CURRENT (NANOAMPS) Type: REAL
Lower Limit: 0.0
Upper Limit: 1.7e38

The PIN dark current in nanoamps.

INPUT SIGNAL MAGNITUDE Type: REAL
Lower Limit: 3.0e-39
Upper Limit: 1.7e38

this is the gain constant for the gain block. it must be a single precision real number.
the block output = gain coeff * block input .

ATTENUATION FACTOR Type: REAL
Lower Limit: 0.0
Upper Limit: 1.0

this is the gain constant for the gain block. it must be a single precision real number.
the block output = gain coeff * block input .

3RD HARMONIC LEVEL Type: REAL
Lower Limit: -1.7e38
Upper Limit: 1.7e38

Level of third harmonic (in dB) relative to the fundamental. If the parameter "harm/coef" is .false., this parameter is the coefficient of the cubed term in the polynomial.

BIAS POWER Type: REAL
Lower Limit: 3.0e-39
Upper Limit: 1.7e38

Power output at bias point (corresponding current specified by the parameter "bias current"). Units should be same as the output power signal.

THRESHOLD CURRENT Type: REAL
Lower Limit: 0.0
Upper Limit: 1.7e38

Current at threshold corresponding to the measured harmonic values. The units should be the same as the bias current parameter. This parameter should always be less than the bias current. The laser module is not designed to accurately model the laser near threshold, but this parameter is required to relate the test modulation index to the test sinusoid magnitude.

TEST MOD INDEX Type: REAL
Lower Limit: 0
Upper Limit: 1

The input modulation index used during measurement of the given harmonic levels. This number must be between zero and one inclusive.

EFFICIENCY Type: COMPLEX
Lower Limit: 3.0e-39
Upper Limit: 1.7e38

Slope of the output power vs input current characteristic at the bias point. The units of this parameter must correspond to the units of the output power/input current.

2ND HARMONIC LEVEL Type: REAL
Lower Limit: -1.7e38
Upper Limit: 1.7e38

Level of second harmonic (in dB) relative to the fundamental.
If the parameter "harm/coef" is .false., this parameter is the coefficient of the squared term in the polynomial.

4TH HARMONIC LEVEL Type: REAL
Lower Limit: -1.7e38
Upper Limit: 1.7e38

Level of fourth harmonic (in dB) relative to the fundamental. If the parameter "harm/coef" is .false., this parameter is the coefficient of the fourth order term in the polynomial.

5TH HARMONIC LEVEL Type: REAL
Lower Limit: -1.7e38
Upper Limit: 1.7e38

Level of fifth harmonic (in dB) relative to the fundamental. If the parameter "harm/coef" is .false., this parameter is the coefficient of the fifth order term in the polynomial.

HARM/COEF Type: LOGICAL
Lower Limit: NIL
Upper Limit: NIL

When this logical parameter is .true., the values of parameters "XXX harmonic level" are interpreted as harmonic levels. When .false., they are interpreted as coefficents of the 5th order polynomial (efficiency is the first order term).

BIAS CURRENT Type: REAL
Lower Limit: 3.0e-39
Upper Limit: 1.7e38

The units of this parameter should be the same as the input current, and the parameter "test tone magnitude".

T-ON Type: REAL
Lower Limit: 0.0
Upper Limit: 1.7e38

Time (seconds) in which enable becomes true.

MODULES USED IN BLOCK DIAGRAM:

FM MOD
IMPULSE TRAIN
SINUSOIDAL
TABULAR PLOT VIA ITERATION
SAMPLE & HOLD
LOGICAL TRUE COUNTER
= INTGR
TERMINATE SIMULATION
SNR RATIO
T >= T ON
CONST GEN
SAMPLER CMPLX
COMLX LASER
CMPLX DC BLOCK
FM BALANCED DISCRIMINATOR
BUTWTH FILTER (REAL)
REAL TO CMPLX
SUBTRACTOR
BUTTERWORTH BANDPASS
UNIT VECTOR
VARIABLE-DELAY
REAL COEFF GAIN
CMPLX PIN DETECTOR
ADDER
AVERAGE POWER OF REAL SIGNAL
REAL OF CMPLX
GAUSSIAN RAN_GEN
MAKE CMPLX

INITIALIZATION CODE: (none)

FM/TDM USING PIN PHOTODETECTOR

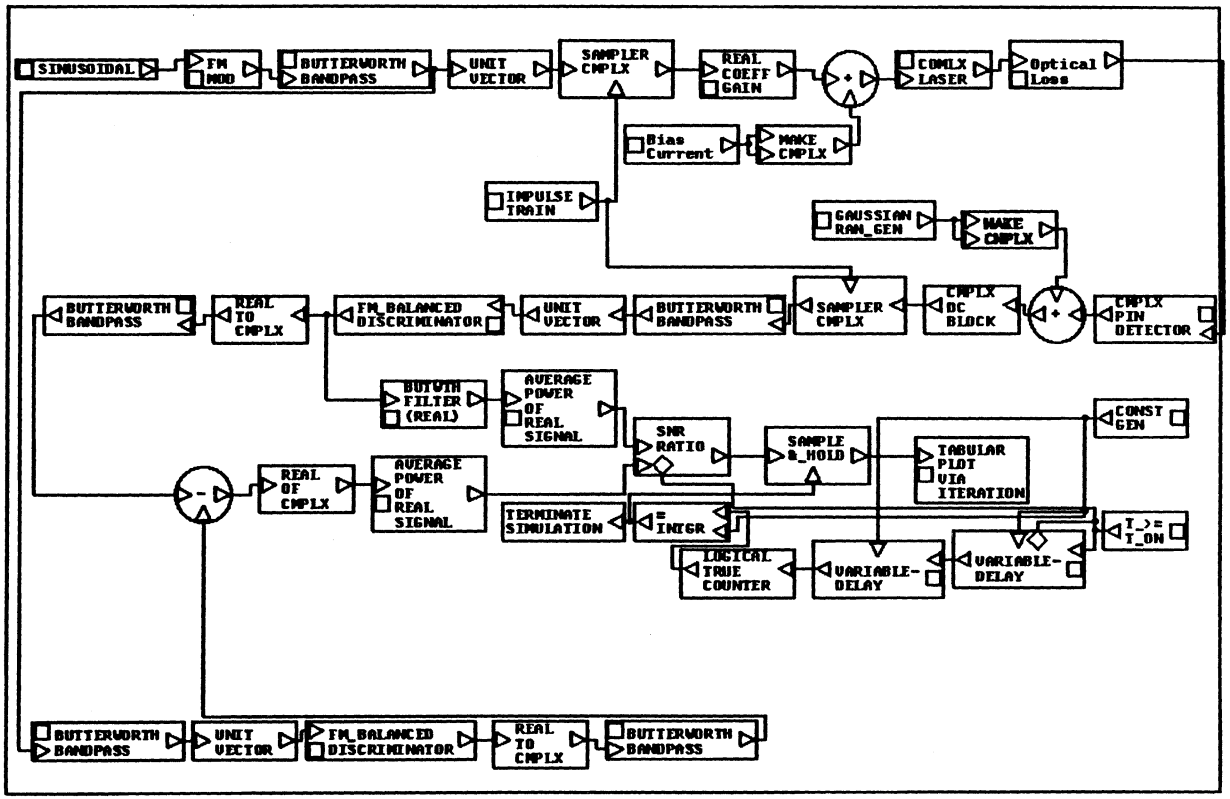

MODULE NAME: SNR VS OMD
GROUP: SYSTEM
DATABASE: DUA0:[USERS.ALFRED.TEST]
AUTHOR: ALFRED
CREATION DATE: 1-Dec-1991 17:12:49

DESCRIPTION:

This system modue finds the IF signal-to-noise ratio as a function of the optical modulation depth. Multiple simulations will result in IF S/N vs OMD.

REVISIONS:

Author : ALFRED
Date : 1-Dec-1991 17:12:49
Description:

1-Dec-1991 17:13:07
Module CREATION.

INPUT SIGNALS: (none)

OUTPUT SIGNALS: (none)

PARAMETERS:

STOP-TIME Type: REAL
Lower Limit: 3.0e-39
Upper Limit: 1.7e38

Specifes the maximum value of time for the simulation (in seconds).
The simulation clock runs from time=0.0 to time=STOP-TIME in steps of DT, all in seconds.

DT Type: REAL
Lower Limit: 3.0e-39
Upper Limit: 1.7e38

Time between discrete simulation signal samples (in seconds).
DT must be small enough to satisfy the Nyquist Sampling Theorem for all signals at all points in the simulation.

NOTE:
If the specified period or rate of a periodic function results
in a period that is not a multiple of DT, then BOSS will round
the period to the nearest value that IS a multiple of DT.
For example, if DT=0.125(sec) and a rate was specified as rate=1.4(hz) which corresponds to a period of T=0.714(sec) which is 5.7*DT , then BOSS will round this period to be 6.0*DT and thus the effective rate will be 1.333(hz).

Because of this, the choice for DT can affect the periods of the periodic signals in the simulation.

OPTICAL BIAS POWER Type: REAL
Lower Limit: NIL
Upper Limit: NIL

This is the value to be output by the module.

BIAS POWER Type: REAL
Lower Limit: 3.0e-39
Upper Limit: 1.7e38

Power output at bias point (corresponding current specified by the parameter "bias current"). Units should be same as the output power signal.

THRESHOLD CURRENT Type: REAL
Lower Limit: 0.0
Upper Limit: 1.7e38

Current at threshold corresponding to the measured harmonic values. The units should be the same as the bias current parameter. This parameter should always be less than the bias current. The laser module is not designed to accurately model the laser near threshold, but this parameter is required to relate the test modulation index

to the test sinusoid magnitude.

TEST MOD INDEX Type: REAL
Lower Limit: 0
Upper Limit: 1

The input modulation index used during measurement of the given harmonic levels. This number must be between zero and one inclusive.

EFFICIENCY Type: REAL
Lower Limit: 3.0e-39
Upper Limit: 1.7e38

Slope of the output power vs input current characteristic at the bias point. The units of this parameter must correspond to the units of the output power/input current.

2ND HARMONIC LEVEL Type: REAL
Lower Limit: -1.7e38
Upper Limit: 1.7e38

Level of second harmonic (in dB) relative to the fundamental.
If the parameter "harm/coef" is .false., this parameter is the coefficient of the squared term in the polynomial.

3RD HARMONIC LEVEL Type: REAL
Lower Limit: -1.7e38
Upper Limit: 1.7e38

Level of third harmonic (in dB) relative to the fundamental. If the parameter "harm/coef" is .false., this parameter is the coefficient of the cubed term in the polynomial.

4TH HARMONIC LEVEL Type: REAL
Lower Limit: -1.7e38
Upper Limit: 1.7e38

Level of fourth harmonic (in dB) relative to the fundamental. If the parameter "harm/coef" is .false., this parameter is the coefficient of the fourth order term in the polynomial.

5TH HARMONIC LEVEL Type: REAL
Lower Limit: -1.7e38
Upper Limit: 1.7e38

Level of fifth harmonic (in dB) relative to the fundamental. If the parameter "harm/coef" is .false., this parameter is the coefficient of the fifth order term in the polynomial.

HARM/COEF Type: LOGICAL
Lower Limit: NIL
Upper Limit: NIL

When this logical parameter is .true., the values of parameters "XXX harmonic level" are interpreted as harmonic levels. When .false., they are interpreted as coefficents of the 5th order polynomial (efficiency is the first order term).

INPUT SIGNAL MAG. Type: REAL
Lower Limit: 0.0
Upper Limit: 1.7e38

output = gain constant * input

BIAS CURRENT Type: REAL
Lower Limit: 3.0e-39
Upper Limit: 1.7e38

The units of this parameter should be the same as the input current, and the parameter "test tone magnitude".

BASEBAND FREQUENCY Type: REAL
Lower Limit: 0.0
Upper Limit: 1.7e38

The frequency of the generated sinuaoidal tone in Hertz.

T-ON Type: REAL
Lower Limit: 0.0
Upper Limit: 1.7e38

Time (seconds) in which enable becomes true.

MODULES USED IN BLOCK DIAGRAM:

FM MOD
BUTTERWORTH BANDPASS
IMPULSE TRAIN
SINUSOIDAL
REAL OF CMPLX
TABULAR PLOT VIA ITERATION
SAMPLE & HOLD
LOGICAL TRUE COUNTER
= INTGR
TERMINATE SIMULATION
SNR RATIO
VARIABLE-DELAY
REAL TO CMPLX
T_>= T_ON
GAIN
ADDER
SAMPLER
BUTWTH FILTER (REAL)
AVG CMPLX POWER
LASER DIODE
SUBTRACTOR
CONST GEN

INITIALIZATION CODE: (none)

SNR VS OMD

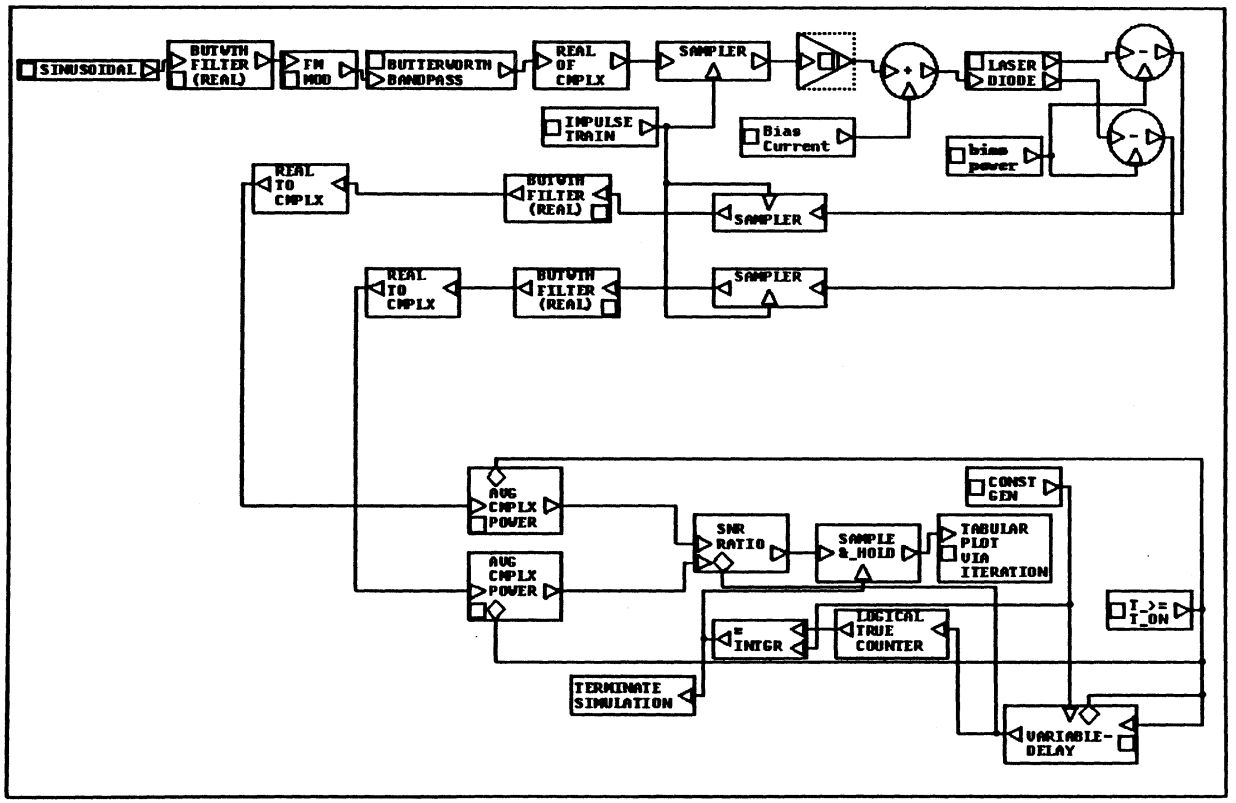
SINUSOIDAL
BUTWTH FILTER (REAL)
FM MOD
BUTTERWORTH BANDPASS
REAL OF CMPLX
SAMPLER
LASER DIODE
IMPULSE TRAIN
Bias Current
bias power
REAL TO CMPLX
BUTWTH FILTER (REAL)
SAMPLER
REAL TO CMPLX
BUTWTH FILTER (REAL)
SAMPLER
AVG CMPLX POWER
AVG CMPLX POWER
SNR RATIO
SAMPLE & HOLD
CONST GEN
TABULAR PLOT VIA ITERATION
I_>= I_ON
= INTGR
LOGICAL TRUE COUNTER
TERMINATE SIMULATION
VARIABLE-DELAY

MODULE NAME: SNR VS NONLINEARITIES
GROUP: SYSTEM
DATABASE: DUA0:[USERS.ALFRED.TEST]
AUTHOR: ALFRED
CREATION DATE: 1-Dec-1991 17:23:20

DESCRIPTION:

This module finds the baseband signal-to-noise ratio as a function of laser's nonlinearities.

REVISIONS:

Author : ALFRED
Date : 1-Dec-1991 17:23:20
Description:

1-Dec-1991 17:23:36
Module CREATION.

INPUT SIGNALS: (none)

OUTPUT SIGNALS: (none)

PARAMETERS:
STOP-TIME Type: REAL
Lower Limit: 3.0e-39
Upper Limit: 1.7e38

Specifes the maximum value of time for the simulation (in seconds).
The simulation clock runs from time=0.0 to time=STOP-TIME
in steps of DT, all in seconds.

DT Type: REAL
Lower Limit: 3.0e-39
Upper Limit: 1.7e38

Time between discrete simulation signal samples (in

seconds).
  DT must be small enough to satisfy the Nyquist Sampling Theorem for all signals at all points in the simulation.

NOTE:
  If the specified period or rate of a periodic function results
in a period that is not a multiple of DT, then BOSS will round
the period to the nearest value that IS a multiple of DT.
  For example, if DT=0.125(sec) and a rate was specified as rate=1.4(hz) which corresponds to a period of T=0.714(sec) which is 5.7*DT , then BOSS will round this period to be 6.0*DT and thus the effective rate will be 1.333(hz).

  Because of this, the choice for DT can affect the periods of the periodic signals in the simulation.

BASEBAND FREQUENCY Type: REAL
Lower Limit: -1.7e38
Upper Limit: 1.7e38

The frequency of the generated sinuaoidal tone in Hertz.

INPUT SIGNAL MAGNITUDE Type: REAL
Lower Limit: 3.0e-39
Upper Limit: 1.7e38

  this is the gain constant for the gain block. it must be a single precision real number.
  the block output = gain coeff * block input .

BIAS POWER Type: REAL
Lower Limit: 3.0e-39
Upper Limit: 1.7e38

Power output at bias point (corresponding current specified by the parameter "bias current"). Units should be same as the output power signal.

THRESHOLD CURRENT Type: REAL
Lower Limit: 0.0

Upper Limit: 1.7e38

Current at threshold corresponding to the measured harmonic values. The units should be the same as the bias current parameter. This parameter should always be less than the bias current. The laser module is not designed to accurately model the laser near threshold, but this parameter is required to relate the test modulation index to the test sinusoid magnitude.

TEST MOD INDEX Type: REAL
Lower Limit: 0
Upper Limit: 1

The input modulation index used during measurement of the given harmonic levels. This number must be between zero and one inclusive.

EFFICIENCY Type: COMPLEX
Lower Limit: 3.0e-39
Upper Limit: 1.7e38

Slope of the output power vs input current characteristic at the bias point. The units of this parameter must correspond to the units of the output power/input current.

2ND HARMONIC LEVEL Type: REAL
Lower Limit: -1.7e38
Upper Limit: 1.7e38

Level of second harmonic (in dB) relative to the fundamental.
If the parameter "harm/coef" is .false., this parameter is the coefficient of the squared term in the polynomial.

HARM/COEF Type: LOGICAL
Lower Limit: NIL
Upper Limit: NIL

When this logical parameter is .true., the values of parameters "XXX harmonic level" are interpreted as harmonic levels. When .false., they are interpreted as coefficents

of the 5th order polynomial (efficiency is the first order term).

BIAS CURRENT Type: REAL
Lower Limit: 3.0e-39
Upper Limit: 1.7e38

The units of this parameter should be the same as the input current, and the parameter "test tone magnitude".

T-ON Type: REAL
Lower Limit: 0.0
Upper Limit: 1.7e38

Time (seconds) in which enable becomes true.

MODULES USED IN BLOCK DIAGRAM:

FM MOD
IMPULSE TRAIN
SINUSOIDAL
TABULAR PLOT VIA ITERATION
SAMPLE & HOLD
LOGICAL TRUE COUNTER
= INTGR
TERMINATE SIMULATION
SNR RATIO
T_>= T_ON
ADDER
SAMPLER CMPLX
CONST GEN
MAKE CMPLX
COMLX LASER
CMPLX DC BLOCK
FM_BALANCED DISCRIMINATOR
BUTWTH FILTER (REAL)
REAL TO CMPLX
SUBTRACTOR
BUTTERWORTH BANDPASS
UNIT VECTOR
VARIABLE-DELAY
REAL COEFF GAIN
AVERAGE POWER OF REAL SIGNAL
REAL OF CMPLX

INITIALIZATION CODE: (none)

SNR VS NONLINEARITIES

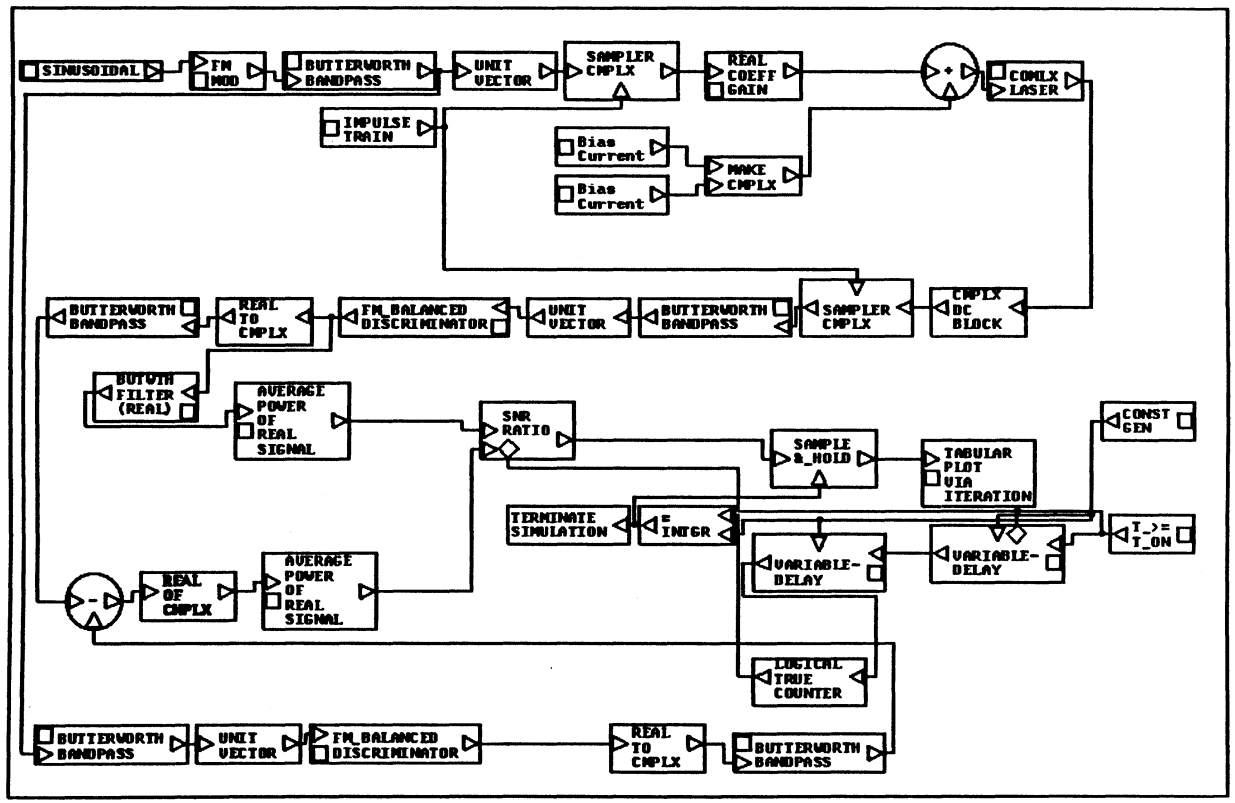

MODULE NAME: COMLX LASER
GROUP: ANALOG MODULATORS
DATABASE: DUA0:[USERS.ALFRED.BASICS]
AUTHOR: ALFRED
CREATION DATE: 28-May-1991 18:58:35

DESCRIPTION:

This module models the optical power output vs current input characteristic for a laser diode above threshold. The laser is represented by an AM-AM, memoryless nonlinearity which is approximated by a fifth order polynomial. Laser diodes are biased for analog applications above the threshold (lasing region). The input current, output optical power, and slope of the characteristic (the output efficiency) at the bias point must be given. The coefficients of the remaining terms in the polynomial approximation may be entered directly (if "harm/coef" is .false.) or as the levels of the 2nd through 5th harmonics (if ""harm/coef" is .true.), measured relative to the fundamental with a test tone of peak magnitude equal to "test mod index" * ("bias current" - "threshold current").

The polynomial approximation assumes that the input current remains above the threshold current. If the input drops below this, the calculated output power may be <0. In this case, the output power is set to 0, since power output cannot be negative. In this case, the results will not be accurate for samples near or below threshold.

The input and the output types are complex, the nonlinear distortion is added to both real and imaginary part equally.

REVISIONS:

Author : ALFRED
Date : 1-Dec-1991 17:41:21
Description:

Edited 1-Dec-1991 17:41:21, No Edit Description Entered.

Author : ALFRED
Date : 3-Jun-1991 21:57:51
Description:

Edited 28-May-1991 19:15:39, No Edit Description Entered.
Edited 29-May-1991 9:46:54, No Edit Description Entered.
Edited 3-Jun-1991 21:08:40, No Edit Description Entered.
Edited 3-Jun-1991 21:35:27, No Edit Description Entered.

Edited 3-Jun-1991 21:57:51, No Edit Description Entered.

Author : ALFRED
Date : 28-May-1991 19:17:08
Description:

Edited 28-May-1991 19:17:08, No Edit Description Entered.

Author : ALFRED
Date : 28-May-1991 18:58:35
Description:

28-May-1991 18:59:02
Module CREATION.

INPUT SIGNALS:
INPUT CURRENT Type: COMPLEX
Lower Limit: (-1.7e38 -1.7e38)
Upper Limit: (1.7e38 1.7e38)

Laser input current. Should always be greater than the threshold current.

OUTPUT SIGNALS:
OPTICAL PWR OUT Type: COMPLEX
Lower Limit: (-1.7e38 -1.7e38)
Upper Limit: (1.7e38 1.7e38)

Laser optical power output.

PARAMETERS:
HARM/COEF Type: LOGICAL
Lower Limit: NIL
Upper Limit: NIL

When this logical parameter is .true., the values of parameters "XXX harmonic level" are interpreted as harmonic levels. When .false., they are interpreted as coefficents

of the 5th order polynomial (efficiency is the first order term).

5TH HARMONIC LEVEL Type: REAL
Lower Limit: -1.7e38
Upper Limit: 1.7e38

Level of fifth harmonic (in dB) relative to the fundamental. If the parameter "harm/coef" is .false., this parameter is the coefficient of the fifth order term in the polynomial.

4TH HARMONIC LEVEL Type: REAL
Lower Limit: -1.7e38
Upper Limit: 1.7e38

Level of fourth harmonic (in dB) relative to the fundamental. If the parameter "harm/coef" is .false., this parameter is the coefficient of the fourth order term in the polynomial.

3RD HARMONIC LEVEL Type: REAL
Lower Limit: -1.7e38
Upper Limit: 1.7e38

Level of third harmonic (in dB) relative to the fundamental. If the parameter "harm/coef" is .false., this parameter is the coefficient of the cubed term in the polynomial.

2ND HARMONIC LEVEL Type: REAL
Lower Limit: -1.7e38
Upper Limit: 1.7e38

Level of second harmonic (in dB) relative to the fundamental.
If the parameter "harm/coef" is .false., this parameter is the coefficient of the squared term in the polynomial.

EFFICIENCY Type: COMPLEX

Lower Limit: 3.0e-39
Upper Limit: 1.7e38

Slope of the output power vs input current characteristic at the bias point. The units of this parameter must correspond to the units of the output power/input current.

TEST MOD INDEX Type: REAL
Lower Limit: 0
Upper Limit: 1

The input modulation index used during measurement of the given harmonic levels. This number must be between zero and one inclusive.

THRESHOLD CURRENT Type: REAL
Lower Limit: 0.0
Upper Limit: 1.7e38

Current at threshold corresponding to the measured harmonic values. The units should be the same as the bias current parameter. This parameter should always be less than the bias current. The laser module is not designed to accurately model the laser near threshold, but this parameter is required to relate the test modulation index to the test sinusoid magnitude.

BIAS POWER Type: REAL
Lower Limit: 3.0e-39
Upper Limit: 1.7e38

Power output at bias point (corresponding current specified by the parameter "bias current"). Units should be same as the output power signal.

BIAS CURRENT Type: REAL
Lower Limit: 3.0e-39
Upper Limit: 1.7e38

The units of this parameter should be the same as the input current, and the parameter "test tone magnitude".

COMPUTED PARAMETERS:

A2 Type: COMPLEX
Lower Limit: -1.7e38
Upper Limit: 1.7e38

Computed.

A3 Type: COMPLEX
Lower Limit: -1.7e38
Upper Limit: 1.7e38

Computed.

A4 Type: COMPLEX
Lower Limit: -1.7e38
Upper Limit: 1.7e38

Computed.

A5 Type: COMPLEX
Lower Limit: -1.7e38
Upper Limit: 1.7e38

Computed.

MODULES USED IN BLOCK DIAGRAM:

SUBTRACTOR
GAIN
MULTIPLIER
ADDER
CONST GEN
MAKE CMPLX

INITIALIZATION CODE:

Subroutine: laser_pwr_series
Arguments:
EFFICIENCY

2ND HARMONIC LEVEL
3RD HARMONIC LEVEL
4TH HARMONIC LEVEL
5TH HARMONIC LEVEL
TEST MOD INDEX
HARM/COEF
BIAS POWER
BIAS CURRENT
THRESHOLD CURRENT
A2
A3
A4
A5

Description:

This subroutine calculates the coefficients of the second through fifth order terms of the polynomial approximation of the power output vs current input characteristic of the laser diode. These values are determined from the levels of the 2nd through 5th harmonics (relative to the fundamental), the magnitude of the test tone, the output efficiency (ie, slope of the characteristic at the bias point). If "harm/coef" is .false., then the entered harmonic level parameters are used as the polynomial coefficients.

COMLX LASER

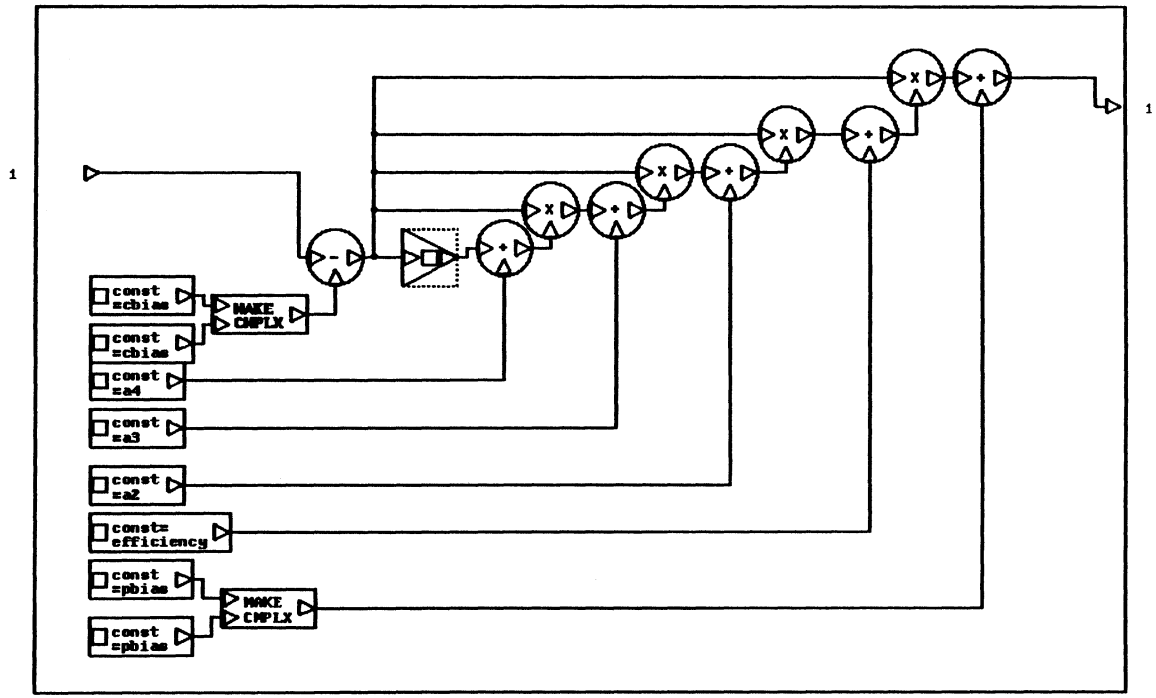

ON 1 OPTICAL PWR OUT

IN 1 INPUT CURRENT

MODULE NAME: LASER DIODE
GROUP: ANALOG MODULATORS
DATABASE: DUA0:[USERS.ALFRED.BASICS]
AUTHOR: ALFRED
CREATION DATE: 4-Jul-1991 13:09:18

DESCRIPTION:

This module models the optical power output vs current input characteristic for a laser diode above threshold. The laser is represented by an AM-AM, memoryless non-linearity which is approximated by a fifth order polynomial. Laser diodes are biased for analog applications above the threshold (lasing region). The input current, output optical power, and slope of the characteristic (the output efficiency) at the bias point must be given. The coefficients of the remaining terms in the polynomial approximation may be entered directly (if "harm/coef" is .false.) or as the levels of the 2nd through 5th harmonics (if ""harm/coef" is .true.), measured relative to the fundamental with a test tone of peak magnitude equal to "test mod index" * ("bias current" - "threshold current").

The polynomial approximation assumes that the input current remains above the threshold current. If the input drops below this, the calculated output power may be <0. In this case, the output power is set to 0, since power output cannot be negative. In this case, the results will not be accurate for samples near or below threshold.

The output quantity a1*i is routed from output#1 while the the rest of the terms in the power series are routed from output#2.

REVISIONS:

Author : ALFRED
Date : 1-Dec-1991 17:46:33
Description:

Edited 1-Dec-1991 17:46:33, No Edit Description Entered.

Author : ALFRED
Date : 4-Jul-1991 13:09:18
Description:

4-Jul-1991 13:09:43
Module CREATION.

INPUT SIGNALS:

INPUT CURRENT — Type: REAL
Lower Limit: 0.0
Upper Limit: 1.7e38

Laser input current. Should always be greater than the threshold current.

OUTPUT SIGNALS:

DISTORTION OUTPUT — Type: REAL
Lower Limit: 0.0
Upper Limit: 1.7e38

Nonlinear distortion signal.

OPTICAL PWR OUT — Type: REAL
Lower Limit: 0.0
Upper Limit: 1.7e38

Desired optical signal.

PARAMETERS:

HARM/COEF — Type: LOGICAL
Lower Limit: NIL
Upper Limit: NIL

When this logical parameter is .true., the values of parameters "XXX harmonic level" are interpreted as harmonic levels. When .false., they are interpreted as coefficents of the 5th order polynomial (efficiency is the first order term).

5TH HARMONIC LEVEL — Type: REAL
Lower Limit: -1.7e38
Upper Limit: 1.7e38

Level of fifth harmonic (in dB) relative to the fundamental. If the parameter "harm/coef" is .false., this parameter is the coefficient of the fifth order term in the polynomial.

4TH HARMONIC LEVEL Type: REAL
Lower Limit: -1.7e38
Upper Limit: 1.7e38

Level of fourth harmonic (in dB) relative to the fundamental. If the parameter "harm/coef" is .false., this parameter is the coefficient of the fourth order term in the polynomial.

3RD HARMONIC LEVEL Type: REAL
Lower Limit: -1.7e38
Upper Limit: 1.7e38

Level of third harmonic (in dB) relative to the fundamental. If the parameter "harm/coef" is .false., this parameter is the coefficient of the cubed term in the polynomial.

2ND HARMONIC LEVEL Type: REAL
Lower Limit: -1.7e38
Upper Limit: 1.7e38

Level of second harmonic (in dB) relative to the fundamental.
If the parameter "harm/coef" is .false., this parameter is the coefficient of the squared term in the polynomial.

EFFICIENCY Type: REAL
Lower Limit: 3.0e-39
Upper Limit: 1.7e38

Slope of the output power vs input current characteristic at the bias point. The units of this parameter must correspond to the units of the output power/input current.

TEST MOD INDEX Type: REAL
Lower Limit: 0
Upper Limit: 1

The input modulation index used during measurement of the given harmonic levels. This number must be between zero and one inclusive.

THRESHOLD CURRENT Type: REAL
Lower Limit: 0.0
Upper Limit: 1.7e38

Current at threshold corresponding to the measured harmonic values. The units should be the same as the bias current parameter. This parameter should always be less than the bias current. The laser module is not designed to accurately model the laser near threshold, but this parameter is required to relate the test modulation index to the test sinusoid magnitude.

BIAS POWER Type: REAL
Lower Limit: 3.0e-39
Upper Limit: 1.7e38

Power output at bias point (corresponding current specified by the parameter "bias current"). Units should be same as the output power signal.

BIAS CURRENT Type: REAL
Lower Limit: 3.0e-39
Upper Limit: 1.7e38

The units of this parameter should be the same as the input current, and the parameter "test tone magnitude".

COMPUTED PARAMETERS:

A2 Type: REAL
Lower Limit: -1.7e38
Upper Limit: 1.7e38

Computed.

A3 Type: REAL
Lower Limit: -1.7e38
Upper Limit: 1.7e38

Computed.

A4 Type: REAL
Lower Limit: -1.7e38
Upper Limit: 1.7e38

Computed.

A5 Type: REAL
Lower Limit: -1.7e38
Upper Limit: 1.7e38

Computed.

MODULES USED IN BLOCK DIAGRAM:

SUBTRACTOR
GAIN
MULTIPLIER
CONST GEN
3 INPUT MULTIPLIER
>= REAL
SELECT
ADDER

INITIALIZATION CODE:

Subroutine: laser_pwr_series
Arguments:
- EFFICIENCY
- 2ND HARMONIC LEVEL
- 3RD HARMONIC LEVEL
- 4TH HARMONIC LEVEL
- 5TH HARMONIC LEVEL
- TEST MOD INDEX
- HARM/COEF
- BIAS POWER

BIAS CURRENT
THRESHOLD CURRENT
A2
A3
A4
A5

Description:

This subroutine calculates the coefficients of the second through fifth order terms of the polynomial approximation of the power output vs current input characteristic of the laser diode. These values are determined from the levels of the 2nd through 5th harmonics (relative to the fundamental), the magnitude of the test tone, the output efficiency (ie, slope of the characteristic at the bias point). If "harm/coef" is .false., then the entered harmonic level parameters are used as the polynomial coefficients.

LASER DIODE

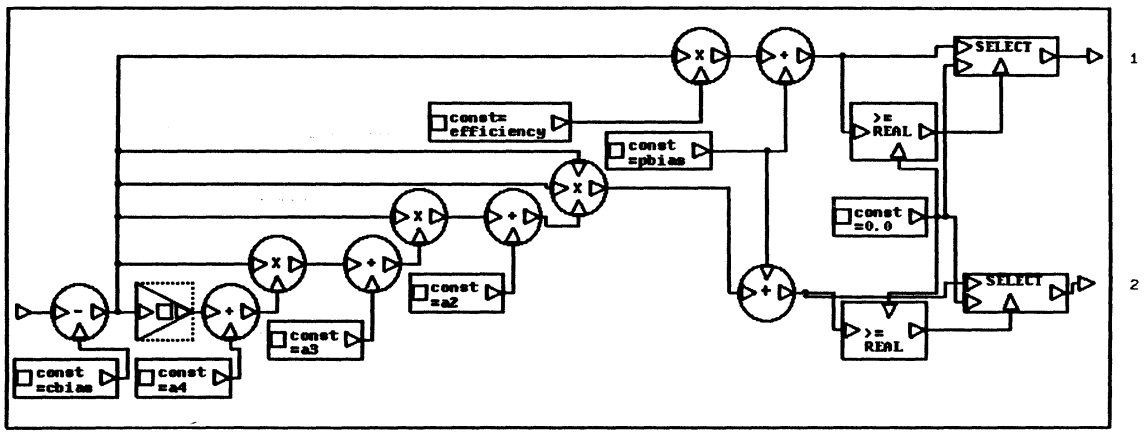

I# 1 INPUT CURRENT

O# 1 OPTICAL PWR OUT
O# 2 DISTORTION OUTPUT

MODULE NAME: SAMPLER CMPLX
GROUP: ANALOG MODULATORS
DATABASE: DUA0:[USERS.ALFRED.BASICS]
AUTHOR: ALFRED
CREATION DATE: 7-Jun-1990 16:39:32

DESCRIPTION:

This module is a sampler for complex signals. That is to say it samples tha magnituse and the phase of the input signal.

REVISIONS:

Author : ALFRED
Date : 1-Dec-1991 17:51:08
Description:

Edited 1-Dec-1991 17:51:08, No Edit Description Entered.

Author : ALFRED
Date : 4-Jun-1991 11:48:18
Description:

Edited 4-Jun-1991 11:48:18, No Edit Description Entered.

Author : ALFRED
Date : 7-Jun-1990 16:39:32
Description:

7-Jun-1990 16:39:59
Module CREATION.

INPUT SIGNALS:

TRIGGER INPUT Type: LOGICAL
Lower Limit: NIL
Upper Limit: NIL

trigger input (inpulse train)

SIGNAL TO BE SAMPLED — Type: COMPLEX
Lower Limit: (-1.7e38 -1.7e38)
Upper Limit: (1.7e38 1.7e38)

signal to be sampled (real).

OUTPUT SIGNALS:

SAMPLED OUTPUT (REAL) — Type: COMPLEX
Lower Limit: (-1.7e38 -1.7e38)
Upper Limit: (1.7e38 1.7e38)

sampled output (real).

PARAMETERS: (none)

MODULES USED IN BLOCK DIAGRAM:

SAMPLE & HOLD
MULTIPLIER
LOGICAL TO NUMERIC

INITIALIZATION CODE: (none)

SAMPLER CMPLX

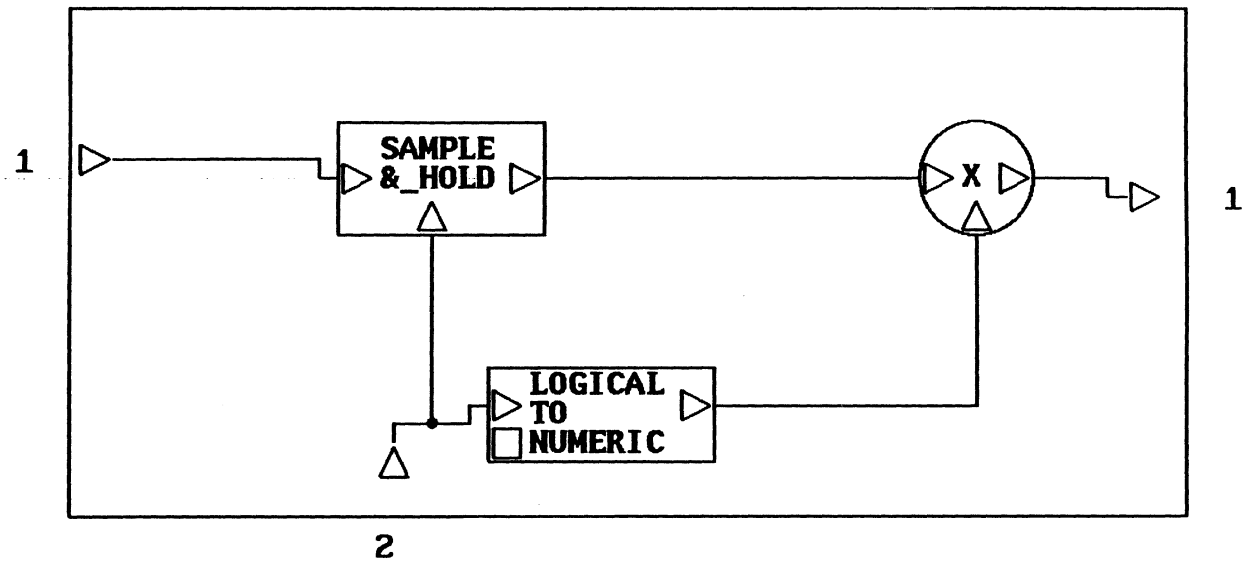

I# 1 SIGNAL TO BE SAMPLED
I# 2 TRIGGER INPUT

O# 1 SAMPLED OUTPUT (REAL)

MODULE NAME: CMPLX PIN DETECTOR
GROUP: NOISE AND INTERFERENCE
DATABASE: DUA0:[USERS.ALFRED.BASICS]
AUTHOR: ALFRED
CREATION DATE: 29-May-1991 9:42:23

DESCRIPTION:

This module implements a PIN diode photo detector. The input signal should be an optical power signal (Watts). Any small amount of negative power on this input will be ignored by the module (this may occur in an FFT filter, for example). Shot noise effects are simulated using a Poisson random number generator. The output current is in units of microamps.
The type of the input signal is complex. the signal is internally separated to real and imaginary. The p-i-n diode discribed above is repeated twice, once for each part of the complex number.

REVISIONS:

Author : ALFRED
Date : 1-Dec-1991 18:07:39
Description:

Edited 1-Dec-1991 18:07:39, No Edit Description Entered.

Author : ALFRED
Date : 29-May-1991 9:42:23
Description:

29-May-1991 9:42:52
Module CREATION.

INPUT SIGNALS:
OPTICAL POWER IN Type: COMPLEX
Lower Limit: (0.0 0.0)
Upper Limit: (1.7e38 1.7e38)

The incident optical power in watts.

OUTPUT SIGNALS:

OUTPUT CURRENT Type: COMPLEX
Lower Limit: (0.0 0.0)
Upper Limit: (1.7e38 1.7e38)

The pin diode output current in MICROAMPS.

PARAMETERS:

DARK CURRENT (NANOAMPS) Type: REAL
Lower Limit: 0.0
Upper Limit: 1.7e38

The PIN dark current in nanoamps.

INITIAL SEED Type: INTEGER
Lower Limit: 1
Upper Limit: 2147483647

Initial seed for Poisson random number generator. Should be large and odd.

QUANTUM EFFICIENCY Type: REAL
Lower Limit: 0.0
Upper Limit: 1.0

The quantum efficiency of the pin diode.

SOURCE CENTER WAVELENGTH Type: REAL
Lower Limit: 0.0
Upper Limit: 1.7e38

Center wavelength of the source in micrometers. This is used to determine the optical frequency.

COMPUTED PARAMETERS:

ELECTRON CONST Type: REAL
Lower Limit: 0.0

Upper Limit: 1.7e38

Electron constant, computed.

DARK CONST Type: REAL
Lower Limit: 0.0
Upper Limit: 1.7e38

Dark constant, computed.

POWER CONST Type: REAL
Lower Limit: 0.0
Upper Limit: 1.7e38

Power constant, computed.

MODULES USED IN BLOCK DIAGRAM:

>= REAL
SELECT
ADDER
POISSON RAN_GEN
MULTIPLIER
REAL OF CMPLX
IMAG OF CMPLX
MAKE CMPLX
CONST GEN

INITIALIZATION CODE:

Subroutine: pin_photo_detector
Arguments:
QUANTUM EFFICIENCY
SOURCE CENTER WAVELENGTH
DARK CURRENT (NANOAMPS)
POWER CONST
DARK CONST
ELECTRON CONST

Description:

This routine calculates 3 constants: "power const", "dark const", and "electron const". "Power const" equals the product of "source center wavelength", "quantum

efficiency", and "dt", divided by 1.989e-13. "Power const" converts the input optical power units to average number of charge carriers. "Dark const" is the number of dark charge carriers in delta t seconds. "Electron const" converts charge into current in microamps.

CMPLX PIN DETECTOR

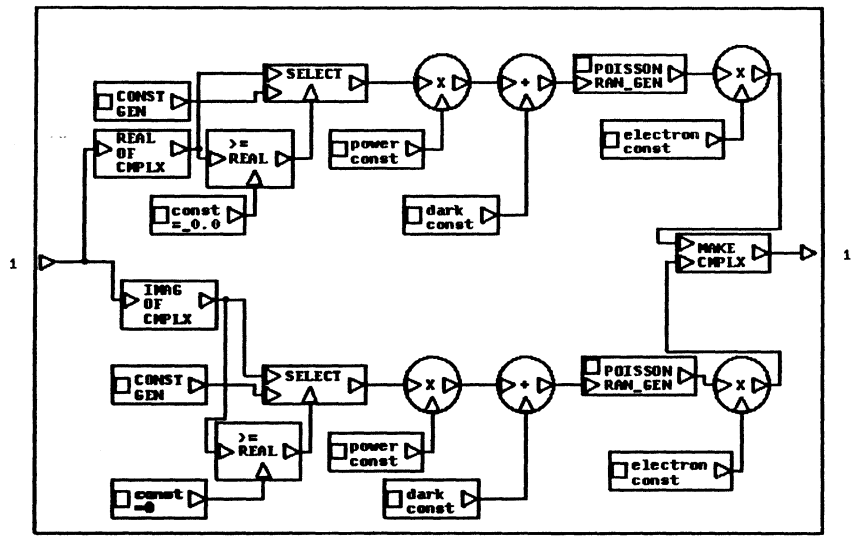

I# 1 OPTICAL POWER IN

O# 1 OUTPUT CURRENT

MODULE NAME: SNR RATIO
GROUP: CALIBRATION DEVICES/METERS
DATABASE: DUA0:[USERS.ALFRED.BASICS]
AUTHOR: ALFRED
CREATION DATE: 25-Jun-1990 10:40:57

DESCRIPTION:

The output of this module is found as

output = 10*log(input#1/input#2)

the two inputs are real signal. The two signals should be syncronized and have the same power units.

REVISIONS:

Author : ALFRED
Date : 1-Dec-1991 18:21:50
Description:

Edited 1-Dec-1991 18:21:50, No Edit Description Entered.

Author : ALFRED
Date : 1-Jun-1991 14:12:55
Description:

Edited 27-Jul-1990 11:30:06, No Edit Description Entered.
Edited 27-Jul-1990 12:16:08, No Edit Description Entered.
Edited 28-Aug-1990 15:28:15, No Edit Description Entered.
Edited 5-Sep-1990 15:34:16, No Edit Description Entered.
Edited 19-Sep-1990 10:14:20, No Edit Description Entered.
Edited 1-Jun-1991 14:12:55, No Edit Description Entered.

Author : ALFRED
Date : 16-Sep-1990 10:54:41
Description:

Edited 25-Jun-1990 14:07:57, No Edit Description Entered.
Edited 5-Sep-1990 13:04:56, No Edit Description Entered.
Edited 5-Sep-1990 13:11:01, No Edit Description Entered.
Edited 16-Sep-1990 10:54:41, No Edit Description Entered.

Author : ALFRED
Date : 25-Jun-1990 10:40:57
Description:

25-Jun-1990 10:41:18
Module CREATION.

INPUT SIGNALS:
DISTORTED SIGNAL Type: REAL
Lower Limit: -1.7e38
Upper Limit: 1.7e38

Distorted signal, which could be delayed also.

REFERRANCE SIGNAL Type: REAL
Lower Limit: -1.7e38
Upper Limit: 1.7e38

Referance signal, which is not distorted undelayed signal.

OUTPUT SIGNALS:
S/N(DB) Type: REAL
Lower Limit: -1.7e38
Upper Limit: 1.7e38

Signal-to-noise in db. Note that this value is not valid until the delay time is passed.

PARAMETERS: (none)

MODULES USED IN BLOCK DIAGRAM:
DIVIDER ZERO PROTECT
RUNNING AVERAGE
REAL TO DB

SNR RATIO

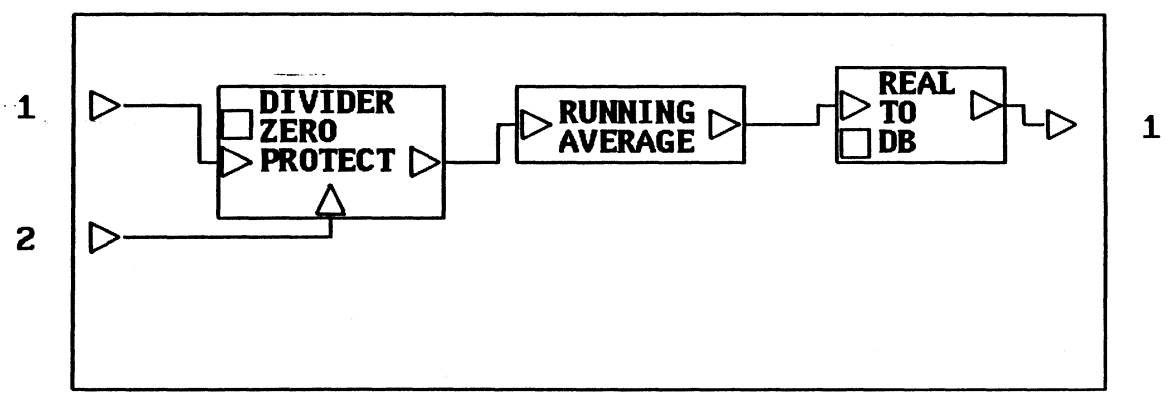

I# 1 REFERRANCE SIGNAL
I# 2 DISTORTED SIGNAL

O# 1 S/N (DB)

The vita has been removed from the scanned document